

# Fate of Persistent Organic Pollutants in the marine environment

Dissertation  
with the aim of achieving a doctoral degree  
at the Faculty of Mathematics, Informatics and Natural Sciences Department of Earth Sciences  
at Universität Hamburg

submitted by  
**Elena Mikheeva**

Hamburg, 2024



**Department of Earth Sciences**

Date of Oral Defense:

18.12.2024

Reviewers:

Prof. Dr. Corinna Schrum  
Dr. Johannes Bieser

Members of the examination commission:

Prof. Dr. Corinna Schrum  
Dr. Johannes Bieser  
Prof. Dr. Ralf Ebinghaus  
Prof. Dr. Gerhard Schmiedl  
Prof. Dr. Tatiana Ilyina

Chair of the Subject Doctoral Committee  
Earth System Sciences:

Prof. Dr. Hermann Held

Dean of Faculty MIN:

Prof. Dr.-Ing. Norbert Ritter

## Eidesstattliche Versicherung | Declaration on Oath

Hiermit erkläre ich an Eides statt, dass ich die vorliegende Dissertationsschrift selbst verfasst und keine anderen als die angegebenen Quellen und Hilfsmittel benutzt habe.

Sofern im Zuge der Erstellung der vorliegenden Dissertationsschrift generative Künstliche Intelligenz (gKI) basierte elektronische Hilfsmittel verwendet wurden, versichere ich, dass meine eigene Leistung im Vordergrund stand und dass eine vollständige Dokumentation aller verwendeten Hilfsmittel gemäß der Guten wissenschaftlichen Praxis vorliegt. Ich trage die Verantwortung für eventuell durch die gKI generierte fehlerhafte oder verzerrte Inhalte, fehlerhafte Referenzen, Verstöße gegen das Datenschutz- und Urheberrecht oder Plagiate.

I hereby declare and affirm that this doctoral dissertation is my own work and that I have not used any aids and sources other than those indicated.

If electronic resources based on generative artificial intelligence (gAI) were used in the course of writing this dissertation, I confirm that my own work was the main and value-adding contribution and that complete documentation of all resources used is available in accordance with good scientific practice. I am responsible for any erroneous or distorted content, incorrect references, violations of data protection and copyright law or plagiarism that may have been generated by the gAI.

A handwritten signature in blue ink, appearing to read 'Elena Mikheeva', with a long horizontal flourish extending to the right.

Elena Mikheeva

Hamburg, 19/08/2024

# Contents

<b>1</b>	<b>Introduction</b>	<b>13</b>
1.1	Persistent Organic Pollutants . . . . .	13
1.1.1	<i>General challenges of POPs research</i> . . . . .	15
1.1.2	<i>Current state-of-art for Pollution Models Development</i> . . . . .	17
1.1.3	<i>Development of a Modeling Framework for This Study</i> . . . . .	18
<b>2</b>	<b>Chemical and scientific justification</b>	<b>19</b>
2.1	Chosen pollutants . . . . .	19
2.1.1	<i>Polychlorinated Biphenyls (PCB) and Polybrominated Diphenyl Ethers (PBDEs)</i> . . . . .	19
2.1.2	<i>PFAS</i> . . . . .	23
2.2	Chemical processes . . . . .	25
2.2.1	Photolytical processes . . . . .	25
2.2.2	Photolysis of PFAS . . . . .	29
2.3	Biological degradation . . . . .	29
2.4	Research questions . . . . .	31
<b>3</b>	<b>Model description</b>	<b>33</b>
3.1	General information . . . . .	33
3.2	<b>GOTM – The hydrodynamic host model</b> . . . . .	35
3.3	ECOSMO . . . . .	38
3.4	Model coupling, initial and boundary conditions . . . . .	38
3.5	Chemical model . . . . .	40
3.5.1	Particle partitioning (kinetic sorption) . . . . .	40
3.5.2	Photolytic degradation . . . . .	42
3.5.3	Biological degradation . . . . .	45
3.5.4	Freely dissolved POPs . . . . .	45
3.6	Boundary forcing and external processes . . . . .	46
3.6.1	Air-sea exchange . . . . .	46
3.6.2	Sedimentation, resuspension and burial . . . . .	49
3.7	Regional Characteristics for Model Implementation . . . . .	50
<b>4</b>	<b>Results and Discussion</b>	<b>53</b>
4.1	The environmental fate of specific congeners of a group of POPs . . . . .	54
4.1.1	<i>Atmospheric flux</i> . . . . .	55
4.1.2	<i>Dergadation</i> . . . . .	59
4.1.3	<i>Partitioning to detritus and sediment concentrations</i> . . . . .	60
4.2	Hydrodynamic Impacts on the Fate of hydrophobic POPs in the Marine Environment . . . . .	61
4.2.1	The Deep Region with Permanent Stratification — The Gotland Deep . . . . .	63
4.2.2	Permanently Mixed Region with Low Atmospheric Input and the Late Onset of Production due to Sea Ice Cover—The Bothnian Bay . . . . .	66
4.2.3	The North Sea — Tides Influenced Area with High Primary Production . . . . .	69

4.3	Changes in aquatic POPs distribution under the conditions of enhanced nitrate concentrations . . . . .	79
4.3.1	Gotland Basin - the stratified region of high nutrient content and UV irradiation . . . . .	80
4.3.2	Bothnian Bay - the region of low UV irradiation and winter sea ice coverage . . . . .	83
4.3.3	Northern North Sea - seasonally stratified area of high nutrients content and UV irradiation . . . . .	86
4.3.4	Southern North Sea - shallow permanently mixed region with high UV irradiation and high biological production . . . . .	90
<b>5</b>	<b>Summary and Conclusions</b>	<b>95</b>
5.1	RQ1: The environmental fate of specific POP congeners . . . . .	95
5.2	RQ2: Hydrodynamic Impacts on the Fate of hydrophobic POPs in the Marine Environment . . . . .	97
5.3	RQ3: Changes in aquatic POPs distribution under the conditions of enhanced nitrate concentrations . . . . .	100

## Abstract

Over the past several decades, Persistent Organic Pollutants (POPs) have garnered significant attention due to their persistence in the environment and harmful effects on human health. POPs include a broad range of chemical species, each characterized by a long half-life, widespread distribution, high bioaccumulation, and toxicity. Despite these shared traits, individual POPs can exhibit markedly different chemical properties, influencing their behavior in natural environments. Coastal aquatic areas are particularly vulnerable to POP contamination due to their proximity to emission sources, high biological productivity, and additional inputs from atmospheric deposition and terrestrial runoff.

Modeling the fate of POPs is essential for understanding their distribution and identifying areas of accumulation within the water column. This knowledge is critical for developing strategies to mitigate and eventually eliminate these pollutants. This dissertation introduces a newly developed numerical model designed to simulate the cycling of various POPs in aquatic environments. A detailed fate analysis was conducted using a new chemical model, based on the GOTM-ECOSMO-FABM framework, which integrates hydrodynamic and biogeochemical components with a chemical module accounting for the specific physicochemical properties of each selected pollutant. One of the key advantages of this model is its flexibility, allowing the chemical module to be coupled with any hydrophysical and biogeochemical model setup. The study includes 1D simulations at various locations in the North and Baltic Seas, investigating how different hydrodynamic and biogeochemical conditions influence the fate of five POPs from three distinct chemical classes.

This dissertation is structured into three parts, each addressing a specific research question. The study builds complexity with each section, highlighting the processes impacting the fate of POPs.

The first part examines the differing behaviors of five POPs based on their unique chemical characteristics. Despite sharing certain properties, these POPs show variations in their distribution patterns. While all POP classes exhibit an affinity for organic matter, the rate of sorption and desorption is dictated by their chemical structure, resulting in differences in seasonal distribution even within the same class. Additionally, the specific properties of each chemical influence exchange processes between water and atmosphere, leading to variations in the balance of influx and outflux and the pathways of degradation. Their persistent nature allows these pollutants to remain in the environment for extended periods, undergoing long-range transport and slow degradation, ultimately influencing their long-term fate.

The second part of the dissertation focuses on the impact of hydrophysical properties on pollutant behavior within the North and Baltic Seas. The study area exhibits diverse hydrodynamic and biogeochemical conditions that are crucial in determining pollutant distribution. This section explores the roles of resuspension, mixing, the biological pump, sea ice, and tides in shaping the final phase distribution of various POPs. These factors create specific pollutant accumulation zones, or "hotspots," significantly influencing POP uptake and concentration within the water column. Two key dynamics predominantly govern pollutant fate in coastal regions: i) Primary

production facilitates the adsorption of POPs onto organic material, leading to their removal from the surface ocean and enhancing atmospheric influx; ii) Tidal-induced resuspension and mixing regulate benthic–pelagic exchange and vertical distribution of POPs. Sediments act as either permanent sinks (e.g., Gotland Deep) or seasonal sinks (e.g., Northern North Sea), while areas with permanent mixing, like the Southern North Sea, exhibit minimal pollutant accumulation in sediments.

The final section examines system responses to elevated nitrate concentrations in the studied regions. Increased nitrate levels boost organic matter production, a critical matrix for POP partitioning. In regions with distinct stratification, like the Gotland Basin, this leads to enhanced removal of detritus and bound pollutants from the surface layer, but also increases atmospheric flux. In seasonally stratified areas, resuspension of organic matter within the water column leads to greater pollutant accumulation, reducing dissolved concentrations. Elevated nitrate and DOM concentrations stimulate hydroxyl radical production, driving indirect photolysis and forming highly toxic compounds like BDE-OH, particularly in permanently mixed areas with low light penetration.

This dissertation offers new insights into the fate of POPs in coastal aquatic environments, highlighting overlooked processes in existing models. The developed model effectively captures the distinct behaviors of pollutants, even within the same class, and is designed to be coupled with any hydrodynamic and biogeochemical host model.

## Zusammenfassung

In den letzten Jahrzehnten haben persistente organische Schadstoffe oder POPs (im Englischen "persistent organic pollutants") aufgrund ihrer gefährlichen Eigenschaften, insbesondere ihrer Persistenz in der Umwelt und ihrer schädlichen Auswirkungen auf die menschliche Gesundheit, große Aufmerksamkeit in der wissenschaftlichen Gemeinschaft erlangt. POPs umfassen eine Vielzahl chemischer Verbindungen, die durch eine lange Halbwertszeit, globale Verbreitung, hohe Bioakkumulation und Toxizität gekennzeichnet sind. Trotz dieser gemeinsamen Merkmale können einzelne POPs sehr unterschiedliche chemische Eigenschaften aufweisen, die ihr Verhalten in der Umwelt beeinflussen. Küstennahe aquatische Gebiete sind besonders anfällig für POP-Kontaminationen aufgrund ihrer Nähe zu Emissionsquellen, ihrer hohen biologischen Produktivität und zusätzlichen Einträgen durch atmosphärische Deposition und terrestrischen Abfluss.

Die Modellierung des Verbleibs von POPs ist entscheidend, um ihre Verteilungsmuster zu verstehen und Akkumulationsgebiete innerhalb der Wassersäule zu identifizieren. Dieses Wissen ist unerlässlich, um Strategien zur Minderung und letztendlichen Beseitigung dieser Schadstoffe zu entwickeln. Die in dieser Dissertation vorgestellte Forschung führt ein neu entwickeltes numerisches Modell ein, das den Kreislauf verschiedener POPs im Ozean simuliert. Zur detaillierten Analyse des Verbleibs einzelner Kongenere wurde ein neues chemisches Modell entwickelt. Dieses Modell berücksichtigt alle bekannten relevanten Prozesse basierend auf spezifischen physikochemischen Eigenschaften jedes ausgewählten Schadstoffs. Ein wesentlicher Vorteil dieses Systems ist seine Flexibilität, da das chemische Modul mit verschiedenen hydrodynamischen und biogeochemischen Modellen gekoppelt werden kann. Diese Studie umfasst Simulationen für verschiedenen Standorten in der Nord- und Ostsee mit dem Ziel zu untersuchen wie unterschiedliche hydrodynamische und biogeochemische Bedingungen den Verbleib von fünf POPs aus drei verschiedenen chemischen Klassen beeinflussen.

Diese Dissertation ist in drei Teile gegliedert, von denen jeder eine spezifische Forschungsfrage behandelt. Die Komplexität der Studie nimmt mit jedem Teil zu und beleuchtet die spezifischen Prozesse, die den Verbleib von POPs beeinflussen.

Der erste Teil konzentriert sich auf das unterschiedliche Verhalten von fünf POPs basierend auf ihren einzigartigen chemischen Eigenschaften. Die Studie untersucht drei verschiedene Klassen von POPs und hebt Unterschiede in ihren Verteilungsmustern hervor, selbst wenn sie bestimmte Eigenschaften teilen. Während alle POP-Klassen eine Affinität zu organischem Material zeigen, wird die Sorptions- und Desorptionsrate durch ihre chemische Struktur bestimmt. Dies führt zu Unterschieden in der saisonalen Verteilung der Schadstoffe, selbst innerhalb derselben POP-Klasse. Zudem beeinflussen die spezifischen Eigenschaften jedes chemischen Stoffs die Austauschprozesse zwischen Wasser und Atmosphäre, was zu Variationen im Gleichgewicht von Zufluss und Abfluss sowie den Abbauprozessen führt. Trotz ihrer persistenten Natur, die auf kurzen Zeitskalen biologische Abbauprozesse und photolytische Transformationen relativ unbedeutend macht, bleiben diese Schadstoffe aufgrund ihrer Persistenz über lange Zeiträume in der Umwelt erhalten. Sie können sogar über weite Strecken transportiert werden. Im Laufe der Zeit summieren sich die langsamen Abbau- und Transformationsprozesse und verändern den langfristi-

gen Verbleib dieser Schadstoffe.

Der zweite Teil dieser Dissertation befasst sich mit der Klärung des Einflusses hydrophysikalischer Eigenschaften auf den Verbleib von Schadstoffen in der Nord- und Ostsee. Das Untersuchungsgebiet weist eine Vielzahl hydrodynamischer und biogeochemischer Bedingungen auf, die entscheidend dafür sind, wie sich Schadstoffe verhalten und innerhalb der marinen Umwelt verteilen. In diesem Abschnitt werden die Rollen von Resuspension, Durchmischung, der biologischen Pumpe, Meereis und Gezeiten bei der Bildung der finalen Phasenverteilung verschiedener POPs untersucht. Das Zusammenspiel dieser Faktoren führt zur Entstehung spezifischer Schadstoff-Akkumulations-zonen oder "Hotspots" und beeinflusst maßgeblich die Gesamtaufnahme und Konzentration von POPs in der Wassersäule.

Der letzte Abschnitt untersucht die Reaktion des Systems auf erhöhte Nitratkonzentrationen in den untersuchten Regionen. Erhöhte Nitratwerte führen zu einer gesteigerten OM-Produktion, die als kritische Matrix für die Partitionierung von POPs dient.

Diese Dissertation ergibt neue Erkenntnisse über den Verbleib verschiedener POPs in der küstennahen aquatischen Umgebungen und hebt Unterschiede und Schlüsselprozesse hervor, die in Modellierungsansätzen oft keine Berücksichtigung finden. Die Ergebnisse zielen darauf ab, den Einfluss verschiedener Komponenten des aquatischen Systems auf die Verteilungsmuster und die endgültige Akkumulation von POPs mit unterschiedlichen chemischen Eigenschaften zu untersuchen.

## List of Abbreviations

<b>POP</b>	Persistent organic pollutants
<b>EC</b>	Emerging contaminants
<b>PCB</b>	Polychlorinated biphenyls
<b>CB</b>	Chlorinated biphenyls (biphenyls with one chlorine in the structure)
<b>BDE(PBDE)</b>	Polybrominated Diphenyl Ethers
<b>PFAS</b>	Per- and polyfluoroalkyl substances
<b>PFOA</b>	Perfluorooctanoic acid
<b>DDT</b>	Dichlorodiphenyltrichloroethane
<b>NO<sub>3</sub></b>	Nitrate
<b>NO<sub>2</sub></b>	Nitrite
<b>OH·</b>	Hydroxyl radical
<b>CO<sub>3</sub><sup>-</sup></b>	Carbonate anion
<b>CDOM</b>	Chromophoric dissolved organic matter
<b>SC</b>	Stockholm Convention
<b>SNS</b>	Southern North Sea
<b>NNS</b>	Northern North Sea
<b>GOTM</b>	'General Ocean Turbulence Model' [ <a href="#">Umlauf et al., 2024</a> ]
<b>ECOSMO</b>	'ECOSystem MOdel', is a 3D fully coupled physical–biogeochemical model [ <a href="#">Daewel and Schrum, 2013</a> ]
<b>FABM</b>	The Framework for Aquatic Biogeochemical Models [ <a href="#">Bruggeman and Bolding, 2014</a> ]
<b>NPZD (model)</b>	Nutrients, phytoplankton, zooplankton, detritus ecosystem model
<b>TKE</b>	Turbulent Kinetic Energy
<b>CTD</b>	Oceanography instrument used to measure the electrical conductivity, temperature, and pressure of seawater
<b>WOA</b>	World Ocean Atlas
<b>EMEP</b>	'European Monitoring and Evaluation Programme' [ <a href="#">EMEP, 2024</a> ]
<b>LRT</b>	Long-range transport
<b>LRTP</b>	Long-Range transport on Plastic
<b>OM</b>	Organic matter
<b>POM</b>	Particulate organic matter
<b>DOM</b>	Dissolved organic matter
<b>SSE</b>	Sea surface elevation
<b>SSA</b>	Sea Salt Aerosols
<b>SML</b>	Surface mixed layer
<b>BML</b>	Bottom mixed layer
<b>TLS</b>	Turbulence length scale
<b>ORCM</b>	Oxidative ring cleavage mechanism
<b>MFC</b>	Micelle formation concentration
<b>ES</b>	Excited state
<b>HSC</b>	High (Higher) Substituted Congener
<b>LSC</b>	Low (lower) Substituted Congener

**LFER** Linear free-energy relationships  
**BCF** Bioconcentration Factor  
**LC<sub>50</sub>** Lethal concentration of 50 % species  
**UV** Ultra-violet (refers to the part of the light spectrum)  
**GC-MS** Gas Chromatography Mass Spectrometer  
**LC-MS** Liquid Chromatography Mass Spectrometer

# 1 Introduction

## 1.1 Persistent Organic Pollutants

As the previous century drew to a close, heightened public awareness of the emission of hazardous chemical substances into the environment brought about growing concerns regarding their impact on human health. The dawn of the 21st century marked a significant milestone with the introduction of the Stockholm Convention on Persistent Organic Pollutants (POPs) [SC, 2019].

The group of pollutants commonly referred to as POPs encompasses numerous chemical species that meet specific criteria: they possess exceptionally long half-lives, are widely distributed throughout various environmental matrices (including soil, water, and air) [Miniero et al., 2015, SC, 2019, Schwarzenbach et al., 2016], exhibit high bioaccumulation and/or biomagnification factors, and pose significant hazards to both human health and wildlife [IARC, 2016, Ren et al., 2017, Wu et al., 2022, Rokni et al., 2023, Alharbi et al., 2018, Qing Li et al., 2006].

The primary sources of POPs are generally of anthropogenic origin, stemming from various pathways such as industrial processes [Breivik et al., 2007], pesticide usage [Vijgen et al., 2018, Wong et al., 2005], bleaching from landfills/wastelands [Ng and von Goetz, 2017, Kohler et al., 2005, Ruiz-Fernández et al., 2014], and unintentional production [SC, 2019]. The first two types of POPs are intentionally produced by humans, and we are aware of their use or release into the environment. The latter two types can be considered as secondary sources of POPs production [Mishra et al., 2022, SC, 2019]. Despite being unintentionally released, their effects remain significant.

Following the banning of some POPs under the Stockholm Convention's Annexes A and B [SC, 2019], the production of these restricted chemicals has decreased or ceased altogether. However, they can still be found in various environmental compartments [Ruiz-Fernández et al., 2014, Ng and von Goetz, 2017, Guo et al., 2019]. This persistence is not only due to their long half-life but also because of additional releases from industrial and electronic waste [Kohler et al., 2005, Ruiz-Fernández et al., 2014, Ng and von Goetz, 2017, Guo et al., 2019, SC, 2019]. Moreover, by definition, POPs are compounds of organic origin containing carbon and hydrogen atoms in their structure, which persist in the environment. Once released, they enter the ecosystem and can remain there for decades.

While POPs are known for their resistance to degradation, certain natural processes can still affect them [Schwarzenbach et al., 2016]. In aquatic environments, there are two common ways in which these pollutants can be transformed into other compounds [Eriksson et al., 2004, Boyle et al., 1992, Agulló et al., 2019, Zhang et al., 2015].

The first is through photochemical transformation. Most hydrophobic POPs absorb sunlight in the UV range. When exposed to photon flux, these compounds can become activated and enter an excited state, enabling them to transform into other compounds [Lores et al., 2002, Schwarzenbach et al., 2016, Eriksson et al., 2004]. While this process results in a decrease

in the initial concentration of the pollutant, in some cases, the newly formed compounds can be even more hazardous than the parent ones. This phenomenon is observed with polybrominated diphenyl ethers (PBDEs) [Eriksson et al., 2004] (Figure 6).

Another way in which POPs undergo transformation is through biodegradation. Certain bacterial communities possess the capability to metabolize specific POPs. For example, aerobic bacteria belonging to genera such as *Pseudomonas* and *Acinetobacter* can degrade polychlorinated biphenyls (PCBs) with particular chemical structures, such as PCB<sub>28</sub>, but are unable to degrade other PCBs like PCB<sub>153</sub> [Boyle et al., 1992, Agulló et al., 2019]. In a recent study, Zhang and colleagues demonstrated that the cyanobacterium *Anabaena* PD-1 can degrade PCB<sub>153</sub>, albeit to a lesser extent compared to PCB<sub>28</sub> (34.5:100%) [Zhang et al., 2015].

Due to their physical and chemical persistence, POPs tend to accumulate in various environmental compartments [Schwarzenbach et al., 2016, Beyer and Biziuk, 2009, IARC, 2016, SC, 2019, Nadal et al., 2015]. Additionally, these contaminants can be transported over long distances in the atmosphere and open water matrices through a process known as long-range transport (LRT) [SC, 2019, Nadal et al., 2015]. There are two primary modes of LRT for POPs: atmospheric and oceanic [de Wit et al., 2004, Lohmann et al., 2007].

Atmospheric LRT is considered the faster route for pollutant transport [Kallenborn et al., 2015]. Through mechanisms such as global distillation or the grasshopper effect [Gouin et al., 2004], pollutants released into the atmosphere in regions of high production can travel vast distances to remote areas, including polar regions and the deep ocean [Jamieson et al., 2017, Sobek et al., 2023, Kallenborn et al., 2015]. In the northern hemisphere, these pollutants are often transported towards the Arctic, where they can persist for extended periods.

Oceanic transport, while slower, also contributes significantly to the dissemination of POPs to remote areas, even decades after their production [Luarte et al., 2023]. The open ocean's lack of organic matter and degradation sources allows hydrophobic POPs to remain in the water column and undergo LRT.

Recently, attention has been drawn to another mechanism in aquatic LRT involving plastic debris. Chemical additives in plastic debris, as well as POPs that accumulate on micro- and nano-plastics, can travel long distances in higher concentrations than when freely dissolved [Andrade et al., 2021]. Moreover, micro plastic particles can trap other emerging contaminants (EC) and transport them to polar regions. This means that contaminants with short half-lives can also reach the Arctic Circle, posing a threat to local communities and wildlife. The persistent nature of POPs and the slow movement of oceanic currents have led to the underestimation of oceanic LRT by the scientific community. However, Andrade et al. [Andrade et al., 2021] have emphasized that the oceanic LRT of pollutants on plastic (L RTP) should be included in the Stockholm Convention's considerations due to its significant impact.

The exposure of humans and the environment to POPs remains a critical concern. Despite their poor solubility in water, pollutants like PCBs and PBDEs exhibit high lipophilicity ( $K_{ow} = 10^4$ - $10^7$ ) [ChemSpider, 2024], which enhances their affinity for fatty tissues in biota [IARC,

2016, Lippold et al., 2019]. This characteristic, combined with the slow metabolism of these hydrophobic substances, leads to their bioaccumulation within organisms and increasing concentrations along the food chain—a process known as biomagnification [Schwarzenbach et al., 2016]. Consequently, animals at the top of the food chain, particularly birds and mammals, including humans, accumulate the highest concentrations of POPs [Khairy et al., 2021, IARC, 2016, Andvik et al., 2020, Lippold et al., 2019].

Once in the body, POPs have an extended half-life. For instance, PCBs can persist in the human body for 2.6 to 15.5 years, depending on the specific congener [Ritter et al., 2011, IARC, 2016]. The bioaccumulation of POPs is associated with numerous serious health issues, including cancer, immune system effects, reproductive and neurological disorders, endocrine disruption, and other significant health problems [IARC, 2016, Lippold et al., 2019, Ren et al., 2017, Wu et al., 2022, Rokni et al., 2023, Alharbi et al., 2018, Qing Li et al., 2006].

Lipophilic toxic chemicals are efficiently concentrated in high-fat fluids such as semen and breast milk, which leads to their higher accumulation in these fluids compared to other body tissues. This property facilitates the direct transfer of these pollutants to fetuses or infant offspring during pregnancy and breastfeeding [IARC, 2016, Lippold et al., 2019].

Intentional and unintentional releases of POPs affect every link in the ecosystem. Understanding their behavior in natural matrices is crucial for finding safe and effective solutions for their elimination. Knowledge about the mechanisms governing POP behavior in the environment can help evaluate their distribution patterns and prevent undesirable accumulation in remote areas with high biological productivity. This understanding is also essential for developing conscious and responsible elimination techniques that can efficiently remove POPs from the environment without causing further harm.

Given our limited knowledge of the environment, predicting the precise effects of POPs in advance is challenging. However, current scientific capabilities allow us to measure and assess the presence of POPs in both present and past contexts. Environmental modeling enables us not only to describe and understand the current behavior of POPs in natural compartments but also to project their future behavior.

Therefore, modeling the fate of POPs in the environment is the focus of this research. The presented study aims to incorporate specific chemical pathways of various selected pollutants into a multi-compartment, complex biogeochemical numerical model to evaluate their accumulation areas in the marine environment. This approach will provide valuable insights into the long-term impact and distribution of POPs, aiding in the development of more effective and safer remediation strategies.

### 1.1.1 *General challenges of POPs research*

The Stockholm Convention (SC) regulates over 30 different groups of POPs under categories such as elimination (Annex A), restriction (Annex B), and unintentional production (Annex C)

[SC, 2019]. Each category encompasses hundreds of substances or congeners. For instance, the PCB group contains 209 congeners, each differing in the number of chlorine atoms in their chemical structure. While these congeners share some general properties, such as hydrophobicity and a low Henry's law constant, other critical properties can vary significantly [ChemSpider, 2024].

For example, lower substituted congeners (LSC) like PCB<sub>28</sub> are susceptible to degradation by bacterial communities, whereas higher substituted congeners (HSC) like PCB<sub>209</sub> are not degradable in the same manner [Boyle et al., 1992, Zhang et al., 2015, Agulló et al., 2019]. Nevertheless, PCB<sub>209</sub> can be transformed into PCB<sub>28</sub> through photo-induced dechlorination [Wong and Wong, 2006]. Thus, it is essential to distinguish between different congeners within the same contaminant class and to simulate the specific pathways for each, including their unique reactions and mechanisms. This approach ensures a more accurate understanding of their behavior and impact in the environment.

In addition to the vast number of pollutant classes and the numerous compounds they encompass, there are several other complexities in POPs research. In natural compartments, hydrophobic pollutants tend to bind to non-polar organic matrices such as particulate organic matter (POM), dissolved organic matter (DOM), and plastics [Schwarzenbach et al., 2016, Rodrigues et al., 2019, Cui et al., 2023]. The sorption of POPs to these matrices is influenced not only by the specific properties of each congener or type of chemical but also by various characteristics of the organic matter. These characteristics include the carbon content and origin, particle size, pH, salinity, ionic strength, chemical structure, density, and crystallinity of the matrix, as well as the polymer type (with different types of micro- and nanoplastics exhibiting different sorption rates) [Rodrigues et al., 2019, Cui et al., 2023, van Noort et al., 2003, Sobek et al., 2023]. This complexity introduces significant uncertainty into the available data and parameters required for model implementation.

Direct measurement of specific chemicals or congeners in the environment poses significant challenges. Congeners within the same pollutant class often exhibit similar and overlapping signals on analytical instruments such as GC-MS and LC-MS, making separation and accurate identification difficult. Additionally, these measurement processes are extremely costly.

Laboratory experiments on POPs in water also face various obstacles. Due to their hydrophobic nature, these experiments are typically conducted in polar solvents like alcohols (propanol, ethanol, methanol, etc.). Consequently, the results of such experiments may not be directly applicable to natural water conditions [Wong and Wong, 2006].

As POPs have a tendency to accumulate on OM, measuring concentrations on DOM can be a problematic issue - it is difficult to separate POPs in dissolved form from POPs sorbed to DOM [Garrido Reyes et al., 2021]. Understanding the distribution of hydrophobic chemicals on OM is crucial for estimating the overall fate of POPs in the marine environment. Pollutants such as PCBs and PBDEs have a significant fraction bound to DOM, which enhances the bioaccumulation of POPs in marine biota through consumption. However, with the knowledge of sorption coefficients, these processes can be effectively simulated using biogeochemical models [Daewel et al., 2020, Mikheeva et al., 2022].

### 1.1.2 *Current state-of-art for Pollution Models Development*

Although this approach is widely accepted in the scientific community, there is currently no high-resolution 3D model that comprehensively describes the detailed behavior of these contaminants in coastal and other marine environments. Most research in this field has relied on either box models or numerical models. Each of those approaches suits for different research questions and has its own advantages and disadvantages.

Box models were the first step in the development of POPs modelling. Originally, they were employed to estimate fluxes of POPs between different environmental compartments [Scheringer et al., 2004, Scheringer, 1996, Kong et al., 2014, Lamon et al., 2012, Webster et al., 2004], spatial distribution such as latitudinal zones [Scheringer et al., 2000, MacLeod et al., 2001], and generally to estimate areas of accumulation [Wania and Mackay, 1995]. This approach is simple but useful for those research purposes. Although the POPs model development made a huge leap forward, this approach is still widely used for making first estimations of the system response and comparison of its results to measurements [Wang et al., 2020].

Alongside box models, numerical modeling is another widely used approach, ranging from one-dimensional (1D) [Jurado et al., 2007] to three-dimensional (3D) models [Daewel et al., 2020, Ilyina et al., 2006, Alekseenko et al., 2018, Huang et al., 2007]. This method accounts for specific parameters of the simulated region, encompassing physical, chemical, and biogeochemical characteristics, depending on the model's design. Typically, these models are applied to either aquatic [Daewel et al., 2020, Ilyina et al., 2006, O'Driscoll et al., 2013] or atmospheric environments [Hansen et al., 2004, Huang et al., 2007, EMEP, 2024, Van Jaarsveld et al., 1997]. Spatially, they can vary from selected locations (1D models) [Jurado et al., 2007, Mikheeva et al., 2022] to local [Alekseenko et al., 2018], regional [O'Driscoll et al., 2013, Ilyina et al., 2006, Daewel et al., 2020, Van Jaarsveld et al., 1997], or global scales [Huang et al., 2007]. While these models demand significant computational resources, smaller domains are generally easier and faster to simulate. However, the computational demand strongly depends on the model's resolution.

The aforementioned studies primarily focus on the influence of environmental conditions on the fate and transport of POPs, considering factors such as hydrodynamic regimes [Jurado et al., 2007, O'Driscoll et al., 2013, Mikheeva et al., 2022], biogeochemical processes [Ilyina et al., 2006, Daewel et al., 2020], and the specific conditions required for long-range transport (LRT) [Huang et al., 2007]. Research on LRT has predominantly been applied to atmospheric global models, owing to the relative lack of studies in the aquatic environments in this area.

To investigate the distribution and accumulation of persistent pollutants, as well as their seasonality and the importance of various system factors, numerical modeling is an appropriate tool, especially for pollutants with long half-lives. However, the chemistry of POPs is often oversimplified in these models. Rather than accounting for congener-specific physical and chemical properties—which are essential for understanding the degradation and accumulation processes—these models typically group POPs into a single category or simplify their degradation patterns. This approach neglects the differing behaviors and impacts of various PCB congeners, thereby limiting the accuracy and comprehensiveness of the simulations. Typically, these pro-

cesses are deliberately neglected to conserve computational time.

Dynamic modeling of the transport and transformation of individual contaminants in coastal areas holds promise for estimating the global fate of POPs. However, existing state-of-the-art models have notable limitations that hinder their effectiveness in accurately capturing POP dynamics. Coastal environments are characterized by significant variability in hydrodynamic and biogeochemical conditions across various time scales. Additionally, these systems are influenced by benthic-pelagic feedback mechanisms, which involve frequent shifts between processes such as sedimentation and resuspension of organic matter [Daewel and Schrum, 2013]. These complexities present challenges for modeling POP behavior in coastal regions.

### 1.1.3 *Development of a Modeling Framework for This Study*

The numerical model, used in this study is designed to simulate the cycling of various classes of POPs within marine ecosystems. The introduction of this model was first published in 2022 [Mikheeva et al., 2022] and the results from that article are incorporated into the current study. This model integrates biogeochemical and physical processes occurring in the water column, as well as the coupling between benthic and pelagic environments, while considering the unique chemical characteristics of each POP species. Our aim is to investigate the influence of different processes within the water column on the behavior of each selected pollutant, accounting for their specific physicochemical properties.

To elucidate the dominant hydrodynamic effects on POP transformation, we conducted initial simulations using 1D model configurations. Four distinct hydrodynamically varied regions within the North Sea and the Baltic Sea were selected for these simulations. The North Sea sites exhibit tidal influences with varying depths and levels of biological productivity. The Gotland Basin, situated in the Baltic Sea, is characterized by strong stratification due to its considerable depth. Finally, the Bothnian Bay experiences advective mixing, particularly during seasons of ice cover. These seas, located in Northern Europe, have historically been associated with high levels of POP production [SC, 2019, Berdowski et al., 1997, McLachlan et al., 2018, Breivik et al., 2002]. Despite regulatory efforts such as those implemented by the Stockholm Convention to ban the production of these pollutants [SC, 2019], POPs persist in both marine environments and the atmosphere [EMEP, 2024].

The developed comprehensive dynamic model is designed to be versatile and capable of predicting the fate of all POPs, considering their individual characteristics. In this research, we focus on simulating the behavior of three major classes of POPs: polychlorinated biphenyls (PCBs), polybrominated biphenyl ethers (PBDEs), and per- and polyfluorinated substances (PFAS).

## 2 Chemical and scientific justification

### 2.1 Chosen pollutants

For the detailed study of the marine environmental fate, we decided to focus on 3 specific groups of industrial POPs: *Polychlorinated Biphenyls (PCB)*, *PolyBrominated Diphenyl Ethers (PBDE)* and *Per- and PolyFluoroAlkyl Substances (PFAS)*. These pollutants have been earmarked for elimination by the Stockholm Convention. While PCBs were among the initial POPs classified by the SC, PBDEs and PFAS fall under the category of "new POPs" as designated by the convention [SC, 2019].

Two of the chosen pollutant categories exhibit hydrophobic characteristics. Both PCBs and PBDEs demonstrate extremely low solubility in water. On the other hand, PFAS possess a surfactant nature—featuring one hydrophobic head and one water-soluble head. Consequently, apart from sharing physical properties with PCBs and PBDEs, PFAS possess unique attributes that influence their behavior in the water column. All these contaminant classes can exist in a freely dissolved state but exhibit a strong affinity for binding to organic carbon [Schwarzenbach et al., 2016, Mackay et al., 2006, Beyer and Biziuk, 2009].

In shelf waters, the concentration of recently released ("fresh") POPs tends to be higher compared to the open ocean, primarily due to their proximity to land-based sources. The absence of organic matter and degradation sources allows these chemicals to persist in the open ocean. Coastal waters serve as the initial phase of the journey for selected POPs from land to the open ocean [Hemond and Fechner, 2015, Mackay et al., 2006, Olenycz et al., 2015, Schwarzenbach et al., 2016]. A comprehensive understanding of their behavior in these regions is crucial for predicting their environmental fate under changing external conditions, such as variations in emissions and climate change.

The objective of this chapter is to provide a comprehensive overview of selected pollutants, outlining their primary characteristics, and rationalizing the choice of specific congeners for simulations and analysis.

#### 2.1.1 *Polychlorinated Biphenyls (PCB) and Polybrominated Diphenyl Ethers (PBDEs)*

Polychlorinated biphenyls (PCBs) and polybrominated diphenyl ethers (PBDEs) belong to the class of POPs. Despite being banned from production in most countries [SC, 2019], they persist in the environment due to their long half-life and legacy sources.

PCBs, along with other chlorinated pollutants such as dichlorodiphenyltrichloroethane (DDT) and aldrin, were among the first substances identified as toxic and persistent environmental contaminants [Fulton and Matthews, 1936]. These compounds are notable for their ability to accumulate within ecosystems, particularly within trophic levels of food webs. The large-scale production of PCBs commenced in the early 1930s [Markowitz, 2018]. During this period, PCBs were manufactured and marketed as industrial mixtures under the trade name Aroclor. These mixtures comprised various PCB congeners, each denoted by a specific numerical identifier reflecting the chlorine content by weight. For instance, Aroclor-1242, one of the most widely used

formulations, contains 42% chlorine by weight [Katsikantami et al., 2024].

Initially, PCBs were intended for use as dielectric fluids in transformers and capacitors due to their excellent insulating properties [Fulton and Matthews, 1936]. However, their application rapidly expanded to a broad array of industrial and commercial uses. PCBs were employed as fire retardants and incorporated into paints, varnishes, adhesives, lacquers, and transparent, moisture-resistant paper. Additionally, they served as heat transfer fluids, impregnation agents, plasticizers for a diverse range of products, and were even used in inks and chewing gum formulations [Markowitz, 2018].

Nowadays, main sources of banned PCBs release include improperly managed electronics and manufacturing landfills, illegal disposal of old PCB-containing transformer fluids, and leaks from such sources, as well as disposal of PCB-containing consumer products in non-hazardous waste landfills [Wolska et al., 2012]. Legislation

Polybrominated diphenyl ethers (PBDEs) were introduced approximately half a century after the inception of PCBs, specifically in the 1970s [Environment Agency, 2019]. These compounds are predominantly recognized for their efficacy as flame retardants. PBDEs have been extensively incorporated into a wide variety of consumer products, including electrical and electronic equipment, textiles, and polyurethane foams used in furniture [Environment Agency, 2019, EPA, 2009, Abbasi, 2015]. The primary function of PBDEs in these applications is to inhibit the ignition and slow the spread of fire, thereby enhancing the fire safety of these products. Simultaneously, research has demonstrated that decabromodiphenyl ether (decaBDE) can act as a precursor to other lower brominated congeners through various transformation processes [Pan et al., 2016, Zhao et al., 2015]. These processes include photolytic degradation, where exposure to light causes the breakdown of decaBDE, and biological degradation, where microorganisms metabolize decaBDE into less brominated forms. Consequently, decaBDE contributes to the formation of a range of polybrominated diphenyl ethers with differing degrees of bromination, which can exhibit distinct environmental behaviors and toxicological profiles [Schmitt et al., 2021, Environment Agency, 2019, Pan et al., 2016, Zhao et al., 2015, Abbasi, 2015].

Since the production of PBDEs has been banned in most countries, the primary source of these pollutants in aquatic environments has become unintentional. This unintentional release occurs primarily through leaching from discarded electronic devices and manufacturing waste in landfills. As a result, these persistent organic pollutants continue to pose significant risks to biological communities, perpetuating their presence and adverse effects in ecosystems despite the cessation of their production [IARC, 2016, Wolska et al., 2012, EPA, 2009]. Legislation

Both PCBs and PBDEs are hydrophobic contaminants with a strong tendency to bind to organic matter (OM) [Beyer and Biziuk, 2009, Mackay et al., 2006]. This behavior stems from their low water solubility and high affinity for organic carbon matrices [Schwarzenbach et al., 2016]. PCBs adsorbed on particulate organic matter (PCB<sub>POM</sub>) are transported downward due to the sinking velocity of particulate organic carbon (POC) particles, leading to their accumulation in sediments. Additionally, PCBs and PBDEs form strong bonds with dissolved organic matter [Schwarzenbach et al., 2016, ChemSpider, 2024, van Noort et al., 2003, Jonker and Smedes,

2000]. While this type of DOM does not sink, it remains in the dissolved phase and absorbs freely dissolved PCBs ( $PCB_{free}$ ) and PBDEs ( $PBDE_{free}$ ). Freely dissolved contaminants and those absorbed on DOM are readily available for direct biological uptake, as they can diffuse through cell membranes and bioconcentrate inside phytoplankton [Alava et al., 2018, Schwarzenbach et al., 2016]. PCBs and PBDEs attached to detritus are not directly available for diffusive bioconcentration due to particle size but can accumulate in higher trophic levels through feeding.

These processes are general for all PCBs and PBDEs, but specific properties of the pollutants determine their partitioning between all three phases ( $POP_{POM}$ ,  $POP_{DOM}$  and  $POP_{free}$ ). The ability of PCBs and PBDEs to bind to OM is described by the octanol-water partition coefficient  $K_{ow}$ . For PCBs  $\log K_{ow}$  varies from 4.46 ( $CB_1$ ) to 8.27 ( $PCB_{209}$ ) [ChemSpider, 2024, Zhou et al., 2005]. PBDEs exhibit a similar range, with  $\log K_{ow}$  values spanning from 4.34 ( $BDE_1$ ) to 9.87 ( $BDE_{209}$ ) [Bao et al., 2011]. Furthermore, variations in the chemical and physical properties of each congener result in distinct transport and degradation patterns, particularly in aquatic environments [Daewel et al., 2020, Ilyina et al., 2006].

Chlorinated biphenyls (CBs) consist of two directly linked to each other phenyl rings, with chlorine atoms, which may substitute hydrogen atoms in *ortho*, *meta*, and/or *para* positions (Figure 1). There exist a total of 209 congeners of CBs, and their properties are primarily dictated by their chemical structure [ChemSpider, 2024]. Notably, photodegradation predominantly affects higher chlorinated congeners, leading to subsequent dechlorination (loss of chlorine atoms under UV irradiation) [Pagni and Sigman, 1999, Wong and Wong, 2006]. Conversely, aerobic biological degradation necessitates a specific structure in the PCB molecule, with two chlorine-free carbon atoms positioned in *ortho* and *meta* positions on the same side of the benzene ring (Figure 1) [Borja et al., 2005, Boyle et al., 1992]. Without this arrangement, bacteria within the microbial community cannot cleave the carbon-carbon bond.

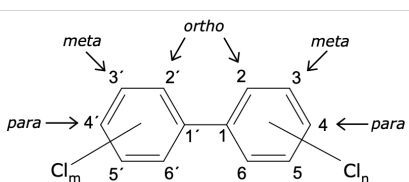


**Figure 1:** General chemical structure of chlorinated biphenyls (PCBs)

Polybrominated diphenyl ethers (PBDEs) represent another class of hydrophobic POPs, comprising 209 congeners [ChemSpider, 2024]. Widely used as flame retardants, PBDEs have been banned alongside PCBs under the SC [SC, 2019]. Despite this, PBDEs exhibit structural disparities from PCBs [ChemSpider, 2024]. Primarily, bromine atoms replace hydrogen atoms in the benzene rings. However, the most significant structural deviation lies in the linkage of benzene rings by an oxygen atom, rendering the structure more flexible. With bromine being larger than chlorine, the PBDE molecule may bend at certain positions in the ring to optimize bond energy, resulting in diverse structural configurations among BDE congeners — classified as planar and non-planar [ChemSpider, 2024]. These variations are crucial for energy transfer in photolytic processes or bacterial degradation [Zhang et al., 2013, Schwarzenbach et al., 2016]. Analogous

to PCBs, certain BDE congeners experience higher biodegradation and bioconcentration due to their structural features. Moreover, some BDE congeners can undergo transformation under photochemical processes into hydroxylated chemicals and furans (Figure 6), which exhibit greater toxicity, longer half-lives, and higher bioaccumulation factor (BCF) values than BDEs themselves.

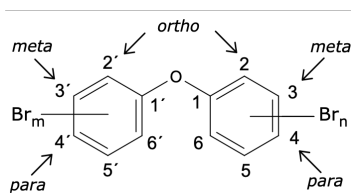


**Figure 2:** General structure of Polybrominated Biphenyl Ethers (PBDEs)

Finally, the atmospheric exchange is dictated by the Henry's law constant, a parameter highly contingent on the enthalpy and entropy of dissolution, which vary based on the chemical properties of each pollutant [Bamford et al., 2000].

In this study, two congeners from each class are under scrutiny—one with a higher degree of substitution and one with a lower degree. Research indicates that higher substituted congeners (HSC) exhibit greater persistence in aquatic environments and may even permeate to the deepest depths of the planet [Jamieson et al., 2017]. However, such congeners have been observed to undergo halogenation reduction under solar irradiation, a process known as photolytic dechlorination/debromination (e.g., for BDE, see Figure 6). Lower substituted congeners (LSC), on the other hand, tend to display lower resistance to biodegradation but are relatively less affected by photolytic processes.

For PCBs, considering the aforementioned factors, we selected the higher substituted congener PCB<sub>153</sub> and the lower substituted congener PCB<sub>28</sub> (Figure 3a). The hypothesis of transformation from PCB<sub>153</sub> to PCB<sub>28</sub> under sunlight activity opens the possibility of modeling the interlinkage between different pollutant fates under similar conditions.

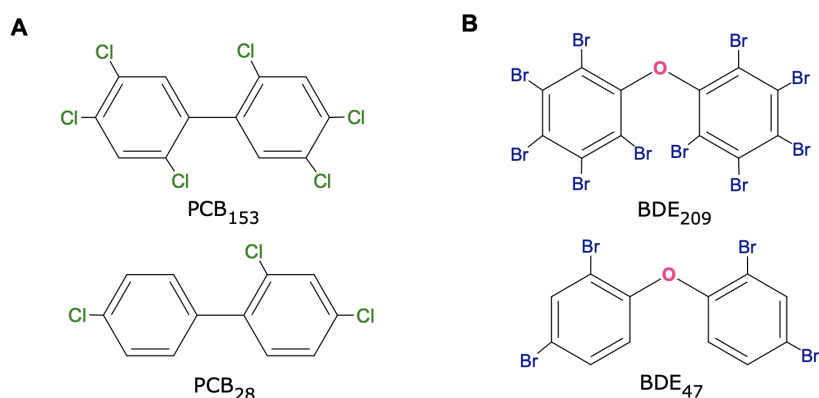


**Figure 3:** Chemical structure of chosen congeners as original (parent) pollutants from **a** - PCB class; **b** - PBDE class

In our selection of BDEs, we focused on HSC BDE<sub>209</sub> and LSC BDE<sub>47</sub> (Figure 3b). Alongside these, we incorporated the processes of hydroxylation of both BDEs to BDE-OH into the model. However, it's important to note that these latter two compounds are included in the model as by-products, and their fate was not explored in this particular study.

It is important to acknowledge the scarcity of available data for BDEs due to the high costs and complexities associated with measuring them in natural waters. Nevertheless, compared to PCBs, the chemistry of photolytic transformations of PBDEs has been subject to more detailed study [Pan et al., 2016, Zhao et al., 2015, Wang et al., 2018, Rayne et al., 2006, Roszko et al., 2015, Usenko et al., 2012, Yang and Chan, 2014, Schmitt et al., 2021]. Consequently, the model was initially applied to PCBs [Mikheeva et al., 2022]. Following the investigation of PCB processes in the marine environment under various hydrodynamic conditions using the developed model, we made the decision to test it on PBDEs and PFAS to explore other chemical processes and variations in their fate.

### 2.1.2 PFAS

PFAS, or Per- and Polyfluorinated Substances, represent another class of anthropogenic organic pollutants. One prominent compound within this group is PFOA (perfluorooctanoic acid), which, due to its persistence in the environment and its toxic and bioaccumulative properties, can also be categorized as a POP [SC, 2019].

Among the three selected groups of POPs, PFAS are particularly notable for several reasons. Although these chemicals were first discovered in the 1930s and began to be widely used in the 1950s [ITRC, 2020], they continue to be incorporated into a broad range of products despite their toxic and persistent nature. This can be attributed to the fact that significant environmental detection of PFAS did not occur until around the year 2000 [ITRC, 2020]. The extensive use of PFAS is primarily attributed to their exceptional chemical stability, which makes them highly effective in various applications. These applications include water and dirt-repellent coatings, food packaging, outdoor apparel, furniture, firefighting foams, aerosol propellants, and heat transfer fluids [Organisation for Economic Co-operation and Development (OECD), 2006, Gluege et al., 2020, Buck et al., 2011].

PFOA consists of a carboxyl group at one end and an aliphatic tail comprising seven carbon atoms with fluorine atoms replacing hydrogen atoms (Figure 4) [ChemSpider, 2024]. Its distinctive physico-chemical properties make it particularly interesting for comparison with the aforementioned POPs [ITRC, 2021]. Unlike PCBs and PBDEs, PFOA features not only a hydrophobic tail but also a hydrophilic part, enhancing its solubility in water. This characteristic confers upon PFOA a surfactant nature, significantly distinguishing its behavior from highly hydrophobic pollutants [ITRC, 2021].

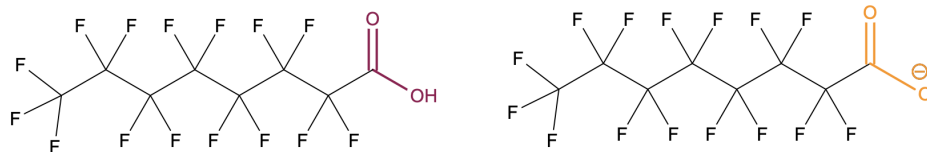


**Figure 4:** PFOA

In addition to the primary properties of PFOA, we delve into those most pertinent for modeling purposes. Firstly, the hydrophobic head of PFOA facilitates its accumulation on OM in a manner akin to PCBs and PBDEs [Fagbayigbo et al., 2021]. However, the other acidic head of this pollutant dissociates in the aquatic environment, enhancing its water solubility compared to PCBs and PBDEs [Fagbayigbo et al., 2021, ITRC, 2021]. This process significantly influences the diffusive atmospheric exchange of PFOA—once dissociated, it tends to remain in the aquatic phase rather than being released back into the atmosphere even under higher dissolved concentrations [ITRC, 2021].

The surfactant nature of PFOA defines several other crucial properties and behavioral patterns. Surfactants exhibit an affinity for accumulating at the interface between two fluids, a condition commonly found at the boundary between water and air in natural marine environments [ITRC, 2021, ITRC, 2020]. On one hand, this characteristic augments the concentration of PFOA in the near-surface water layer [Sha et al., 2022]. On the other hand, this fraction of PFOA is more susceptible to the effects of breaking waves [ITRC, 2021, Johansson et al., 2019]. Pollutants residing in the near-surface water layer can be readily removed through processes like sea salt aerosol and droplet formation [Sha et al., 2022, McMurdo et al., 2008, Johansson et al., 2019].

Another significant property of PFOA is its capacity to form micelles [ITRC, 2021]. When PFOA reaches a sufficient concentration, known as the micelle formation concentration (MFC), the molecules aggregate with their hydrophilic heads outward and hydrophobic heads inward (Figure 5). Consequently, this phenomenon enhances their solubility in water [ITRC, 2021].

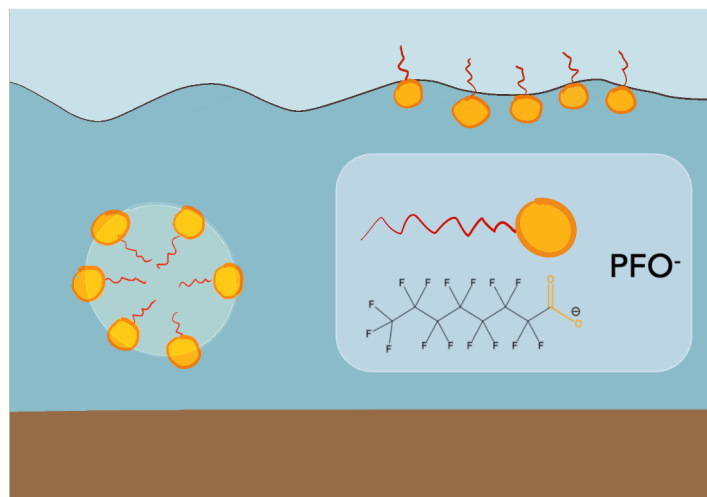


**Figure 5:** Micelle formation of PFOA in aquatic environment: in the water column under MFC and in the border between two fluids (air-water)

Like other POPs, PFOA is subject to solar radiation. Under this process, the hydrophobic fluorine-enriched head is degraded, leading to the transformation of PFOA into other substances.

## 2.2 Chemical processes

PCBs and PBDEs are hydrophobic POPs and share similar mechanisms of chemical transformation within environmental matrices. Conversely, PFAS function as surfactants, and their chemical properties dictate distinct behaviors in the marine environment compared to the other two classes of pollutants. Initially, we will examine the chemical processes common to PCBs and PBDEs.

This chapter serves to encapsulate and provide an overview of the chemical and biological processes pertinent to each of the selected pollutants, aiming to construct a clear depiction of their differences and similarities. It furnishes essential insights for comprehending the varied fates of different POPs in the marine environment, facilitating estimations of distribution pattern hotspots and elucidating their interactions with biota.

### 2.2.1 Photolytical processes

The persistent nature of POPs determines their long half-life and tendency to accumulate over time in various matrices, including sediment, water and living organisms. Nonetheless, two prominent factors shape the fate of these pollutants in the environment: sunlight and bacterial activity. These elements enable POPs to undergo transformations under specific conditions, gradually leading to their degradation over time. It's important to emphasize that these "degradation pathways" do not unfold rapidly; instead, they facilitate the gradual removal of pollutants

from the environment.

This chapter aims to delve into the influence of sunlight on POPs, particularly examining photolytic processes. Generally, most POP classes are impacted by the UV-B segment of the irradiation spectrum. When exposed to light within the range of 100-300 nm [Schwarzenbach et al., 2016, Eriksson et al., 2004, Pagni and Sigman, 1999, Wong and Wong, 2006, Pan et al., 2016, Zhao et al., 2015, Roszko et al., 2015, Giri et al., 2011], POPs absorb photon energy, leading to excitation and triggering various processes [Schwarzenbach et al., 2016, Calza and Vione, 2015]. These processes can vary among pollutant classes, their congeners, and the wavelengths emitted. Even persistent inert POP molecules can undergo transformation into other substances, contingent upon their congener structure and the surrounding water conditions.

In aquatic environments, photolysis unfolds through two primary pathways: *direct* and *indirect* [Schwarzenbach et al., 2016]. Direct photolysis involves photons directly exciting pollutant molecules. However, this pathway is subject to several limiting factors, including water extinction, irradiation intensity, pollutant concentration, and the quantum yield of each step [Schwarzenbach et al., 2016].

Indirect photolysis constitutes a multifaceted process wherein photon energy is transferred to other constituents within the system rather than directly to the pollutant molecule [Schwarzenbach et al., 2016]. In the aqueous environment, the primary species involved in indirect photolysis include dissolved organic matter (DOM),  $NO_3$ , and  $NO_2$  (hereafter referred to as ES - excited states) [Schwarzenbach et al., 2016, Bodrato and Vione, 2013]. Notably, indirect photolysis can generate radicals, which are atoms, molecules, or ions possessing at least one unpaired valence electron, within the aquatic environment. In the water column, transient species such as  $OH\cdot$ ,  $CO_3^{\cdot-}$ ,  $^1O_2$ , and the triplet states of chromophoric dissolved organic matter,  $^3CDOM^*$ , are present, playing a crucial role in the energy transfer of photoreactive species [Bodrato and Vione, 2013].

The energy received can either be transferred to pollutants or quenched by other biogeochemical species [Schwarzenbach et al., 2016]. Although the quenching process diminishes a considerable portion of the energy transmitted to POPs from ES, overall, this process holds significant importance [Bodrato and Vione, 2013, Schwarzenbach et al., 2016]. Firstly, the total concentration of ES surpasses that of POPs, resulting in a greater accumulation of photolytic fluxes within the system. Secondly, in heavily turbid waters where direct photolysis is improbable, the utilization of ES can still facilitate the transformation of POPs through indirect photolysis [Schwarzenbach et al., 2016].

When an POP molecule becomes excited, it can undergo various transformations. The direction of the photolytic reaction is influenced by the structural characteristics of each congener [Pagni and Sigman, 1999, Eriksson et al., 2004, Schwarzenbach et al., 2016]. Each specific congener within each class has a different molar attenuation coefficient ( $\epsilon$ ), which measures how strongly a chemical species absorbs and attenuates light at a given wavelength. As a general pattern, highly substituted pollutants from the PCB and PBDE classes are more likely to absorb more energy and undergo further changes in their chemical structure [Eriksson et al., 2004, Wong and

Wong, 2006].

The detailed description of the implemented processes concerning photolytic transformations is presented in Section 3.5.2. The current section focuses on various pathways of chemical transformation and the resulting compounds.

#### 1. *Dechlorination/debromination:*

The initial photolytic transformation observed in POPs involves sequential dehalogenation, a process evident in both PCBs [Pagni and Sigman, 1999, Wong and Wong, 2006] and PBDEs [Eriksson et al., 2004, Pan et al., 2016]. When higher substituted congeners absorb UV light, they enter an excited state (as depicted in Figure 6). The absorbed energy subsequently breaks the weakest halogen bonds within the structure, leading to the dispersion of residual energy throughout the phenyl structure. This results in the creation of a radical molecule with an unpaired valence electron on the carbon atom, capable of further halogen loss until it attains a stable congener form. Following a series of such transformations, PCB<sub>153</sub> (HSC) is transformed into PCB<sub>28</sub> (LSC) as outlined in [Wong and Wong, 2006]. The LSC molecule exhibits a lower propensity for photon absorption, with its quantum yield of dechlorination being insignificant, rendering it relatively unaffected by solar irradiation.

A similar transformational pathway is observed in the conversion of PBDEs [Eriksson et al., 2004, Wong and Wong, 2006]. Research by Pan et al [Pan et al., 2016] has established that HSC BDE<sub>209</sub> undergoes conversion into LSC BDE<sub>47</sub> through a comparable series of transformations (as illustrated in Figure 6). Consequently, the concentration of HSC decreases while the abundance of LSC in the system increases, both in the cases of PCBs and PBDEs. In the current study, photolytic dehalogenation contributes to the rising concentrations of LSC PCB<sub>28</sub> and BDE<sub>47</sub>.

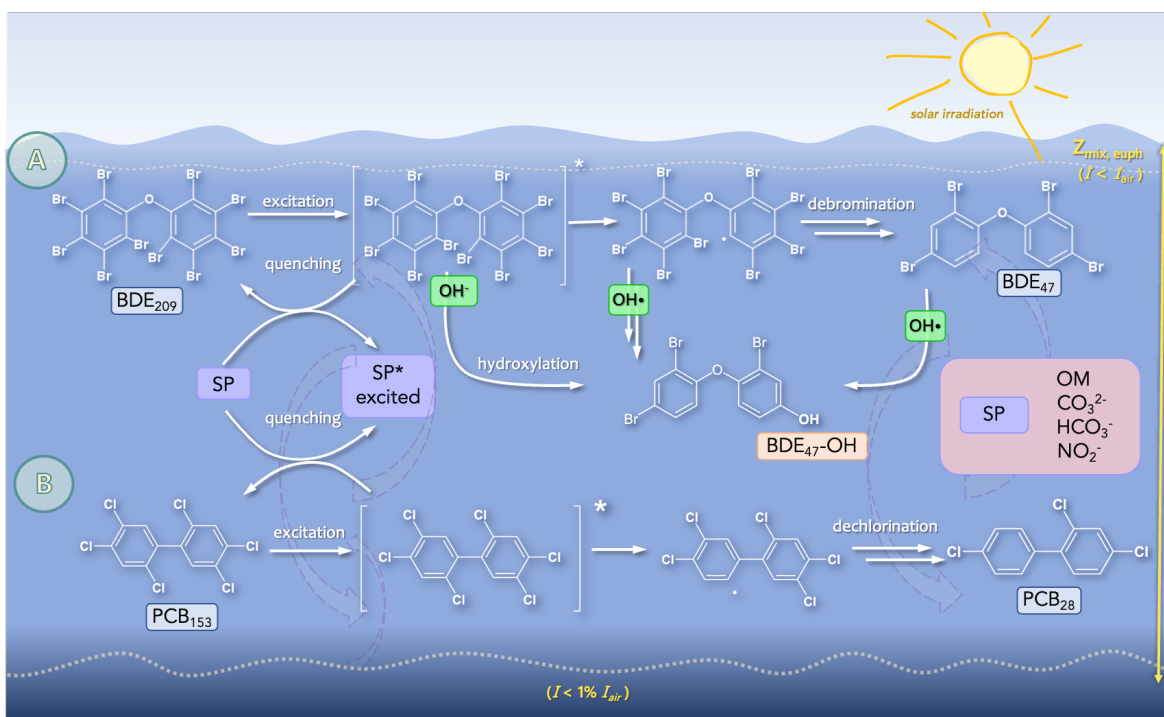


**Figure 6:** Main pathways of direct photolysis for PBDE (A) and PCB (B) in dissolved phase. An example of BDE<sub>209</sub> chemical transformations in surface waters.

## 2. Hydroxylation:

Hydroxylation, the second type of photolytic reaction, is observed in both PCB and PBDE pollutants [Zhao et al., 2015, Tehrani and Van Aken, 2014]. This process initiates with a similar excitation and radical formation as seen in the previous stage. However, the presence of hydroxyl radical OH is necessary, which is generated through indirect photolysis. Subsequently, in the ensuing phase of the reaction, both the molecule and hydroxyl radicals combine to produce a new category of pollutant - PCB-OH and PBDE-OH.

In the final product, the halogen atom positioned in the *ortho*-position to the carbon-oxygen bond is substituted by a hydroxyl group OH (refer to Figure 6). Although the concentration of the product is relatively low, its presence in the aquatic environment is crucial to acknowledge. These new products demonstrate high bioconcentration factors (BCF) and low LC50 values. Notably, PBDE-OH significantly impacts the development of early-stage larvae, leading to a considerable decrease in hatching, as evidenced in studies involving zebrafish [Usenko et al., 2012]. Additionally, it is important to highlight that these pollutants have never been industrially manufactured; their presence in aquatic environments solely arises from photolytic hydroxylation.

Consequently, PCB-OH and PBDE-OH are obtained as derivative products from this reaction. Both are included as side products in the current research.

### 3. Cyclisation:

Another potential pathway for phototransformation involves the production of furans. The chemical structure of PBDE exhibits greater flexibility compared to PCB due to the presence of an oxygen atom linking two phenyl rings [Wang et al., 2018]. This flexibility allows for the inclusion of larger bromine atoms in PBDE's structure, unlike the smaller chlorine atoms found in PCB [Wang et al., 2018, Rayne et al., 2006]. However, this flexibility also results in a wider range of possible products of photolysis [Eriksson et al., 2004].

In this process, a PBDE molecule in its radical form can detach another bromine in the *ortho* position close to the radical formation, leading to the formation of another cycle (refer to Figure 6). Although the quantum yield for this process tends to be low, similar to the previous case [Eriksson et al., 2004], the toxicity and bioconcentration factors (BCF) of furans exceed those of the parent pollutant as well as PBDE-OH [Fernandes and Falandysz, 2020].

#### 2.2.2 Photolysis of PFAS

PFAS, often dubbed "forever chemicals", are notorious for their extreme persistence in the environment. Few processes have demonstrated the ability to degrade or transform them. However, recent research suggests that, like PCBs and PBDEs, PFAS can undergo changes when exposed to UV light. Presently, there are two primary phototransformation pathways identified for PFAS.

One potential degradation pathway for PFOA, known as photolytic chain shortening, has been observed [Giri et al., 2011], [Xin et al., 2023]. This process predominantly occurs in the atmosphere but can also manifest in aquatic environments, albeit with a lower quantum yield. Through this pathway, the parent pollutant transforms into another PFAS compound with a shorter carbon chain. Additionally, PFOA can undergo defluorination, losing fluorine atoms from its structure under UV irradiation [Xin et al., 2023]. For PFOA, the ratio of these two reactions is approximately 50/50. In both cases, the concentration of the parent PFOA decreases in its original environment.

In this study, the transformation of PFOA is conceptualized as degradation without the production of daughter pollutants. This approach is adopted due to the complexity of simulating the specific pathways involved. Particularly relevant is the presence of iron, which plays a crucial role in simulating Fenton reactions [Schlesinger et al., 2022], leading to the production of hydroxyl radicals (OH•). These reactions significantly influence the direction of the photolytic degradation of PFOA. As a result, in this study, PFOA is impacted by UV irradiation, leading to a decrease in its concentration.

### 2.3 Biological degradation

As mentioned above, the interactions between POPs and living organisms are extremely complex and depend on a wide range of parameters. Biological degradation is no exception. This

process depends not only on the structure of the pollutant, but is also strongly determined by the type of bacterial community and the chemical composition of the environment, in particular the oxygen content [Borja et al., 2005]. In the presence of oxygen, some microbial communities are able to break the structure of POP molecules (oxidative degradation) [Schwarzenbach et al., 2016, Alava et al., 2018, Borja et al., 2005]. This process is controlled not only by the class of aerobic bacteria but also by the stereochemical structure of the POP molecule and its affinity for the exact type of enzyme [Borja et al., 2005]. Boyle et al. show in their study that for most aerobic bacteria the oxidative ring cleavage mechanism (ORCM) takes place [Boyle et al., 1992]. In this case, PCB degradation by the bphA enzyme is only possible if the PCB has no substitutional chlorine in both ortho and meta positions on the same side of a ring (e.g. PCB<sub>28</sub>) (Figure 7).

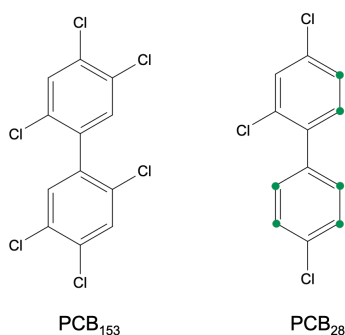


**Figure 7:** Availability of different PCBs chemical structure for aerobic biodegradation.

This means that aerobic bacterial degradation will have an effect on the concentration of such PCB congeners as PCB<sub>28</sub>. However, the congener PCB<sub>153</sub> chosen for the current simulations does not have a suitable structure for this process and aerobic biodegradation is not applicable in this case. However, in more recent study, Zhang and colleagues demonstrated that the cyanobacterium *Anabaena* PD-1 can degrade PCB<sub>153</sub>, at a lesser extent compared to PCB<sub>28</sub> [Zhang et al., 2015]. Hence, the model incorporates biological degradation for all POPs, with higher extent for LSCs.

At the same time, there is another process of biological transformation in the marine environment. This process can be called biological dehalogenation rather than degradation. Without the presence of oxygen, other microbial communities can also degrade PCBs, although by the completely different mechanism of reductive dechlorination [Borja et al., 2005]:



In this case, PCBs are transformed into a lower chlorinated pollutant, but remain in the environment. This pathway occurs mainly under anaerobic conditions, such as in sediments or hypoxic waters [Borja et al., 2005].

## 2.4 Research questions

Pollutants in aquatic environments have a profound impact on every level of the ecosystem, from phytoplankton to humans, causing irreversible damage. Anthropogenic activities contribute significantly to the accumulation of toxic pollutants, affecting not only water bodies but also other environmental matrices such as air and soil. In coastal areas, the constant interaction between these matrices facilitates the exchange, leakage, and deposition of pollutants within the water column. Furthermore, the high biological productivity and nutrient-rich conditions in coastal regions make these areas particularly susceptible to pollutant exposure.

The objective of this study is to develop a model designed to simulate the specific behavior of various POPs in coastal marine environments. The model introduced in this research can simulate the fate of several selected POPs within the marine ecosystem. It incorporates the hydrophysical properties of the chosen regions as well as the chemical and biogeochemical transformations of each pollutant. A significant feature of this model is its adaptability, allowing it to be integrated with any other hydrodynamic and biogeochemical host model.

Given that this model accounts for the major processes and transformations specific to each class of pollutants and their congeners, it was used as a tool to address three research questions. Recognizing the high complexity of the topic, we structured the research questions in a sequence that progressively increases in complexity, starting with more basic scenarios and advancing to most complex ones.

1. *How the specific chemical properties of each pollutant influence their distribution along the water column?*

POPs include chemical classes with hundreds of individual congeners, each exhibiting unique physicochemical properties. This study investigates how these properties influence the environmental fate of POPs. To isolate the effects of these properties from other factors influencing pollutant behavior in the water column, simulations were conducted under consistent conditions in the Gotland Basin of the Baltic Sea. This deep basin features detritus that absorbs POPs, removing a portion of these pollutants from the surface layer affected by atmospheric exchange and biological production. This setup allows for a focused examination of the differences in desorption processes from detritus and DOM that remain in the surface mixed layer. Additionally, the accumulation of POPs in the sediments provides insight into the distinct patterns of pollutant accumulation within the sediment pool.

As first research question, I examine the differences in behavior and accumulation patterns of five POPs from three distinct classes. Under identical conditions and with equal initial concentrations, each of the five pollutants exhibits unique speciation, resulting in distinct distributions between aquatic phases (dissolved, bound with DOM or sorbed on detritus). These differences lead to variations not only in spatial distribution but also in the seasonal hotspots of each POP.

2. *To what extent do the hydrodynamic conditions of the selected region impact the fate of various classes of persistent organic pollutants (POPs)?*

POPs are mostly emitted in populated areas from where they undergo LRT that leads to their global distribution. The coastal oceans are an important entry point of newly emitted POPs into the global cycle. A crucial parameter influencing the fate of POPs in coastal areas are hydrodynamic and biogeochemical processes. To address the research question on the fate of POPs in coastal oceans, we examined four locations in the North and Baltic Seas, each possessing distinct hydrodynamic characteristics.

Turbulent regimes and stratification can affect not only the physical mixing of pollutants but also the production of organic matter. This process is essential in understanding the fate of POPs, due to their high affinity for accumulation on both detritus and DOM. In regions impacted by sea ice formation, the presence of sea ice not only reduces organic matter production within the system but also restricts the exchange of pollutants between the water and the atmosphere. Finally, in the North Sea, we will consider all the aforementioned factors as well as the influence of tides, which can dramatically affect the entire ecosystem's behavior, including the distribution and accumulation of POPs.

### 3. *How does a change in nitrate concentration influence the fate of POPs in the aquatic environment?*

The investigated coastal oceans have been and are subject to heavy eutrophication, strongly impacting the biological activity in these regions. Thus, as third research question, we investigate the impact of nitrate ( $\text{NO}_3^-$ ) concentrations on biological production and the pathways of photolytic transformations of POPs. For this, we simulate the fate of POPs in the North and Baltic Seas under enhanced nitrate loads.

Elevated nitrate levels can lead to a notable increase in biological production, which in turn provides additional organic matter for the partitioning of POPs. Concurrently, nitrate plays a role in the indirect photolysis of POPs, potentially altering the photolytic pathways for specific pollutants such as brominated diphenyl ethers (BDEs). However, an increase in organic matter within the system also attenuates UV light in the water column, which is necessary for photolytic processes. These processes vary in intensity across different hydrodynamic regions, and the specific properties of each POP influence their preferred phase distribution under changing nitrate conditions. Consequently, these factors lead to differences in the concentrations of the five selected POPs between scenarios with enhanced nitrate levels and those with regular nitrate concentrations.

This work is aimed to address each of these research questions separately in detail.

## 3 Model description

### 3.1 General information

The model, introduced in this study, offers the capability to simulate the fate of several selected POPs in marine environments. It not only considers the hydrophysical properties of a given region but also incorporates the chemical-biogeochemical transformations of each pollutant. One of the key features of this model is its adaptability, as it can be implemented using any other hydrodynamic and ecosystem model.

The findings presented in this study encompass simulations of five different pollutants from three POP classes: two congeners from the PCB class, two congeners from the PBDE class, and PFOA from the PFAS class (see Figure 8). Specifically, for the PCB and PBDE classes, we selected one higher substituted congener (HSC) each - PCB<sub>153</sub> and BDE<sub>209</sub>. These chemicals exhibit very low water solubility and a high affinity for partitioning with organic matter. Moreover, they demonstrate a propensity for photolytic dechlorination [Pagni and Sigman, 1999, Wong and Wong, 2006] and are not readily available for aerobic bacterial degradation due to their structural characteristics. Alongside the HSCs, we simulated the fate of the lower substituted congeners (LSC) - PCB<sub>28</sub> and BDE<sub>47</sub>. While these chemicals also possess low water solubility and a high affinity for organic matter, they are considered relatively more stable for phototransformation but are susceptible to biological degradation.

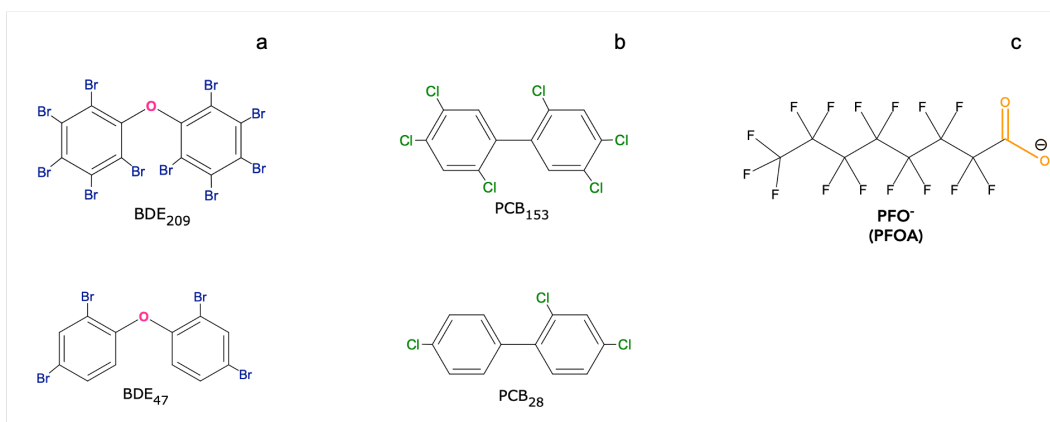


**Figure 8:** All modeled POPs: **a** - BDE class; **b** - PCB class; **c** - PFAS class.

Furthermore, the HSCs undergo transformation into LSCs through the processes of photolytic dechlorination and debromination. Consequently, a reduction in HSC concentration leads to an increase in LSC concentration within the water column.

The chosen PCBs are prevalent in the environment, and comprehensive data required for simulations are readily accessible. Conversely, PBDEs pose a greater challenge for measurement due to their complexity and expense, yet extensive research has been conducted on their chemical transformations in the environment [Roszko et al., 2015, Zhao et al., 2015, Pan et al., 2016]. For a detailed description of the selected pollutants, please refer to Section 2.

PFOA has been selected as an exemplar of POPs with a distinct set of properties owing to its unique structural characteristics. The rationale behind this selection has been extensively expounded upon in Section 2.

For this investigation, we utilize a coupled model system to simulate the transformation and distribution of pollutants within a marine environment. As a primary driver, we employ the 1D hydrodynamic ocean model GOTM [Burchard et al., 1999, Umlauf et al., 2024] (detailed in Section 3.2), in conjunction with the marine ecosystem model ECOSMO [Daewel and Schrum, 2013] (outlined in Section 3.3). The POPs chemistry module is integrated using the Framework for Aquatic Biogeochemical Models (FABM) [Bruggeman and Bolding, 2014] (explained in Sections 3.4 and 3.5) (see Figure 9). This model system operates within 1D water column–sediment setups, thus disregarding horizontal transport. The focus on 1D model setups allows us to isolate the primary structuring hydrodynamic (and consequent biogeochemical) first-order effects on POPs transformation, thereby mitigating the influence of horizontal advection and spatial differences in sources.

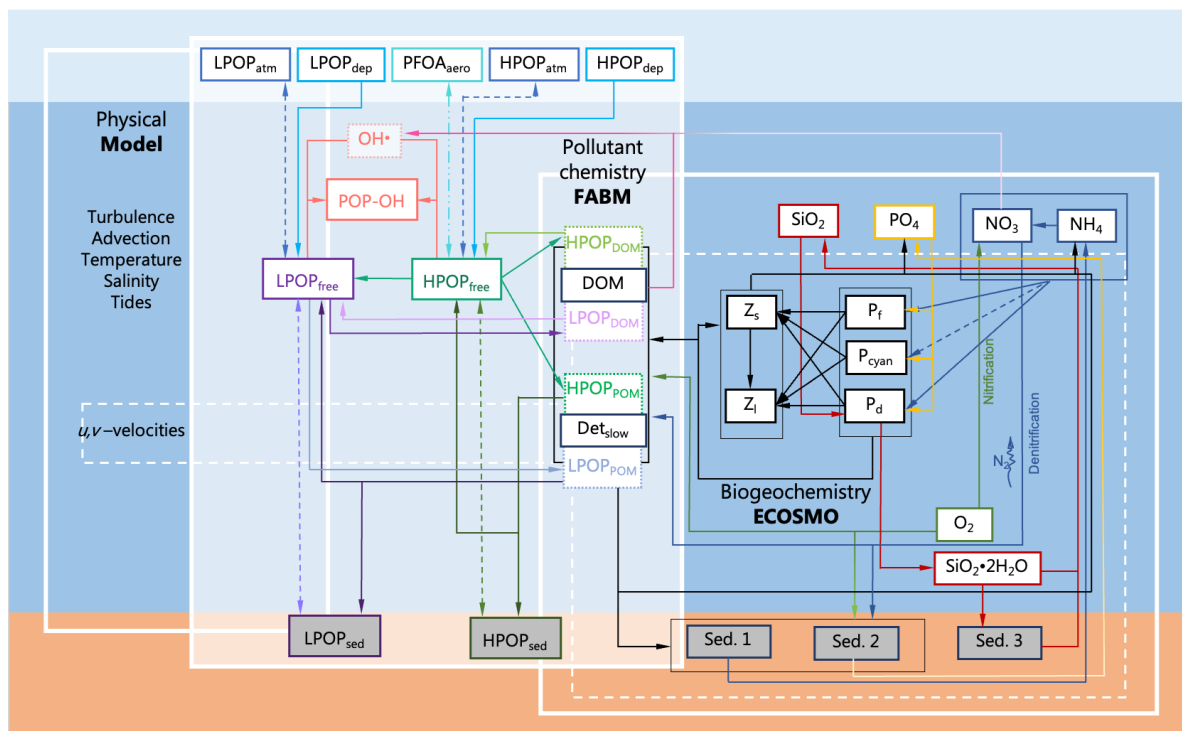


**Figure 9:** Overview of the couple model GOTM-ECOSMO-FABM with an emphasis on the flow between the different model compartments of ECOSMO. **HPOP** - highly substituted congener (PCB<sub>153</sub>, BDE<sub>209</sub>); **LPOP** - lower substituted congener (PCB<sub>28</sub>, BDE<sub>47</sub>). Dashed arrows represent diffusive exchange.

The estimation of the local change in the state variable  $C$  for POPs relies on prognostic equations generalized in equation 2. These equations encompass transport-related terms, comprising advection as the first term, turbulent mixing as the second term, and settling as the third term (as

discussed in section 3.2). Advection and turbulent mixing are computed by the hydrodynamic host model, GOTM, while POP settling is integrated into the POP module within the FABM framework.

The transformation term  $R_c$  encompasses all chemical processes of the POP, including partitioning, chemical reactions, and photolysis (as detailed in Section 3.5).

$$\frac{\delta C}{\delta t} = -\frac{\delta wC}{\delta z} + \frac{\delta}{\delta z}((\nu_t + \nu)\frac{\delta C}{\delta z}) - (w_d)\frac{\delta C}{\delta z} + R_c \quad (2)$$

$\nu$ ,  $\nu_t$  - molecular and turbulent diffusion coefficient;

$w_d$  - sinking velocity ( $1 \text{ m d}^{-1}$ ).

At the boundaries, the intercompartmental fluxes of POPs between the atmosphere and ocean at the surface, and between the ocean and sediment at the bottom, are computed within the POP module and treated as boundary conditions (as discussed in Section 3.6). Detailed descriptions of the transformation terms are provided in Section 3.5.

The presented POP model encompasses all pertinent processes necessary for determining the environmental fate of each selected pollutant under various physical and ecological conditions (refer to Figure 10). Within the water column, these processes include partitioning (Section 3.5.1), degradation, and chemical transformation (Sections 3.5.2 and 3.5.3). At the boundaries, the model accounts for air-sea exchange and sea ice interaction (Section 3.6.1), as well as sedimentation and resuspension (Section 3.6.2). Pollutants resuspended from sediment and those generated from HSCs are regarded as secondary sources of pollutants.

## 3.2 GOTM – The hydrodynamic host model

In this study, we opt to integrate the POP module with a one-dimensional water column model known as GOTM, as discussed earlier [Umlauf et al., 2024]. This model is capable of representing the relevant hydrodynamic and thermodynamic processes associated with vertical turbulent mixing in a 1D model setup [Burchard et al., 1999].

GOTM calculates the vertical turbulent exchange by considering shear and buoyancy production (as depicted in Equation 3) [Burchard et al., 1999, Umlauf et al., 2024].

$$\frac{\delta k}{\delta t} - \frac{\delta}{\delta z}(\nu_t \frac{\delta k}{\delta z}) = P + B - \epsilon \quad (3)$$

$k$  – turbulent kinetic energy;

$\nu_t$  – vertical turbulent diffusivity (eddy);

$P$  – shear production;

$B$  – buoyancy production;

$\epsilon$  – rate of dissipation.

Horizontal advection is integrated by utilizing prescribed salinity and temperature profiles, obtained either from real CTD data or from a three-dimensional hydrodynamic model. GOTM aligns the vertical structure with these prescribed profiles at each time step by employing a relaxation time, denoted as  $\tau_R(A)$ , where  $\tau_R(A) > 0$  (as outlined in Equation 4). The salinity and temperature profiles are sourced from World Ocean Atlas (WOA) data. Simulated profiles undergo relaxation towards the prescribed profiles to accommodate for disregarded horizontal advection and lateral sources. The salinity relaxation is implemented according to the following equation (Equation 4):

$$\frac{\delta A}{\delta t} = \frac{\delta}{\delta z} \left( (\nu_t + \nu) \frac{\delta A}{\delta z} \right) - \frac{1}{\tau_R} (A - A_m) \quad (4)$$

$\nu_t, \nu$  – turbulent and molecular diffusivities;

$\tau_R(A)$  – relaxation time scale;

$A$  – calculated tracer distribution;

$A_m$  – prescribed tracer profile.

The water circulation dynamics in the North and Baltic Seas exhibit distinct time scales, necessitating adjusted relaxation times for the salinity ( $S$ ) and temperature ( $T$ ) profiles to mimic advection simulations by nudging the model towards observed  $S$  and  $T$  data. Salinity profiles are integrated into the model with two distinct relaxation times: 86400 s for the North Sea and 432000 s for the Baltic Sea, as detailed in Table 1. Meanwhile, temperature profiles are incorporated without relaxation.

The vertical grid resolution encompasses both near-surface ( $d_u$ ) and bottom ( $d_b$ ) layers. Consequently, the thickness of the near-surface and bottom layers decreases by up to 10 cm.

**Table 1:** GOTM Specification for current simulations (a,b,c,d – locations of setups on Figure 12)

	Unit	Value	Comment
<i>General</i>			
Turbulence model		second-order model	
TKE method		dynamic equation ( $k$ -epsilon)	
Bottom roughness	(m)	0.03	The North and Baltic Seas
Spin-up	(year)	10	Accumulation of pollutants in sediment reaches equilibrium in 10 years
Calculation time steps	(s)	1800	
Relaxation (Temperature)	(s)	-	The North and Baltic Seas
Zooming factors ( $d_u$ and $d_l$ )	-	1.5;1.0	The North and Baltic Seas
<i>The North Sea</i>			
Number of layers (the North Sea)	-	110; 63	The North Sea (c,d)
Relaxation (Salinity)	(s)	86400	The North Sea
M2 Tidal Amplitude	(m)	0.41; 0.7	The North Sea (c,d)
S2 Tidal Amplitude	(m)	0.16; 0.25	The North Sea (c,d)
M2 Tidal Period	(s)	44714	The North Sea
S2 Tidal Period	(s)	43200	The North Sea
<i>The Baltic Sea</i>			
Number of layers (the Baltic Sea)	-	90; 125	The Baltic Sea (a,b)
Relaxation (Salinity)	(s)	432000	The Baltic Sea

Given that the simulations were conducted in 1D, horizontal transport and movement were disregarded. However, the vertical alterations of the sea surface elevation (SSE) during tidal activity significantly impact the turbulence within the water column. Tides in the North Sea play a crucial role in the turbulent dynamics of the system and are thus accounted for in our study. To enhance the resolution of the modelled tides beyond the observations provided by the TPXO9 atlas (1/30° resolution) [Egbert and Erofeeva, 2002], we have incorporated the two primary harmonics: the solar ( $S2$ ) and lunar ( $M2$ ) semi-diurnal tides. Comprehensive specifications

of GOTM are outlined in Table 1. On the other hand, tides in the Baltic Sea are relatively minor, and tidal turbulence is feeble; hence, tides are disregarded in the Baltic Sea setups.

### 3.3 ECOSMO

ECOSMO is a multicompartment complex biogeochemical numerical model that encompasses multiple compartments, including nutrients, phytoplankton, zooplankton, detritus (POM), and dissolved organic matter (DOM) [Daewel and Schrum, 2013]. The model resolves nutrient cycling and incorporates two key types of non-living organic matter, POM and DOM, which are integral to the chemical module. Additionally, it incorporates five biological functional groups, consisting of three phytoplankton and two zooplankton state variables (see Figure 9).

POM or detritus in marine environments encompasses various labile, non-living organic particles. In ECOSMO, the source terms for POM include mortality components of phytoplankton and zooplankton ( $MORT_{BIO}$ ), which decrease POM concentration. POM concentration further decreases due to temperature-dependent remineralization ( $REMIN_{POM}$ ) and feeding by zooplankton ( $FEEDING_{z-POM}$ ) [Daewel and Schrum, 2013]. The concentration of POM in ECOSMO is calculated based on following equation:

$$\frac{d[POM]}{dt} = (1 - \alpha_{DOM})MORT_{BIO} - REMIN_{POM} - FEEDING_{z-POM} \quad (5)$$

The processes mentioned above are considered for all species of plankton, including microzooplankton, mesozooplankton, and three classes of phytoplankton (flagellates, diatoms, and cyanobacteria) (see Figure 9) [Daewel and Schrum, 2013].

DOM represents the concentration of all types of labile dissolved organic matter. The DOM pool increases due to phytoplankton and zooplankton mortality and decreases as a result of remineralization [Daewel and Schrum, 2013]:

$$\frac{d[DOM]}{dt} = \alpha_{DOM}MORT_{BIO} - REMIN_{DOM} \quad (6)$$

### 3.4 Model coupling, initial and boundary conditions

The hydrodynamic module (GOTM), biogeochemical module (ECOSMO), and chemical module (POP model) are interconnected through FABM. FABM enables the smooth integration of biogeochemical processes, regardless of the hydrodynamic host model. Moreover, FABM facilitates the transfer of state variables between the host model and any number of client models.

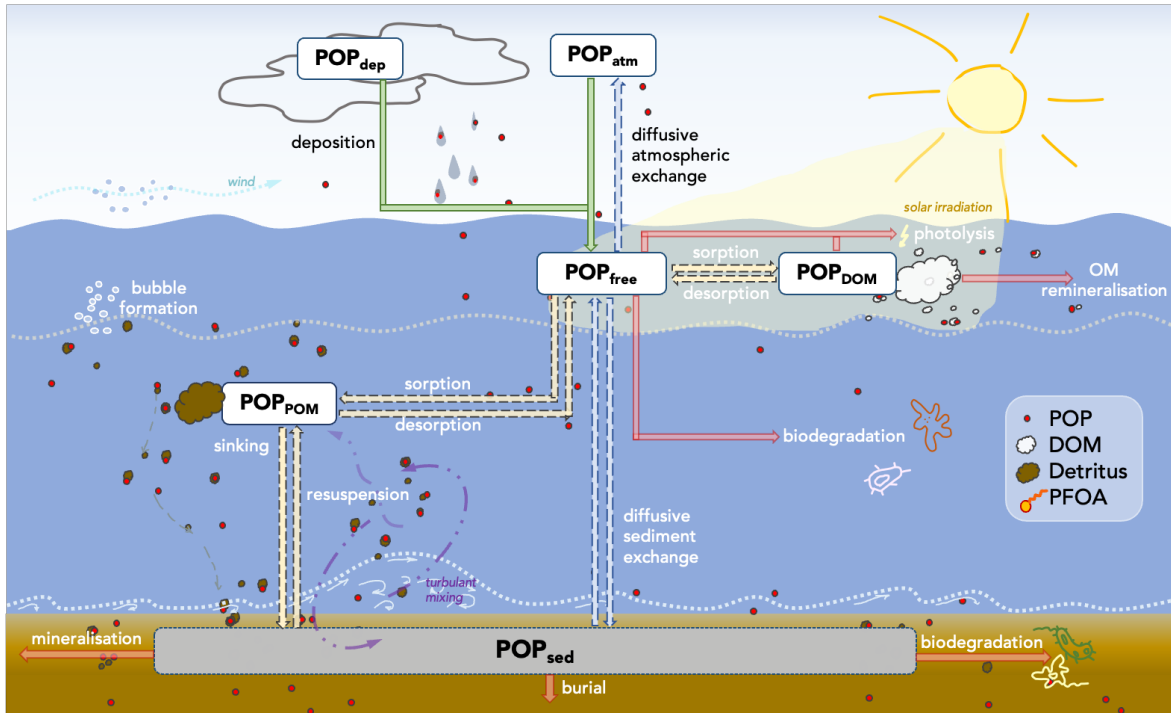


**Figure 10:** Main processes of PCB<sub>153</sub> transformation in current model. Arrows: green – input; yellow – phase transformation; blue - diffusive exchange; red – removing of pollutants from the system.

All processes implemented in FABM (Figure 10) are categorized as either external or internal. External processes involve interactions with the atmosphere, sediment, and related compartments (such as atmospheric PCB concentrations, ice concentration, and wind speed). Internal processes account for transformations of POPs within the water column, including the kinetic sorption of each pollutant onto organic matter (both DOM and POM) and degradation processes (photolytic and biological). Ultimately, these processes collectively determine the concentration of POPs in the dissolved phase ( $POP_{free}$ ). As a result, our model is capable of pinpointing areas with heightened concentrations of POPs and capturing the seasonal variations in these regions. This capability is crucial because it identifies locations where organisms are at an increased risk of absorbing these harmful pollutants.

The initial conditions for each simulated pollutant in the water column are initialized as zero ( $POP_{free}$ ,  $POP_{DOM}$ , and  $POP_{POM}$ ), and the model is allowed to run until establish an equilibrium.

For PFOA, the model incorporates a process involving surface layer formation and exchange between seas salt aerosols (SSA) and  $PFOA_{free}$  fractions (Figure 11).

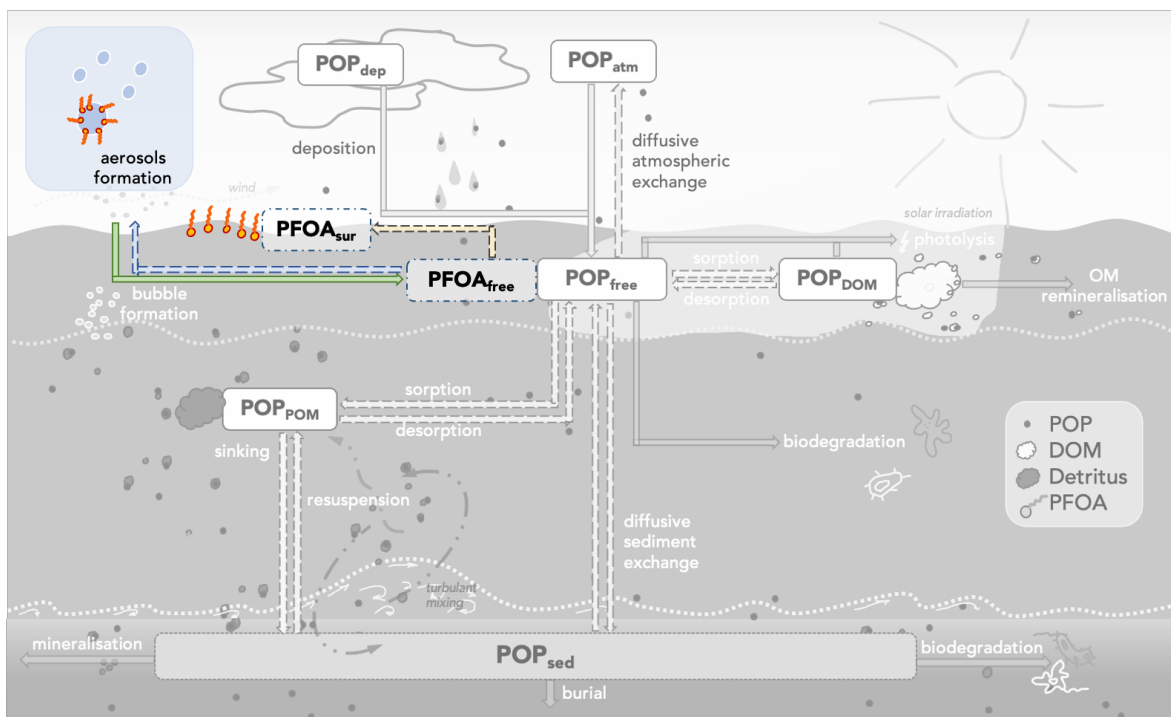


Figure 11: Extra processes of PFOA implemented to the model.

## 3.5 Chemical model

### 3.5.1 Particle partitioning (kinetic sorption)

The inherent chemical structure of hydrophobic POPs predisposes them to exhibit a stronger attraction towards organic carbon matrices in comparison to water. When organic matter is present, these pollutants have an affinity to accumulate on it rather than staying dissolved. In the model, this phenomenon is accounted for through a simplified partitioning mechanism that considers only non-living organic matter (DOM and POM). Sorption to living matrices is neglected in this context, as it involves complex biological processes including accumulation, concentration, and magnification, which fall outside the scope of the present research.

The sorption of POPs onto organic matter is typically quantified by the organic carbon-water partitioning coefficient,  $K_{oc}$ . This coefficient is intricately linked to the chemical makeup of both the pollutants and the absorbing matrix [ChemSpider, 2024, Mackay et al., 2006, Zhou et al., 2005]. Determining  $K_{oc}$  entails detailed knowledge of the chemical composition of each involved compartment, rendering it a challenging task for modeling purposes. However, linear free energy relationships (LFERs) offer a solution by allowing the estimation of  $K_{oc}$  based on the octanol-water coefficient,  $K_{ow}$ .  $K_{ow}$  measurements are relatively more straightforward to obtain and are available for various pollutants in scientific literature [ChemSpider, 2024, Schwarzenbach et al., 2016, Zhou et al., 2005]. For different PCB congeners,  $\log K_{ow}$  ranges from 4.46 (CB<sub>1</sub>) to 8.18 (PCB<sub>209</sub>) [ChemSpider, 2024], a spectrum that significantly influences their partitioning affinity.

In this study, instead of relying on an equilibrium coefficient ( $K_{oc}$ ), we employ the concept of sorption rates ( $k_{sorp}$  and  $k_{desorp}$ ). The concentration of pollutants bound to particulate organic matter ( $POP_{POM}$ ) is calculated using the following equation (Equation 7):

$$\frac{d[POP_{POM}]}{dt} = -(k_{desorp1} + k_{rem1})[POP_{POM}] - (k_{bur} + k_{sed})[POP_{POM}] + k_{sorp1}[POM][POP_{free}] + k_{resusp}[POP_{sed}] \quad (7)$$

Parameters for kinetic sorption ( $k_{sorp1}$ ) are derived from  $K_{oc}$  and  $k_{desorp1}$ , following the method described by Noort et al. and Jonker & Smedes [Jonker and Smedes, 2000, van Noort et al., 2003], or taken from sources [Yan et al., 2016, Fagbayigbo et al., 2021] (refer to Table 2). The rate constants for desorption ( $k_{desorp1}$ ) are sourced from [van Noort et al., 2003] as slow desorption constants, or estimated from sorption constants (if sorption rates were available, instead of desorption).

**Table 2:** Rate constants describing process of PCB<sub>153</sub> sorption on organic matrices.

	PCB <sub>153</sub>	PCB <sub>28</sub>	BDE <sub>209</sub>	BDE <sub>47</sub>	PFOA
POM	0.01064 <sup>2</sup>	0.0095 <sup>1 2</sup>	0.012 <sup>1 3</sup>	0.0086 <sup>3</sup>	0.0024 <sup>4</sup>
DOM	0.007 <sup>1</sup>	0.015 <sup>1</sup>	0.008 <sup>1</sup>	0.015 <sup>1</sup>	0.0026 <sup>1</sup>

<sup>1</sup>Estimated

<sup>2</sup> Calculated from Van Noort et al. [van Noort et al., 2003]

<sup>3</sup> Calculated or estimated from Yan et al. [Yan et al., 2016]

<sup>4</sup> Calculated from Fagbayigbo et al. [Fagbayigbo et al., 2021]

$k_{rem1}(T)$  dictates the process of detritus remineralization, enabling POPs bound to POM to be released back into dissolved form. This parameter is computed in ECOSMO using the following Equation 8 [Daewel and Schrum, 2013]:

$$k_{rem1} = 2 \cdot 10^{-8} \left( 1 + 20 \left( \frac{T^2}{132 + T^2} \right) \right) \quad (8)$$

Another type of organic matter that serves as a reservoir for pollutants in this model system is DOM. Due to the challenges associated with measuring this phase, limited studies on the interactions of POPs with DOM are available in the literature [Lechtenfeld, 2012, Hemond and Fechner, 2015, Kos Durjava et al., 2007, Mackay et al., 2006, Schwarzenbach et al., 2016]. DOM particles are significantly smaller in size compared to POM, resulting in a larger reactive surface area [Pan et al., 2016]. Consequently, DOM serves as an efficient matrix for the absorption of hydrophobic pollutants.

The processes governing sorption to DOM mirror those for POM, albeit at different rates:

$$\frac{d[POP_{DOM}]}{dt} = -k_{desorp2}[POP_{DOM}] + k_{sorp2}[DOM][POP_{free}] - k_{rem2}[POP_{DOM}] \quad (9)$$

However, in the model, DOM is generated through the life cycle of biota, remains in a floating state, and does not accumulate in sediment. As a result, there is no direct exchange between the compartment of  $POP_{DOM}$  concentration and the sediment storage of pollutants, explaining the absence of the last component in Equation 9.

The parameters  $k_{sorp}$  and  $k_{desorp}$  utilized in this context were either directly sourced or derived from existing literature on DOM-related processes [Schwarzenbach et al., 2016, Hemond and Fechner, 2015, Zhou et al., 2005, Jonker and Smedes, 2000, Lechtenfeld, 2012, Kos Durjaya et al., 2007, Pan et al., 2016], as outlined in Table 2.

$k_{rem2}$ , representing DOM remineralization, is computed within ECOSMO and is temperature-dependent [Daewel and Schrum, 2013]:

$$k_{rem2} = 2 \cdot 10^{-7} \left( 1 + 20 \left( \frac{T^2}{13^2 + T^2} \right) \right) \quad (10)$$

### 3.5.2 Photolytic degradation

The chemical composition of each congener within the PCB and PBDE classes plays a crucial role in determining their susceptibility to photochemical alterations. PCBs and PBDEs with higher degrees of chlorination or a planar configuration of phenyl rings are more likely to directly absorb UV light [Pagni and Sigman, 1999, Wong and Wong, 2006]. For instance, PCB<sub>153</sub>, containing 6 chlorine atoms, is particularly prone to photolytic processes.

The intricate nature of photochemical transformation processes and the relative importance of specific photolytic degradation pathways remain topics of ongoing debate within the scientific community [Pan et al., 2016, Zhao et al., 2015, Calza and Vione, 2015, Roszko et al., 2015].

During direct photolysis, photons directly transfer energy to the POP molecule, initiating a stepwise process of dechlorination [Pagni and Sigman, 1999]. This process systematically removes halogen atoms at each stage, leading to the transformation of PCBs and BDEs with higher degrees of chlorination into those with fewer chlorination levels due to photon attacks. Wong and Wong [Wong and Wong, 2006, Roszko et al., 2015] demonstrated that the pattern of photolytic dehalogenation remains consistent across each step, albeit with varying quantum yields. As higher chlorinated congeners, like PCB<sub>153</sub> and BDE<sub>209</sub>, undergo degradation, LSCs such as PCB<sub>28</sub> and BDE<sub>47</sub>, become more prevalent. It's worth noting that while Wong and Wong's experiment was conducted in alcohol solvents, in an aqueous environment, hydroxybiphenyls (PCB-OH) can form from PCBs [Pagni and Sigman, 1999]. However, because of the limited availability of data, our study concentrates exclusively on the degradation of the initial POPs, considering only the degradation product BDE-OH and not PCB-OH.

In this study, we utilize a hybrid approach, incorporating methodologies proposed by Schwarzenbach [Schwarzenbach et al., 2016] and Vione [Calza and Vione, 2015] for direct photolysis analysis. We derive a parameter for the kinetic rate of degradation of the targeted POP by considering factors such as photon flux ( $F_{POP}$ ) and the quantum yield of the reaction ( $Q$ ).

$$k_{photo} = Q \cdot F_{POP} \quad (11)$$

The photon flux absorbed by a pollutant is calculated from the irradiance across various wavelengths within the UV spectrum (Equation 12):

$$F_{POP} = E_{QF} \cdot \left[ \frac{\epsilon(\lambda)[POP_{free}]}{EXT_{TOT}} \right] \quad (12)$$

$E_{QF}$  – photon flux [ $\mu\text{mol}/(\text{m}^2\text{s}) = \mu\text{E}$ ];

$\epsilon$  – extinction coefficient for specific POP [ $\text{m}^2/\text{mol}$ ];

$EXT_{TOT}$  – total extinction, includes marine water, DOM, detritus and phytoplankton [ $\text{m}^2/\text{mol}$ ].

where  $E_{QF}$  represents photon flux (in  $\mu\text{mol}/(\text{m}^2\text{s})$ ), calculated according to equation 13:

$$E_{QF} = \frac{N_p}{N_A \cdot 10^{-6}} = \frac{I[\text{Js}^{-1}\text{m}^{-2}] \cdot \lambda \cdot 10^{-9}[\text{ms}]}{h[\text{Js}] \cdot c[\text{ms}^{-1}] \cdot L[\text{mol}^{-1}] \cdot 10^{-6}} = \lambda I 0.836 \cdot 10^{-2} [\mu\text{molm}^{-2}\text{s}^{-1}] \quad (13)$$

$N_p$  – the number of photons per second and surface unit [ $\text{m}^{-2}\text{s}^{-1}$ ];

$\lambda$  – wavelength [ $\text{nm}$ ];

$I$  – sunlight irradiance in UV range of spectrum [ $\text{W m}^{-2}$ ];

$h$  – Plank constant [ $\text{J s}$ ];

$c$  – speed of light [ $\text{m s}^{-1}$ ];

$L$  – Avogadro number =  $6.022 \cdot 10^{23}$  [ $\text{mol}^{-1}$ ].

The relevant fraction of available UV irradiance is computed to account for light penetration into the water column, which diminishes with increasing depth. This calculation employs 5nm wavelength bins to facilitate the incorporation of wavelength-dependent attenuation coefficients.

The extinction coefficients ( $\epsilon$ ) of different pollutants tend to vary and are typically dependent on wavelength. Unfortunately, there is limited research available to determine these measurements for individual substances in aqueous solutions. To address this challenge, our study incorporates distinct  $\epsilon$  values for each of the five pollutants under investigation. For PBDEs, we adopt values that are dependent on wavelength as outlined in [Eriksson et al., 2004]. However, due to the scarcity of data regarding the extinction coefficients of PCBs and PFOA, our simulations for these pollutants feature a wavelength-independent  $\epsilon$  parameter. Nonetheless, it's worth noting that this model is designed to be adaptable to various hydrophobic POPs. Implementation of photolysis with extinction coefficients dependent on wavelength can be realized with the necessary data.

The photon flux not only affects POP molecules directly but can also impact other particles in the water column, exciting them and providing energy. These particles then become a new energy source that can be transferred to the POP molecule, a phenomenon known as indirect photolysis [Schwarzenbach et al., 2016]. This process is more complex than direct photolysis and requires additional research and data from the scientific community to be fully understood and implemented.

In our investigation, we have introduced the approach of Bodrato & Vione [Bodrato and Vione, 2013] to incorporate the indirect method of  $OH\cdot$  radical formation in surface water, alongside direct photolysis. The formation of  $OH\cdot$  radicals resulting from  $NO_3^-$  and  $DOM$  excitation processes was implemented based on the relevant compartments of ECOSMO. The photon flux for each of these processes was determined using the following equations:

$$P^{NO_3^-} = 10d^{-1} \int_{\lambda} P^{tot}(\lambda) \cdot 100 \cdot \epsilon_{NO_3^-}(\lambda) \cdot [NO_3^-] [A_{tot}(\lambda)]^{-1} d\lambda \quad (14)$$

$$P^{DOM} = 10d^{-1} \int_{\lambda} P^{tot}(\lambda) \cdot A_{DOM}(\lambda) \cdot [A_{tot}(\lambda)]^{-1} d\lambda \quad (15)$$

The formation rate of  $OH\cdot$  radicals by photoactive specie DOM has been determined through Equation 16.

$$R_{OH}^{DOM} = 3.0 \cdot 10^{-5} \cdot P^{DOM} \quad (16)$$

and for  $NO_3^-$  through Equation 17:

$$R_{OH}^{NO_3^-} = 4.3 \cdot 10^{-2} \cdot \frac{[IC] + 0.0075}{2.25[IC] + 0.0075} \cdot P^{NO_3^-} \quad (17)$$

Here the total  $OH\cdot$  formation rate is presented as the sum of the two equations above.

$$R_{OH}^{tot} = R_{OH}^{NO_3^-} + R_{OH}^{DOM} \quad (18)$$

Freshly formed  $OH\cdot$  radicals can react with both surface water pollutants and scavengers. In the natural water environment, the scavenging rate constant of  $OH\cdot$  by present scavengers is:

$$\sum_i k_{Si} [Si] = 5 \cdot 10^4 [NPOC] + 8.5 \cdot 10^6 [HCO_3^-] + 3.9 \cdot 10^8 [CO_3^{2-}] + 1.0 \cdot 10^{10} [NO_2^-] \quad (19)$$

$\sum_i k_{Si} [Si]$  – scavenging rate constant, presented as a sum of all scavengers in the aquatic system ;  
 $[NPOC]$  – Non-Purgeable Organic Carbon (in case of ECOSMO is considered to be total organic carbon content);  
 $[HCO_3^-]$  – concentration of bicarbonate anion ;  
 $[CO_3^{2-}]$  – concentration of carbonate anion;  
 $[NO_2^-]$  – concentration of nitrite anion.

As a result, the reaction rate between POP and OH radical was calculated using the following expression:

$$k_{POP}^{OH} = R_{OH}^{tot} \frac{k_{OH} \cdot [POP_{free}]}{k_{OH} \cdot [POP_{free}] + \sum_i k_{Si}[Si]} \quad (20)$$

The generated  $OH\cdot$  radicals react with POPs and depending on the quantum yield of the reaction and environmental conditions, either a dehalogenation or hydroxylation product is formed.

### 3.5.3 Biological degradation

Incorporating biological degradation into the model necessitates not only data on various bacterial communities and their concentrations in the water column, but also insights into the bioavailability of POPs. However, the specific mechanisms governing these processes remain hypothetical, as the kinetic and thermodynamic parameters are yet to be determined. Moreover, the current version of the ECOSMO biogeochemical model does not explicitly account for bacterial communities, requiring simplifications in the model implementation.

To address these challenges, we have introduced a generalized process of biodegradation, devoid of specificity regarding bacterial communities. Instead, we parameterize this process based on remineralization rates (Equation 21):

$$k_{bio} = K_{BIO} (2 \cdot 10^{-8} (1 + 20 (\frac{T^2}{13^2 + T^2})) (10[DOM] + [POM])) \quad (21)$$

$T$  - temperature [K];

$K_{BIO}$  - parameterisation coefficient [-].

Finally, a biological degradation rate in sediments is implemented as a constant for all POPs and equal to  $3.935 \cdot 10^{-10} \text{ s}^{-1}$  [Davis, 2004] (Table 4).

### 3.5.4 Freely dissolved POPs

All POPs not bound to organic matter exist in a freely dissolved state within the water column, denoted as  $POP_{free}$  (Equation 22). The concentration of POPs in this phase is influenced by all relevant processes, including sorption-desorption and remineralization from non-living organic matter, as well as photolytic and biological degradation. Furthermore, the concentration of  $POP_{free}$  undergoes continual changes due to atmospheric influx (first term) and diffusive exchange with the sediment (last two terms).

$$\begin{aligned} \frac{d[HPOP_{free}]}{dt} = & + \frac{F_d}{dz} - (k_{sorp1}[POM] + k_{sorp2}[DOM])[HPOP_{free}] \\ & + (k_{desorp1} + k_{rem1})[HPOP_{POM}] + (k_{desorp2} + k_{rem2})[HPOP_{DOM}] \\ & - (k_{photo} + k_{POP}^{OH} + k_{bio})[HPOP_{free}] - k_{diff2}[HPOP_{free}] + k_{diff1}[HPOP_{sed}] \end{aligned} \quad (22)$$

$$\begin{aligned} \frac{d[LPOP_{free}]}{dt} = & + \frac{F_d}{dz} - (k_{sorp1}[POM] + k_{sorp2}[DOM])[LPOP_{free}] \\ & + (k_{desorp1} + k_{rem1})[LPOP_{POM}] + (k_{desorp2} + k_{rem2})[LPOP_{DOM}] \quad (23) \\ & + k_{photo}[LPOP_{free}] - (k_{POP}^{OH} + k_{bio})[LPOP_{free}] \\ & - k_{diff2}[LPOP_{free}] + k_{diff1}[LPOP_{sed}] \end{aligned}$$

$$\frac{d[OH-POP_{free}]}{dt} = + \frac{F_d}{dz} + (k_{POP}^{OH}([LPOP_{free}] + HPOP_{free})) \quad (24)$$

*HPOP* - higher substituted congener (PCB<sub>153</sub>, BDE<sub>209</sub>) or PFOA;

*LPOP* - lower substituted congener (PCB<sub>28</sub>, BDE<sub>47</sub>);

*OH-POP* - derivative hydroxylated POP (BDE<sub>47</sub>-OH);

$F_d/dz$  - atmospheric flux of pollutants (detailed description is below (Section 2.6.1));

$k_{diff(1,2)}$  - rates of PCB<sub>153</sub> diffusive exchange with dissolved in water pollutants (detailed description is below (Section 2.6.2)).

The fraction of POP<sub>free</sub> is particularly significant because it is highly susceptible to degradation processes such as photolysis and biodegradation. Additionally, it is more prone to bioaccumulation compared to POPs bound to organic matter.

## 3.6 Boundary forcing and external processes

### 3.6.1 Air-sea exchange

Since horizontal transport is not included in the model, the exchange of POPs with the atmosphere stands as the sole source of these contaminants in the water column. Our model accounts for both diffusive exchange with the atmosphere and the deposition of particulate pollutants. Deposition involves the influx of POPs onto insoluble particles like elemental carbon and organic aerosols. Upon reaching the surface waters, these contaminants augment the pool of POP<sub>free</sub>. The atmospheric concentration and deposition fields utilized in our model are sourced from the EMEP database [EMEP, 2024] and other publications [Degrendele et al., 2018, Paragot et al., 2020].

The influx of POPs from the atmosphere is influenced by various factors beyond just atmospheric concentrations and deposition. Ice cover, surface wind speed, temperature, and the dissolved POP<sub>free</sub> fraction all play crucial roles in shaping this process. In case of PFOA, this list is extended by salinity of surface water layer.

The net direction of the air-sea flux for hydrophobic substances such as POPs depends on the concentration gradient between the liquid and gaseous phases. To determine the net diffusive flux ( $F_d$ ) of hydrophobic substances like POPs between air and water, we adopt a mixed approach proposed by Friedmann and Selin [Friedman and Selin, 2016] and Odabasi [Odabasi, 2008]. This method relies on factors such as the Henry constant, the mass transfer coefficient, and the concentrations in both air and water (Equation 25).

$$\frac{d[C_{atm}]}{dt} = F_d = \frac{(\frac{C_a}{H} - [POP_{free}])}{\frac{1}{k_w} + \frac{1}{(Hk_a)}} = \frac{(C_a - [POP_{free}]H)}{\frac{1}{(k_wH)} + \frac{1}{k_a}} \quad (25)$$

$k_a$  – mass transfer coefficient in air [m/s];

$k_w$  – mass transfer coefficient in water [m/s];

$C_a$  – POP concentration in air [pg/m<sup>3</sup>];

$POP_{free}$  – POP concentration in water [pg/m<sup>3</sup>].

Here  $H$  is the temperature dependent constant for POP according to Henry's law. This parameter is implemented in the model by the equation 26 (Table 3):

$$H = \exp\left(\frac{-\Delta H}{RT} + \frac{\Delta S}{R}\right) \quad (26)$$

$\Delta H$  – enthalpy of dissolution [J mol<sup>-1</sup>];

$\Delta S$  – entropy of dissolution [J mol<sup>-1</sup> K<sup>-1</sup>];

$R$  – gas constant [J K<sup>-1</sup> mol<sup>-1</sup>];

$T$  – temperature [K].

Following the Odabasi concept, these parameters were calculated based on wind speed and specific diffusivity. The wind speed data for the current simulations are taken from the ECMWF ERA5 dataset (0.25°/hour resolution).

$$k_w = \left[ \frac{(0.24u_{10}^2 + 0.061u_{10})}{3600} \right] \left[ \frac{Dw_i}{Dw_{CO_2}} \right] \quad (27)$$

$$k_a = [0.2u_{10} + 0.3] \left[ \frac{Da_i}{Da_{H_2O}} \right] \quad (28)$$

$u_{10}$  – wind speed at 10 m above a water [m/s];

$D_{wi}$  and  $D_{ai}$  – diffusivities of POP in the air and water [cm<sup>2</sup>/s];

$Dw_{CO_2}$  – CO<sub>2</sub> diffusivities in the water [cm<sup>2</sup>/s];

$Da_{H_2O}$  – H<sub>2</sub>O diffusivities in the air [cm<sup>2</sup>/s].

**Table 3:** Parameters, used in calculations of air-water exchange

Parameter ( <i>units</i> )	<i>BDE</i> <sub>209</sub>	<i>BDE</i> <sub>47</sub>	<i>PCB</i> <sub>153</sub>	<i>PCB</i> <sub>28</sub>	<i>PFOA</i>	Source
<i>MW</i> <sub>air</sub> (g/mol)	28.97	28.97	28.97	28.97	28.97	Calculated
<i>MW</i> <sub>POP</sub> (g/mol)	959.17	485.79	360.88	257.54	414.07	[ChemSpider, 2024]
<i>MV</i> <sub>air</sub> (cm <sup>3</sup> /mol)	20.1	20.1	20.1	20.1	20.1	Calculated
<i>MV</i> <sub>POP</sub> (cm <sup>3</sup> /mol)	321.9	224.8	226.4	190.6	237.3	[ChemSpider, 2024]
<i>H</i> <sub>2</sub> <i>O</i> (cm <sup>2</sup> /s)	0.0089	0.0089	0.0089	0.0089	0.0089	[Schwarzenbach et al., 2016]
<i>D</i> <sub>aH<sub>2</sub>O</sub> (cm <sup>2</sup> /s)	0.3	0.3	0.3	0.3	0.3	[Schwarzenbach et al., 2016]
<i>D</i> <sub>wCO<sub>2</sub></sub> (cm <sup>2</sup> /s)	0.00002	0.00002	0.00002	0.00002	0.00002	[Schwarzenbach et al., 2016]
$\Delta H$ (J mol <sup>-1</sup> )	82600	62000	66100	32500	46800	[Bamford et al., 2000]
$\Delta S$ (J mol <sup>-1</sup> K <sup>-1</sup> )	120	130	190	74	143	[Bamford et al., 2000]

These parameters were taken from Schwarzenbach [Schwarzenbach et al., 2016] as constants (Table 3), while  $D_{wi}$  and  $D_{ai}$  were calculated using the following equations 29, 30. [Odabasi, 2008]:

$$D_{ai} = \frac{T \cdot 10^{-3} \left[ \frac{1}{MW_{air}} + \frac{1}{(MW_{POP} \cdot 10^3)} \right]^{0.5}}{P(V_{air}^{0.33} + V_{POP}^{0.33})^2} \quad (29)$$

$$D_{wi} = \frac{13.26 \cdot 10^{-5}}{P(100\nu_{H_2O})^{1.14} \cdot V_{POP}^{0.589}} \quad (30)$$

$MW_{air}$ ,  $MW_{POP}$  – molar weight of an air and chosen POP [g/mol];

$V_{air}$ ,  $V_{POP}$  – molar volume of an air and chosen POP [cm<sup>3</sup>/mol];

$P$  – air pressure [atm];

$\nu_{H_2O}$  – kinematic viscosity (at 25 °C) [cm<sup>2</sup>/s].

In the case of PFOA, the calculation of atmospheric exchange differs due to its immediate dissociation upon entering the water column, resulting in minimal diffusive exchange. Consequently, all parameters are applied to PFO<sup>-</sup> rather than PFOA. Enthalpy and entropy of vaporization data for this substance were unavailable to the authors. However, another crucial process representing atmospheric exchange of PFOA is the formation of sea salt aerosol (SSA). The parameterization approach for this process was synthesized from studies by Neumann et al. [Neumann et al., 2016], Gong [Gong, 2003], and Sha [Sha et al., 2022]. The total exchange of PFOA with the atmosphere is determined by Equation 31.

$$\frac{d[C_{PFOatm}]}{dt} = F_{ap} = PFOA_{dep} - \frac{MW_{PFO} \cdot EF \cdot [PFO_{free}] \cdot Sal}{35 \cdot [Na^+] \cdot L} \cdot Fr_{80} \quad (31)$$

$MW_{PFO}$  – molar weight of PFO<sup>-</sup> [g/mol];

$EF$  – enrichment factor [-];

$[PFO_{free}]$  – concentration of PFOA in water [pg/m<sup>3</sup>];

$Sal$  – salinity [g/kg];

$[Na^+]$  – concentration of sodium in water at surface layer [ $pg/m^3$ ].

$L$  – Avogadro Number [ $mol^{-1}$ ];

$Fr_{80}$  represent number of particle flux per second and depends on particle size  $r_{80}$  and wind speed  $u_{10}$ :

$$Fr_{80} = 3.84 \cdot 10^{-6} \cdot u_{10}^{3.41} \cdot 3.576 \cdot 10^5 \cdot r_{80}^{-A} (1 + 0.057 \cdot r_{80}^{3.45}) \cdot 10^{1.607 \cdot e^{-B^2}} \quad (32)$$

$$A = 4.7 \cdot (1 + 30 \cdot r_{80})^{-0.017 \cdot r_{80}^{-1.44}} \quad (33)$$

$$B = (0.433 - \log(r_{80}))/0.433 \quad (34)$$

The presence of surface water ice not only affects the availability of incoming atmospheric pollutants but also influences the overall distribution patterns of POPs. Our current simulations take into account the fraction of ice coverage, obtained from ECOSMO simulations [Daewel and Schrum, 2013]. ECOSMO provides a partial exchange of sea ice cover scaled by  $(1 - A_i)$ , where  $A_i$  represents the sea ice compactness, i.e., the fraction of the cell covered by sea ice. Additionally, the atmospheric flux and SSA formation are adjusted according to Equation 35, where  $F_{ow}$  denotes the flux over open water.

$$F = (1 - A_i) \cdot F_{ow} \quad (35)$$

Furthermore, the UV irradiation in the water column has been also adjusted to account for the presence of sea ice.

### 3.6.2 Sedimentation, resuspension and burial

The sedimentation process is primarily governed by the sinking of particles. In our simulations, the sinking of POP on particles is accounted for by assigning a constant sinking velocity of 1  $m/d$  [Daewel and Schrum, 2013]. It's important to note that  $POP_{DOM}$  and free dissolved contaminants do not undergo sedimentation. Therefore, sinking velocities are only considered for POP associated with POM.

In our model, the quantity of POPs stored in sediments is influenced by various processes, including direct sedimentation, diffusive exchange with the water column, degradation, and burial.

The concentration of POP in the sediment is represented in the model as:

$$\frac{d[POP_{sed}]}{dt} = -(k_{bur} + k_{deg} + k_{rem3})[POP_{sed}] - k_{diff1}[POP_{sed}] - k_{resusp}[POP_{sed}] + k_{diff2}[POP_{free}] + k_{sed}[POP_{POM}] \quad (36)$$

$k_{bur}$  – burial rate of POP (equal for a POM burial rate in ECOSMO);

$k_{deg}$  – rate constant of pollutant degradation in sediments;

$k_{diff(1,2)}$  – rates of POP diffusive exchange with dissolved in water pollutants;

$k_{resusp}$  – resuspension rate (bottom shear stress depended);  
 $k_{sed}$  – sedimentation rate of POP<sub>POM</sub>;  
 $POP_{POM}$  – concentration of POP on POM [ $\mu\text{g}/\text{m}^3$ ];  
 $POP_{free}$  – dissolved in water POP [ $\mu\text{g}/\text{m}^3$ ];  
 $k_{rem3}$  – rate of sediment remineralisation.

Rate of sediment remineralisation is calculated as:

$$k_{rem3} = 2 \cdot 10^{-8} \exp(temp_C \cdot T) \quad (37)$$

$temp_C$  – temperature control factor [ $^{\circ}\text{C}^{-1}$ ];  
 $T$  – temperature [ $^{\circ}\text{C}$ ].

**Table 4:** Rate constants, used in modelling of POPs sedimentation

	$k_{bur} \cdot 10^{-9} \text{ (s}^{-1}\text{)}$	$k_{diff} \cdot 10^{-10} \text{ (s}^{-1}\text{)}$	$k_{deg} \cdot 10^{-10} \text{ (s}^{-1}\text{)}$	$k_{ex} \cdot 10^{-5} \text{ (s}^{-1}\text{)}^*$
Sediment POP	1.157 <sup>1</sup>	(1) 0.139 <sup>2</sup>	3.935 <sup>2</sup>	28.935 <sup>1</sup>
POP <sub>free</sub>	–	(2) 4.05 <sup>2</sup>	–	–
POP <sub>POM</sub>	–	–	–	4.051 <sup>1</sup>

\* exchange rate constants:  $k_{resusp}$  for POP<sub>sed</sub> and  $k_{sed}$  for POP<sub>POM</sub>

<sup>1</sup> ECOSMO [Daewel and Schrum, 2013]

<sup>2</sup> Jay A. Davis SETAC [Davis, 2004]

Finally, resuspension is triggered when the friction velocity near the bottom exceeds a critical velocity (Equation 38). The friction velocity ( $u_*^b$ ) is simulated in GOTM, while the critical velocity ( $u_{cr}^b$ ) is set to  $0.07 \text{ ms}^{-1}$  (Equation 39).

$$u_*^b > u_{cr}^b \quad (38)$$

$$u_*^b = r \sqrt{U_1^2 + V_1^2} \quad (39)$$

$U_1, V_1$  – components of mean velocity at the centre of the lowest cell.

### 3.7 Regional Characteristics for Model Implementation

To investigate the influence of hydrodynamic and biogeochemical features on the transformation and mixing processes of persistent organic pollutants in the water column, a column model was applied to four hydrodynamically distinct sites. These simulations depicted conditions in various locations within the North Sea and the Baltic Sea, employing the hydrodynamic column model framework GOTM [Umlauf et al., 2024]. To elucidate the influence of hydrodynamics and biogeochemistry on the destiny of POPs, the water column model was initialized and

subjected to realistic water depths, initial tidal conditions, and atmospheric forcing tailored to each selected region (Figure 12). Detailed specifications of the model and the parameterization for these regions are provided in Section 2.2.

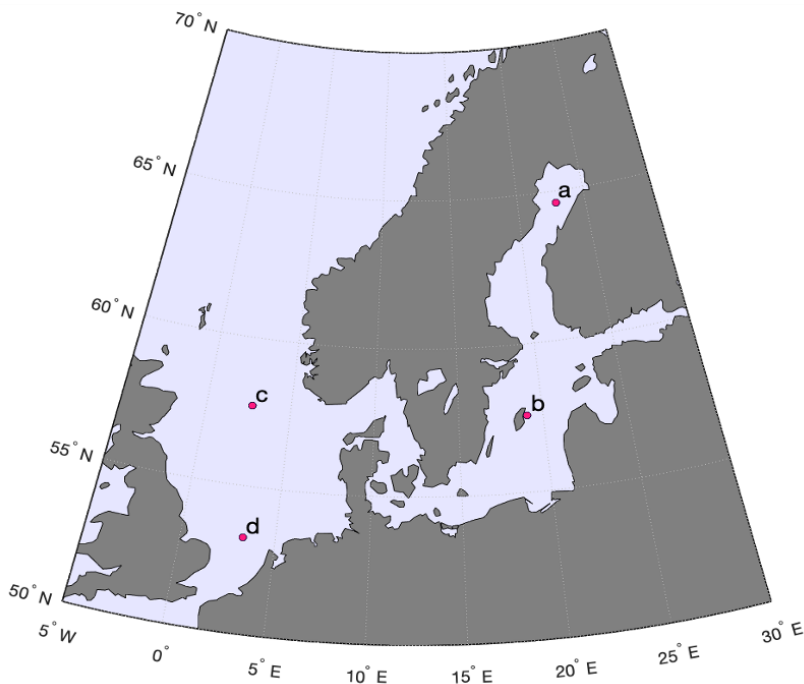


**Figure 12:** The map of chosen locations for a model runs: **a,b** – the Baltic Sea; **c,d** – the North Sea.

The North and Baltic Seas are situated in the European region, surrounded by some of the largest European countries characterized by high levels of industrial production [Lohmann et al., 2007]. Due to the high population density and the proximity of numerous countries, not only those with direct access to the shores of these seas but also those located within the catchment area, this region has experienced significant contamination. Historically, high levels of POP emissions have heavily exposed this region to pollution [Breivik et al., 2002, Breivik et al., 2007, Lohmann et al., 2007]. The high biological productivity of these seas makes them particularly vulnerable to POP exposure [Daewel et al., 2020]. Additionally, the semi-enclosed nature of the Baltic Sea results in the prolonged retention of POPs, limiting their dispersion through long-range transport (LRT).

The choice of these regions as study areas stems from their significant pollutant loads [Breivik et al., 2002] and notable variations in hydrodynamic, meteorological, and biological conditions [Van Leeuwen et al., 2015, Szymczycha et al., 2019, Savchuk and Wulff, 2009]. Moreover, the high primary production in these areas poses a substantial risk of bioaccumulation, raising concerns about food safety [Daewel et al., 2020].

The Baltic Sea, characterized by relatively low salinity levels, is a semi-enclosed water body. This salinity profile arises from the influx of rivers into the sea and its limited exchange with

the open sea, solely through the North Sea [Placke et al., 2021]. Consequently, the Baltic Sea has received high inputs of POPs from terrestrial sources over the past century, with minimal exchange with the open sea. Due to the persistent nature of POPs, they tend to accumulate within this marine environment.

For model simulations in the Baltic Sea, two sites were selected. The first site, denoted as region **b** in Figure 12, lies in the central Baltic Sea. This region is known as the Gotland Basin. Area **b** features brackish water and is characterized by a stable two-layer stratified system: a fresh surface layer and a deeper, more saline layer, often oxygen-depleted [Lehmann et al., 2022, Rodhe et al., 2010]. The surface layer in location **b** experiences thermocline formation during winter and summer, occasionally forming sea ice during severe winters. In contrast, the deeper layer undergoes minimal seasonal changes. The second chosen location aims to capture conditions in the northernmost region of the Baltic Sea, the Bothnian Bay (region **a** in Figure 12). This area is distinguished by nearly freshwater conditions and regular seasonal ice cover lasting several months [Rodhe et al., 2010].

The North Sea's dynamics are significantly shaped by tidal activity, resulting in distinctive regional characteristics. Corresponding to the bathymetry, the North Sea encompasses various areas with distinct mixing regimes: seasonally stratified (Figure 12c), permanently mixed (Figure 12d), and permanently stratified [Van Leeuwen et al., 2015, Zhao et al., 2019]. These characteristics reflect different configurations of surface and bottom mixed layers (SML and BML).

In this study, we focus on two regions where the SML and BML either merge during winter but remain separate in summer (Figure 12c) or constantly overlap (Figure 12d). The northern region, situated in the central-northern part (region **c** in Figure 12), is characterized by seasonal stratification [Van Leeuwen et al., 2015]. This area, with a depth of 110 meters, experiences tides with an M2 amplitude of 0.41 meters and S2 amplitude of 0.16 meters [Egbert and Erofeeva, 2002, NAO, 2024]. Additionally, it is influenced by the North Atlantic inflow, exhibiting lower nutrient content and biological production compared to the southern part [Daewel and Schrum, 2013].

Conversely, the southern part (region **d** in Figure 12) is a shallow area with a depth of 41 meters, strongly affected by tidal forces [Van Leeuwen et al., 2015]. In this region, M2 amplitudes can peak at 0.7 meters, and S2 amplitudes at 0.25 meters [Egbert and Erofeeva, 2002]. These conditions foster high turbulence, leading to continuous mixing and resuspension, thereby maintaining a mixed water column throughout the year [Van Leeuwen et al., 2015]. The warm mixed water and nutrient-rich environment in this area promote high primary production [Zhao et al., 2019].

## 4 Results and Discussion

All of the stated research questions address the major parameters that determine the final fate of POPs in the marine environment. In the first chapter, we examine in detail how specific chemical properties shape the behaviour of each POP in the water column. Additionally, we consider the importance of their byproducts from photolytic processes and the hazardous characteristics of each chemical.

The second chapter focuses on the importance of the biological parameters of the system on the outcome of POPs' fate. In detail, we examine the pattern of the past and observe how a change in just one parameter influences not only the distribution and accumulation pattern of parent POPs but also shapes the direction of the photolytic pathway.

The final chapter addresses the hydrophysical specifications of the system and their influence on the distribution of POPs. Although the biological pump plays a vital role in the fate of POPs, hydrophysical specifications can also have a significant effect. This section examines how different hydrodynamic regimes shape the overall outcome of POPs. In particular, we compare five regions and investigate the influence of tidal activity, stratification, and sea ice on both atmospheric inflow and the final area of accumulation of POPs.

All simulations were conducted using 1D setups, with results presented in Figures 14 - 41. These figures can generally be categorized into three types: atmospheric flux plots, water column concentration plots, and sediment concentration plots. The X-axis across these plots typically represents a timeline, which can vary from months (e.g., Figure 17, where each letter denotes a specific month) to years (Figure 14).

To introduce the 1D simulation results, Figure 13 is presented as an example. The first type of plot illustrates the exchange between the atmosphere and the water surface. As this graph represents flux, it shows the amount of pollutant crossing the boundary between water and air per second ( $\mu\text{g m}^{-2} \text{s}^{-1}$ ). The information in this plot indicates the quantity of pollutants entering the water column from the atmosphere. This process generally comprises two components, with deposition being a constant and one-directional flux from the atmosphere to the water (Figure 13a). However, other processes, such as diffusive exchange and the formation of sea salt aerosols (SSA), can cause an opposite flux of pollutants from water to atmosphere, thereby decreasing the net compartmental exchange flux.

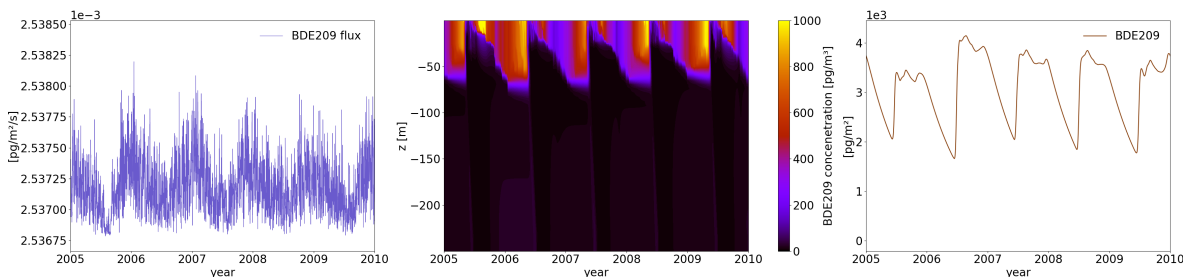


**Figure 13:** Example of plots in this study and their meaning: **a** - atmospheric flux ( $\text{pg m}^{-2} \text{ s}^{-1}$ ); **b** - changes of POP concentration in water column over time ( $\text{pg m}^{-3}$ ); **c** - changes of POP concentration in sediment pool over time ( $\text{pg m}^{-2}$ ).

The second type of plot represents changes in concentration within the water column over time (Figure 13b). The Y-axis denotes water column depth, ranging from 41.5 meters in the Southern North Sea to 250 meters in the Gotland Basin. Concentration ranges are depicted by color variations, with the corresponding values shown in the color bar (in units  $\text{pg m}^{-3}$ ). This type of plots also represent turbulence length scale (TLS) of the water column.

The final plot type represents changes in sediment concentration of POPs (Figure 13c). In this model setup, sediment is implemented as a single pool without differentiation by depth, so concentration changes are presented in units of  $\text{pg m}^{-2}$ .

#### 4.1 The environmental fate of specific congeners of a group of POPs

In the marine environment, the fate of pollutants is influenced by a variety of factors, ranging from hydrophysical and biogeochemical conditions of the region to the specific speciations and properties of each chemical. Similarly, in the simulation or modeling of these processes, it's essential to consider these factors independently. To begin, we will examine the unique characteristics of each POP and analyze how they influence their behavior in the water column.

This chapter aims to delineate the differences in behavioral patterns among five POPs within the same region. Specifically, we will explore how distinct chemical properties shape their distribution patterns within the water column, the diffusive flux between different environmental compartments, and the resulting by-products of their photolytic transformation. The Gotland Basin in the Baltic Sea has been chosen as the site for the 1D simulation of all five POPs. This region is characterized by the absence of sea ice, minimal tidal influence, clear stratification, and high biological production, resulting in a high content of organic matrices for pollutant partitioning. Additionally, detritus in this area has over 200 meters to sink, allowing us to consider the influence of POPs desorption via remineralization. Moreover, once pollutants have descended to the bottom of the water column, they can accumulate in sediments due to low turbulence in the bottom layer. Furthermore, the separation between the bottom and surface mixed layers enables the observation of the dynamic behavior of POPs on detritus and in sediment independently of surface bioproduction and DOM.

To compare how specific parameters influence the distribution pattern of each POP between phases, the experiment was conducted under identical conditions. This involved maintaining consistent hydrodynamic and biogeochemical regimes, as well as initial pollutant concentrations. As outlined in the Methods section 3.4, all aquatic pollutant concentrations were initialized to zero at the beginning of the simulation. However, atmospheric concentrations vary among different POPs, leading to discrepancies in their distribution and accumulation patterns. To address this, we standardized atmospheric concentrations and depositions at 0.1 and 0.001  $\text{pg m}^{-2} \text{s}^{-1}$ , respectively, for each POP, thereby allowing us to focus on specific pollutant properties.

This experiment aims to differentiate the impact of specific properties of POPs on their behavior in the aquatic environment. It's important to note that the results of this experiment do not accurately reflect real concentration distributions.

#### 4.1.1 Atmospheric flux

At the interface between water and air, pollutants can be transferred through two main mechanisms: direct deposition and diffusive flux. Direct deposition is primarily governed by atmospheric concentration and the flux from air to water. Diffusive flux, on the other hand, is more complex. As described in the Methods section 3.4, diffusive flux is influenced by physical factors such as wind speed and temperature [Friedman and Selin, 2016, Odabasi, 2008], as well as chemical properties including the enthalpy and entropy of dissolution, and diffusivities (Table 5). Additionally, the free dissolved concentration of POPs in the water column dictates the direction of the POP flux.

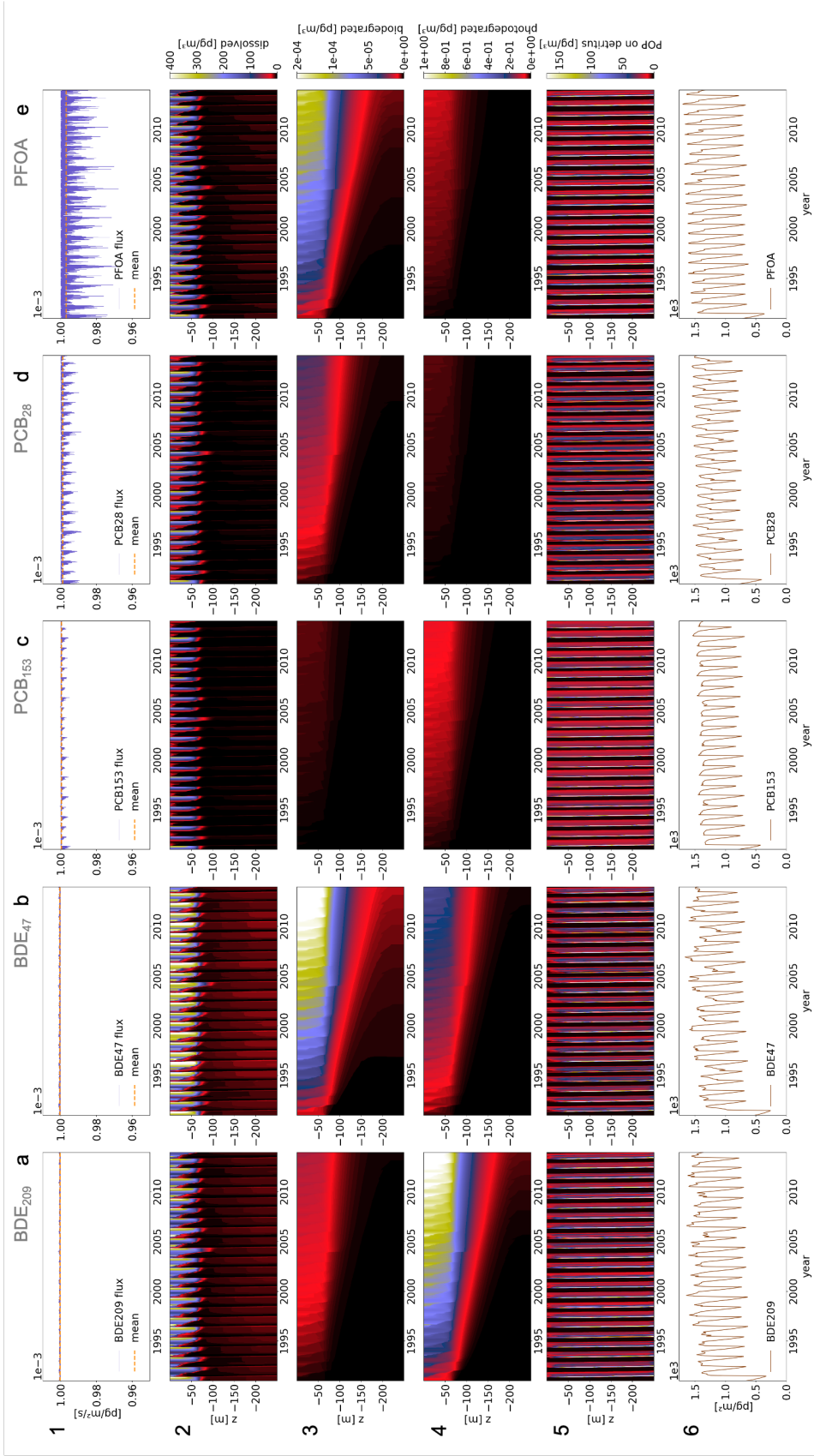
The simulation results indicate that the mobility of selected POPs in diffusive exchange increases as the molar mass and enthalpy of vaporization ( $\Delta Hh$ ) decrease (Fig. 14,a1-a4). This effect, while straightforward, significantly influences the ability of pollutants to remain in dissolved form. Among the selected POPs, BDEs are the heaviest (Table 5), rendering them unlikely to be released back into the atmosphere and instead causing them to distribute within the water column. Consequently, BDEs exhibit the highest dissolved concentrations among all five POPs (Fig. 14,a1,a2,b1,b2).

At low atmospheric concentration levels, pollutants in the water column reach equilibrium with no additional release to the atmosphere. However, the diffusive "pump" facilitating atmospheric exchange is higher for LSCs, resulting in increased dissolved concentrations of BDE<sub>47</sub> compared to BDE<sub>209</sub>.

For the PCB class, the pattern is similar, but they can contribute to the release of pollutants back into the atmosphere under simulated conditions (Fig. 14,a3,a4,b3,b4). PCB<sub>28</sub>, a LSC, has the lowest  $\Delta Hh$  and molar mass (Table 5), resulting in the highest release of POPs via diffusive exchange (Fig. 14,a4). However, both PCB<sub>28</sub> and PCB<sub>153</sub> exhibit a similar range and distribution pattern in dissolved form (Fig. 14,b3,b4), with a slight increase in PCB<sub>28</sub> during summer due to release from dissolved organic matter.

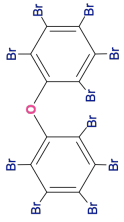
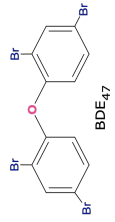
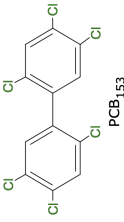
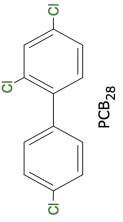
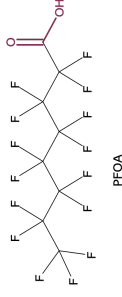
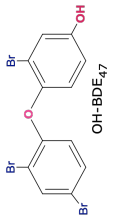
Although PFOA is heavier than PCBs, it has a different mechanism of atmospheric release

through sea salt aerosols. This results in the highest flux of pollutants from the water to the air. However, due to PFOA's solubility and general affinity to water, its dissolved concentration remains high at the surface, with minimal disruptions during summer seasons (Fig. 14b5).



**Figure 14:** Pollutants distribution between different matrices in water column. Results for 5 POPs over 20 years of simulations in Gotland Basin: columns: **a** - BDE<sub>209</sub>; **b** - BDE<sub>47</sub>; **c** - PCB<sub>153</sub>; **d** - PCB<sub>28</sub>; **e** - PFOA. Rows: **1** - atmospheric flux ( $\text{pg m}^{-2} \text{s}^{-1}$ ); **2** - dissolved POP ( $\text{pg m}^{-3}$ ); **3** - biodegraded POP ( $\text{pg m}^{-3}$ ); **4** - photodegraded POP ( $\text{pg m}^{-3}$ ); **5** - POP bound to detritus ( $\text{pg m}^{-3}$ ); **6** - sediment concentration of POP ( $\text{pg m}^{-2}$ ).

**Table 5:** Chemical characteristics of chosen POPs

Class	Molecule	Molar mass <sup>1</sup> (g/mol)	$\Delta H_h^1$ (J/mol)	$\Delta S_h^1$ (J/molK)	Henry <sup>1,2</sup> (atm m <sup>3</sup> /mol)	Partitioning <sup>3,4</sup>	Degradation <sup>5,6,7</sup> pathway	logBCF <sup>1</sup>	LC <sub>50</sub> <sup>1</sup> (mg/L)
PBDE	 BDE <sub>209</sub>	959.17	82600	120	3.95e-7	Detritus	photo	5.97	blank <sup>11</sup>
PBDE	 BDE <sub>47</sub>	485.79	62000	130	1.48e-5	DOM	bio	4.51	4.2 <sup>11</sup>
PCB	 PCB <sub>153</sub>	360.90	66100	190	2.77e-4	Detritus	photo	4.40	5.0 <sup>8</sup>
PCB	 PCB <sub>28</sub>	257.54	32500	74	1.48e-4	DOM	bio	4.20	3.0 <sup>8</sup>
PFAS	 PFOA	414.07	46800	143	2.02e-10	OM fluid borders	photo	0.80-3.20	57.6 <sup>9</sup>
BDE-OH	 OH-BDE <sub>47</sub>	501.79	62000		8.48e-6	-	-	4.51	9.96 <sup>10</sup>

source: <sup>1</sup> [ChemSpider, 2024], <sup>2</sup> [Sander, 2023], <sup>3</sup> [Schwarzenbach et al., 2016], <sup>4</sup> [van Noort et al., 2003], <sup>5</sup> [Pan et al., 2016], <sup>6</sup> [Calza and Vione, 2015], <sup>7</sup> [Zhang et al., 2013], <sup>8</sup> [Sişman et al., 2007], <sup>9</sup> [Wäsel et al., 2020], <sup>10</sup> [Usenko et al., 2011], <sup>11</sup> [Usenko et al., 2012]

#### 4.1.2 Dergadation

Over the long term, POPs can be transported over long distances in the open ocean (LRT). Photolysis is a preferred and viable method for POPs to transform or degrade. Moreover, it's important to note that photolysis occurs exclusively in surface waters, where UV light can penetrate the water column. In the deep ocean, where bacterial communities and sunlight are scarce, POPs can persist almost indefinitely.

The majority of POPs absorb solar irradiation in the UV part of the light spectrum, leading to their transformation into derivative products. This phototransformation process affects PCBs, PBDEs, and PFASs, with some HSCs of the PCB and PBDE classes exhibiting a higher susceptibility to this process compared to LSCs. Although the concentrations of newly developed pollutants are not typically high, studying these phototransformation processes is crucial. Given the persistent nature of POPs, photolysis represents one of the two possible degradation pathways. Over extended periods, there can be a cumulative effect leading to a significant reduction in the concentration of parent POPs. However, POPs undergo different pathways of photolytic transformation in the marine environment and do not always end up in the complete degradation of the original molecule.

For instance, HSCs such as PCB<sub>153</sub> and BDE<sub>209</sub> tend to lose halogens in their structure during direct photolysis, resulting in the formation of LSCs like PCB<sub>28</sub> and BDE<sub>47</sub>. In this case, the reduction in one pollutant results in an increase in the other congener from the same class, rather than complete degradation. For BDE class, HSC transform to LSC BDE<sub>47</sub> (Fig. 15a). This process contributes to an increase in LSCs' dissolved concentrations in the SML, leading to their higher outflux to the atmosphere. PFOA undergoes direct photolysis, resulting in the transformation of the compound into other lighter compounds. In this context, this process is considered degradation.

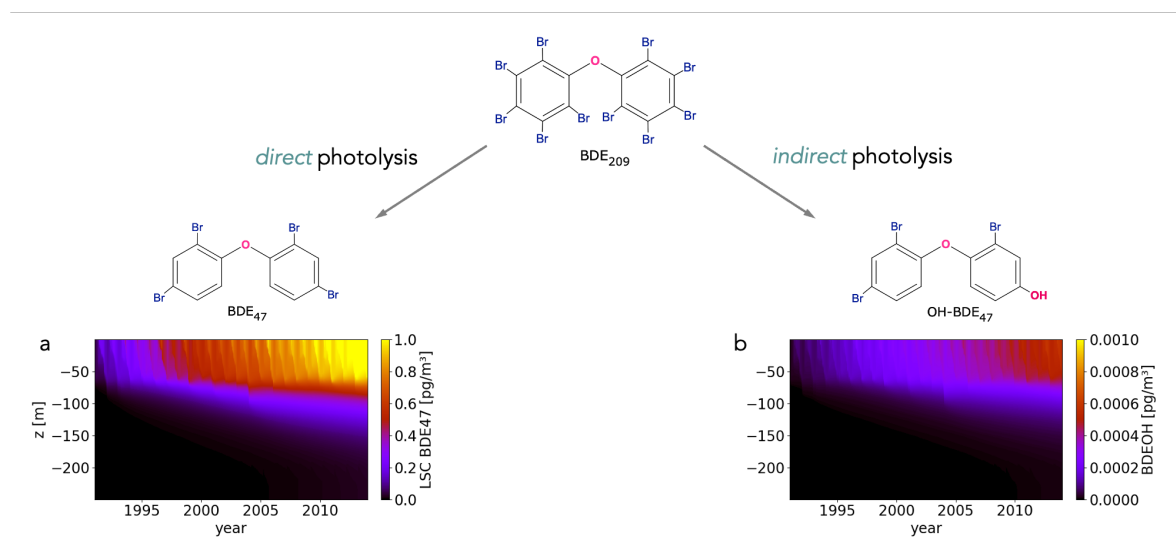


**Figure 15:** Different pathways of BDE phototransformation and their result concentrations: **a** - direct photolysis and BDE<sub>47</sub> formation; **b** - indirect photolysis and BDE-OH formation.

Simultaneously, another process occurs: indirect photolysis. During this process, freshly formed OH radicals interact with POP molecules, resulting in the production of various substances. For instance, PBDE compounds convert into PBDE-OH molecules (Table 5, Fig. 15b). The rate of this process depends not only on the concentration of BDE but also on the availability of OH radicals. Although the creation rate of these new pollutants is relatively low, it's noteworthy that PCB-OH and BDE-OH were never manufactured industrially nor produced by natural activities. These chemicals are persistent, more toxic, and have a significant impact on living organisms compared to their parent pollutants. Moreover, these hydroxylated byproducts also remain mixed within the SML, resulting in greater accessibility to a significant portion of aquatic species (See Section 2).

Although PCB-OH and BDE-OH typically do not reach high concentration levels, their presence can be crucial for local biota.

Biological degradation requires PCBs and BDEs to possess a specific structure that allows bacteria to utilize them as a source of energy. While PCB<sub>153</sub> and BDE<sub>209</sub> do not meet these criteria, PCB<sub>28</sub> and BDE<sub>47</sub> do. Consequently, some percentage of LSC can be degraded. Nevertheless, HSCs are still affected by biological degradation, particularly by cyanobacteria. This process occurs at a much slower rate, resulting in a lower reduction of parent POPs through this degradation pathway.

Here, we delve into various properties of all 5 simulated pollutants and 3 derivatives. This includes information and discussions about their LC<sub>50</sub>, BCF, and their general effects on fetal development. We compare how distribution patterns change across different stages of halogenation and molar mass. Additionally, we explore the identification of hotspots for more dangerous derivatives.

#### 4.1.3 *Partitioning to detritus and sediment concentrations*

One of the most important processes, determining distribution of persistent pollutant between phases in aquatic environment is partitioning with Organic Matter. When both POM and DOM are present, POP partitioning to each matrix can become a competitive process. Within one class of hydrophobic pollutants, different congeners have different preferences for partitioning. HSC BDE<sub>209</sub> and PCB<sub>153</sub> contain a significant amount of halogens in their structures, which greatly increases their weight, molecular size, and flexibility. These molecules can adsorb on the surface of organic particles, but has less affinity for adsorption within the cluster of dissolved organic matter. In contrast, LSC tends to be adsorbed within the clusters of DOM due to their smaller size and lighter mass.

All studied POPs exhibit a high affinity for accumulation on OM, but their adsorption and desorption rates vary. This results in temporal differences in the presence of POPs on POM in the water column throughout the year (Fig. 14e1-e5). BDEs tend to adsorb quickly onto detritus and are released relatively rapidly during both remineralization and desorption processes. This increases the concentration of dissolved BDEs, especially LSC BDE<sub>47</sub>, in the bottom part of the

region (Fig. 14b1,b2). Eventually, BDEs on detritus contribute to the sediment content of these pollutants. While this phenomenon occurs for all five POPs, the PCB class exhibits the slowest desorption rate, resulting in extremely low dissolved concentrations of PCB pollutants below the surface mixed layer (Fig. 14b3,b4).

HSCs like BDE<sub>209</sub>, PCB<sub>153</sub>, and PFOA rapidly adsorb onto detritus, leading to an initial significant decrease in their dissolved concentrations during the plankton bloom season. As POM forms, a substantial portion of these POPs is removed from the dissolved phase and sinks to the sediment. In contrast, LSCs adsorb more slowly onto detritus, allowing them to remain in the dissolved phase for a longer period. Consequently, BDE<sub>47</sub> and PCB<sub>28</sub> exhibit higher concentrations on detritus later in the year. This results in a distinct distribution pattern for these POPs: HSCs and PFOA primarily contribute to sediment concentrations earlier in the year, while LSCs peak later (Fig. 14f1-f5).

## 4.2 Hydrodynamic Impacts on the Fate of hydrophobic POPs in the Marine Environment

In the marine environment, multiple parameters dictate the distribution of POPs. In the previous chapter, we investigated the effect of specific chemical properties of each congener on its behavior in the water column. Another critical factor influencing POP distribution is the hydrodynamic characteristics of the environment. Physical processes such as turbulence regimes and stratification strongly affect the distribution patterns of both organic matter and POPs. Sediments can act as either a permanent or seasonal sink for POPs and detritus, depending on the mixing conditions.

Stratification causes the removal of POPs from the surface layer due to particle settling, which affects the air-sea exchange. This process impacts all chosen pollutants but particularly affects the fate of HSCs, which have a higher affinity for binding with POM. In regions with seasonal stratification, resuspension events may cause significant peaks in dissolved concentrations of POPs previously stored in sediment. These increases in pollutant concentrations can have a major impact on bioaccumulation.

Biological production results in elevated concentrations of organic matter, triggering the transformation of POPs from the dissolved phase to the absorbed phase. Additionally, POM removes POPs from the surface layer through gravitational settling. This alteration in the concentration gradient of POPs between the atmosphere and ocean at the interface leads to an increased atmospheric influx through diffusive exchange. Since the atmosphere serves as the primary source of POPs in the 1D model, the amount of OM at the atmospheric surface is a crucial factor in determining the total amount of POPs in the system.

Resuspension events can increase the quantity of suspended OM, thereby directly enhancing the process of pollutant accumulation by elevating nutrient concentrations. Consequently, this can lead to higher primary production in nutrient-limited regions. This chapter focuses on the impact of the physical characteristics of the system on the behavior of POPs. Section 4.3 provides detailed insights into the influence of changes in OM production on its distribution pattern.

The second driving processes are turbulence regime and stratification. Depending on the mixing condition, sediments can act as either a permanent or seasonal sink for POPs. Regardless of the long-term fate, stratification results in the removal of POPs from the surface layer due to particle settling, which consequently affects air–sea exchange. In regions with seasonal stratification, resuspension events can cause significant peaks in POP concentrations, thereby potentially having a major impact on bioaccumulation.

Here, we assessed four regions with distinct conditions. The two model locations in the Baltic Sea represent contrasting environments: the Gotland Deep, characterized by deep, stratified conditions, and a shallower, mixed region in the north, known for seasonal ice coverage, referred to as the Bothnian Bay. The Gotland Basin area, with a depth of 250 meters, is the deepest part of the Baltic Sea, exhibiting stable stratification [Savchuk and Wulff, 2009]. Surface and bottom mixed layers are permanently separated by a halocline, resulting in rare resuspension events that do not significantly affect the stratified surface layer.

In the Bothnian Bay location, winter sea ice formation restricts the influx of atmospheric POPs and the release of PFOA through sea salt aerosol formation.

In contrast to the Baltic Sea, the North Sea is a much shallower shelf sea with no deep basins. Importantly, it is connected to the Atlantic Ocean, where physical and biological processes determine whether POPs originating from the continent are deposited into the sediments or transported into the open ocean. For our analysis, we modeled POP cycling at two locations in the North Sea, differing due to two key processes: stratification/mixing and primary production/biological pump.

The Northern North Sea (NNS) experiences seasonal stratification with high primary production, whereas the Southern North Sea (SNS) remains mixed throughout the year and exhibits even higher primary production. The stronger vertical mixing in the SNS is attributed to its shallow depth and higher tidal amplitudes. During periods of mixed water column, bottom turbulence (shear stress) prevents POPs from accumulating in the sediments. In cases of seasonal mixing, this can lead to pronounced resuspension peaks.

Furthermore, the high biological production in both regions results in elevated concentrations of dissolved and particulate organic matter. This strongly influences the speciation of POPs and causes sedimentation via POPs bound to detritus (detritus vector). In the Baltic Sea, speciation significantly influences air–sea exchange, as only the dissolved form can exchange between the atmosphere and ocean.

For the North Sea, we assessed two model scenarios for each region. In addition to the default scenario, we conducted simulations without tidal forcing to illustrate the impact of tides on the fate of POPs in this area. The turbulence generated by tides is pivotal in determining whether sediments act as a sink for POPs in this region and has implications for their long-range transport.

On one hand, tides induce more resuspension, reducing net sedimentation. On the other hand, the heightened availability of nutrients in a predominantly nitrogen-limited environment fosters increased primary production, resulting in higher levels of particulate organic carbon (POC) and consequently augmenting the sedimentation flux.

#### 4.2.1 The Deep Region with Permanent Stratification — The Gotland Deep

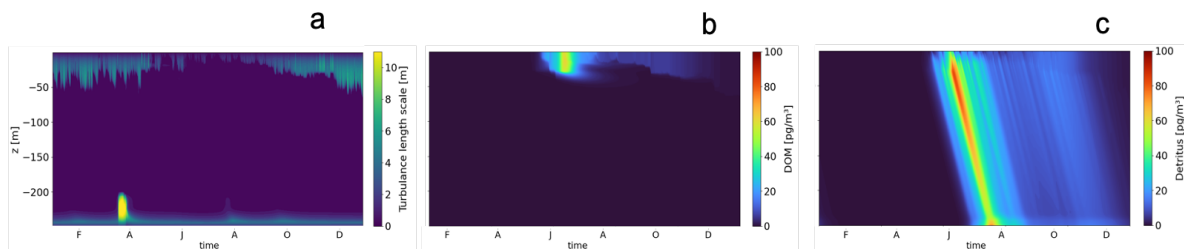


**Figure 16:** Conditions in the Gotland Basin (year 2010): **a** - TLS (m); **b** - DOM ( $\text{mgC m}^{-3}$ ); **c** - detritus ( $\text{mgC m}^{-3}$ ).

In the Gotland region of the Baltic Sea, the surface and bottom mixed layers are distinctly separated (Figure 16a). Primary production in this area begins in May, leading to high concentrations of POM and DOM from decaying phytoplankton (Figure 16b,c). Organic matter subsequently adsorbs  $\text{POP}_{free}$ , and as  $\text{POP}_{POM}$  settles, it effectively scavenges POPs from the surface layer, transporting them toward the ocean floor (Figure 18, column a). Due to the low turbulence and weak currents, there is rarely any resuspension at the bottom of the Gotland Basin, resulting in the permanent accumulation of POPs in the sediment (Figure 18, column b). This process affects all five POPs, though the intensity varies.

PCBs exhibit a high affinity for detritus and sorb quickly, resulting in a intense but short in time  $\text{PCB}_{POM}$  peak in late May to early June (Figure 18 3a, 4a). In contrast, BDEs and PFOA adsorb more slowly onto POM. Consequently, the  $\text{POP}_{POM}$  concentrations for these substances are not as high as for PCBs, but they exhibit a longer peak duration (Figure 18 1a, 2a, 5a).

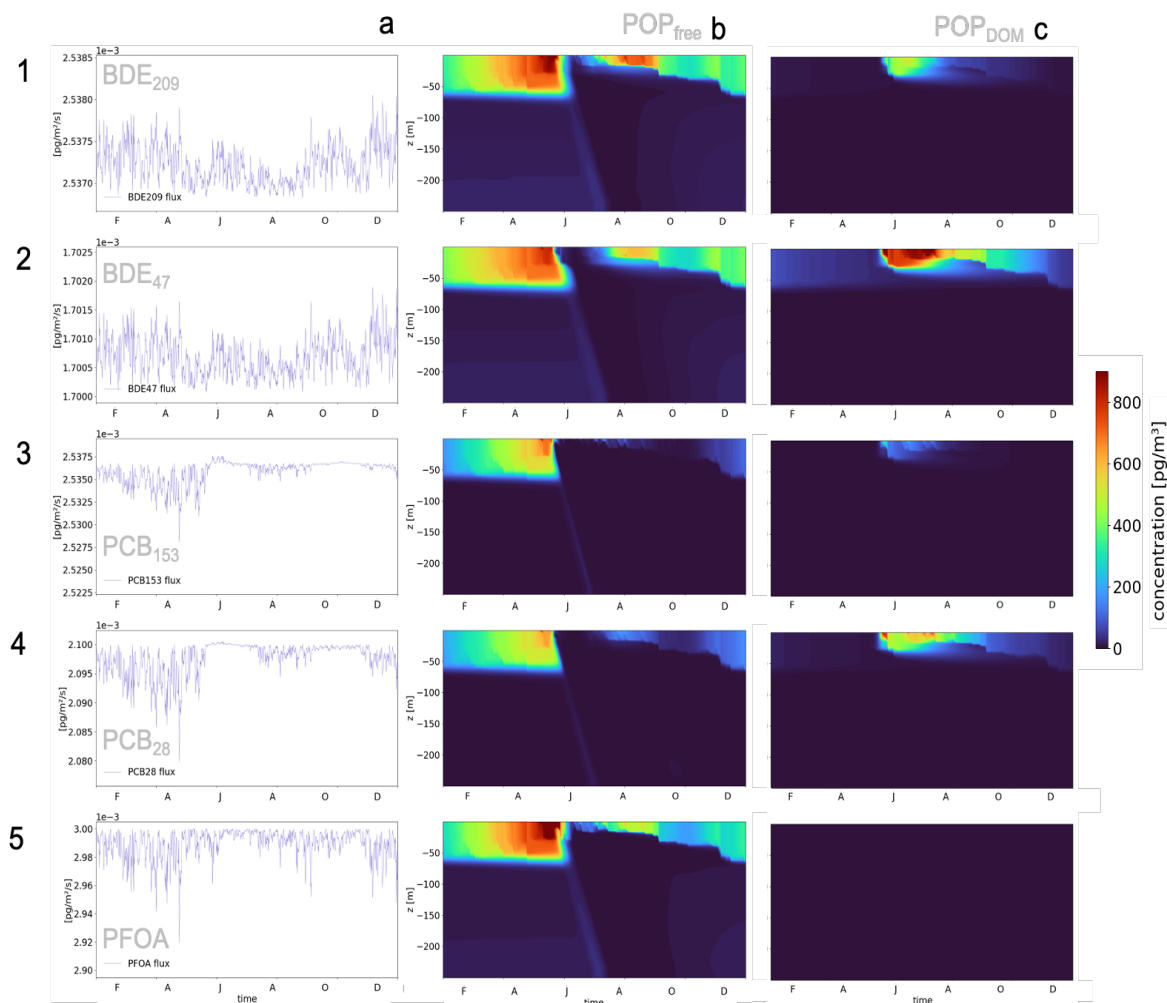


**Figure 17:** Results of simulation in the Gotland Basin (year 2010): column **a** - atmospheric flux of POP ( $\text{pg m}^{-2} \text{s}^{-1}$ ) (direction of flux - from atmosphere to water); **b** -  $\text{POP}_{free}$  concentrations ( $\text{pg m}^{-3}$ ); **c** -  $\text{POP}_{DOM}$  concentrations ( $\text{pg m}^{-2} \text{s}^{-1}$ ); row **1** - BDE<sub>209</sub>; row **2** - BDE<sub>47</sub>; row **3** - PCB<sub>153</sub>; row **4** - PCB<sub>28</sub>; row **5** - PFOA.

In this region, subsurface primary production becomes nutrient-limited early in the summer. Consequently, there is a clear seasonality in the distribution of  $\text{POP}_{free}$ . In early summer, detritus removes pollutants from the dissolved form as biological production begins (Figure 17, column **b**). This effect is observed for all POPs, with the highest impact on the PCB class due to their strong affinity for POM (Figure 17 3b, 4b).

Cyanobacteria bloom in late summer and autumn, keeping the biological pump active almost until the end of the year, though at a lower level (Figure 17b). The increased levels of BDEs and PFOA concentrations in late summer and early autumn are related to the desorption of POPs from decaying DOM. With the initial peak of biological production, all POPs partition with detritus, leading to a temporary removal of freely dissolved POPs in May and June (Figure 17, column **b**).

As a result, the stratified surface layer becomes "cleaned up" from pollutants, and due to the more pronounced concentration gradient, the atmospheric flux of POPs increases, particularly for PCBs (Figure 17 3a, 4a). However, BDEs, being heavier and lacking a tendency for diffusive outflux from the water column, do not exhibit the same effect (Figure 17 1a, 2a). Conversely, a reduction in surface wind speed during the summer months leads to a slight decline in the concentration of incoming BDE compounds, also resulting in a thinner mixed layer during this season. This reduction in wind speed also affects the atmospheric flux of PFOA, albeit in a different manner. Consequently, there is a decrease in the formation of SSA, leading to a reduction in the outflux of PFOA from the water column (Figure 17 5a).

POP entering from the atmosphere initially has no matrix to attach to. As a result, exchange with the atmosphere gradually saturates the thin surface mixed layer with POPs over time (Figure 17, column **b**). Stratification, the absence of detritus, and the high input of atmospheric POPs contribute to the formation of a surface layer primarily composed of  $POP_{free}$ , which accumulates until the next biological production cycle. Ultimately, the high concentration of  $POP_{free}$  at the onset of biological production represents a hotspot of bioavailability.

However, not all removed POPs end up being adsorbed onto POM. A fraction of  $POP_{free}$  associates with DOM, thus remaining in the surface mixed layer. This effect is particularly enhanced for LSCs PCB<sub>28</sub> and BDE<sub>47</sub> (Figure 17, column **c**).

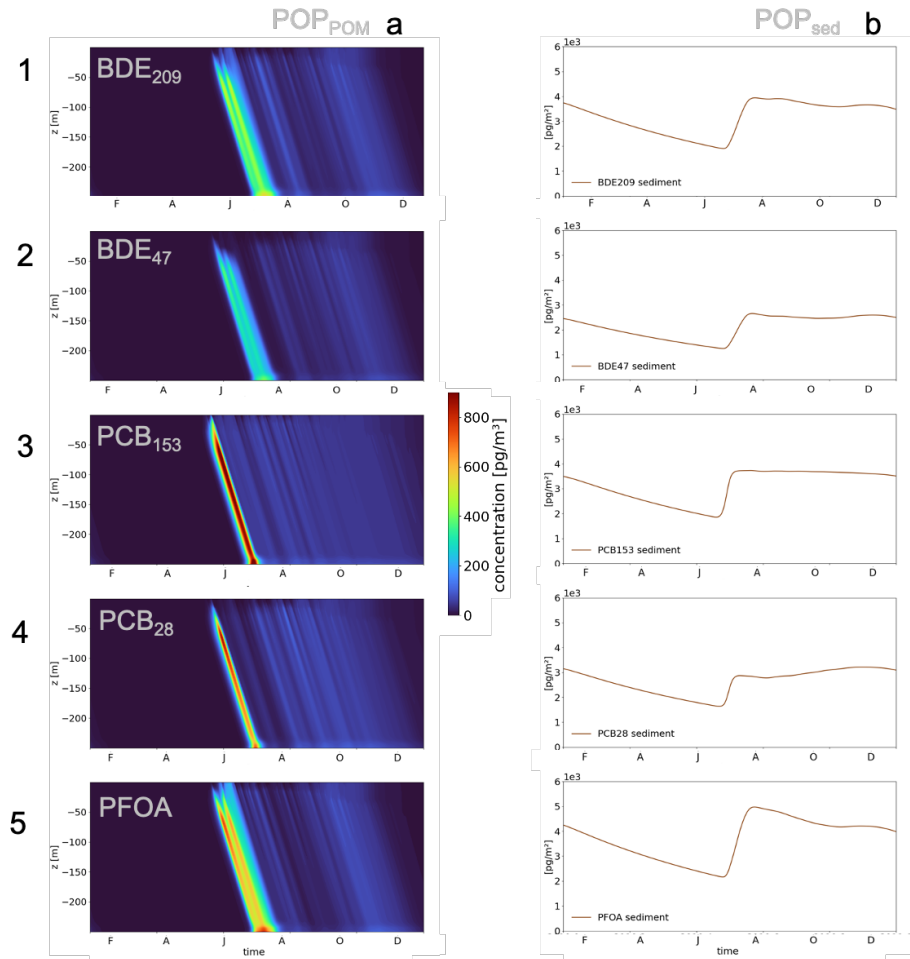


**Figure 18:** Results of simulation in the Gotland Basin (year 2010): column **a** - POP<sub>POM</sub> concentrations ( $pg\ m^{-3}$ ); **b** - sediment POP concentrations ( $pg\ m^{-2}$ ); row 1 - BDE<sub>209</sub>; row 2 - BDE<sub>47</sub>; row 3 - PCB<sub>153</sub>; row 4 - PCB<sub>28</sub>; row 5 - PFOA.

#### 4.2.2 Permanently Mixed Region with Low Atmospheric Input and the Late Onset of Production due to Sea Ice Cover—The Bothnian Bay

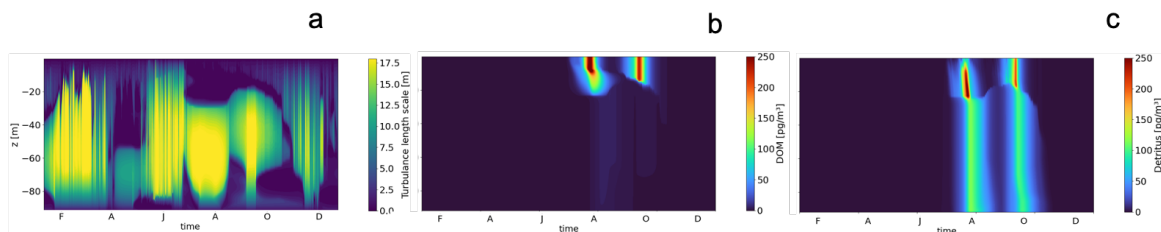


**Figure 19:** Conditions in the Bothnian Bay (year 2010): **a** - TLS (m); **b** - DOM ( $mgC\ m^{-3}$ ); **c** - detritus ( $mgC\ m^{-3}$ ).

In this region, seasonal sea surface ice formation occurs during wintertime, and primary production begins later in the year. Despite being located in the northern part of the Baltic Sea, the water column experiences thorough mixing, with only a brief disruption in mixing occurring in the surface mixed layer (SML) during summer (Figure 19a). This brief disruption in summer facilitates the production of organic matter by biota, resulting in two distinct peaks (the second peak is associated with cyanobacteria bloom) (Figure 19b,c).

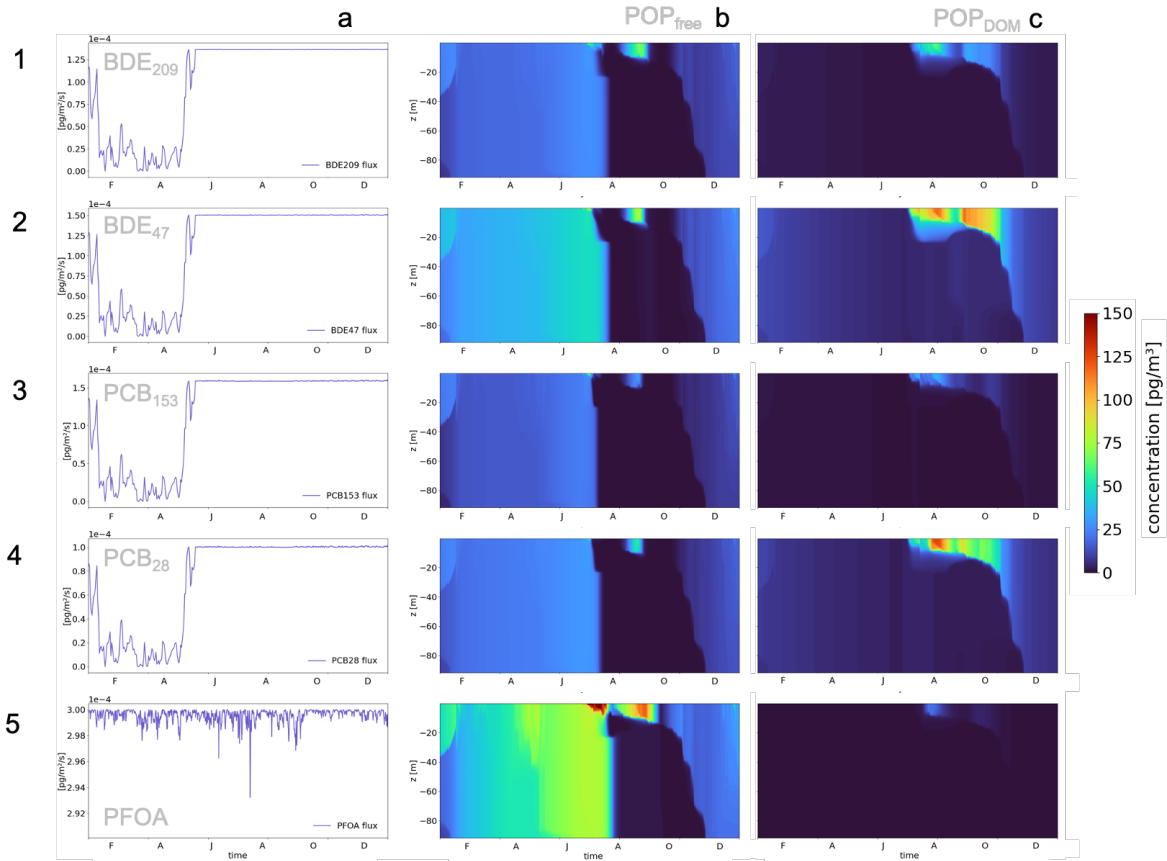


**Figure 20:** Results of simulation in the Bothnian Bay (year 2010): column **a** - atmospheric flux of POP ( $\text{pg m}^{-2} \text{s}^{-1}$ ) (direction of flux - from atmosphere to water); **b** -  $\text{POP}_{free}$  concentrations ( $\text{pg m}^{-3}$ ); **c** -  $\text{POP}_{DOM}$  concentrations ( $\text{pg m}^{-2} \text{s}^{-1}$ ); row **1** - BDE<sub>209</sub>; row **2** - BDE<sub>47</sub>; row **3** - PCB<sub>153</sub>; row **4** - PCB<sub>28</sub>; row **5** - PFOA.

The Bothnian Bay, situated in the northern reaches of the Baltic Sea, represents a more remote location characterized by lower atmospheric concentrations of POPs. During periods of ice coverage, the atmospheric flux of POPs dramatically decreases (Figures 20, column a).

Before the onset of ice formation in winter, incoming atmospheric POPs primarily accumulate on organic matter and subsequently mix within the water column (Figure 21a). A fraction of these pollutants returns to the dissolved form during the remineralization of OM and desorption processes (Figure 20, column b). However, during the brief window of biological production in summer, all forms of OM capture and mix newly arriving pollutants from the atmosphere within

the water column. For PCBs and BDEs, this phenomenon results in a similar pattern of free dissolved pollutants in the water column, commencing with the onset of bioproduction (Figure 20, column b). The variations in concentrations are influenced by the quantity of pollutants suspended in the water column from the previous year during the winter period. LSCs exhibit higher concentrations of POPs associated with dissolved organic matter ( $POP_{DOM}$ ), peaking during the summer DOM production phase. However, a residual amount of this fraction remains mixed within the water column for the subsequent winter season (Figure 20, column c).

The higher solubility of PFOA and its lower susceptibility to diffusive atmospheric flux account for its elevated concentration in the system. During winter, when levels of  $POP_{free}$  are low, sea ice acts as a barrier preventing the influx of PCBs and BDEs from the atmosphere. However, this ice cover also limits the formation of sea salt aerosols (SSA), which are responsible for the outflux of PFOA to the atmosphere. Consequently, over time, PFOA accumulates to higher concentrations in the water column, influencing both the dissolved form ( $PFOA_{free}$ ) and sediment concentrations (Figure 205b, Figure 215b).

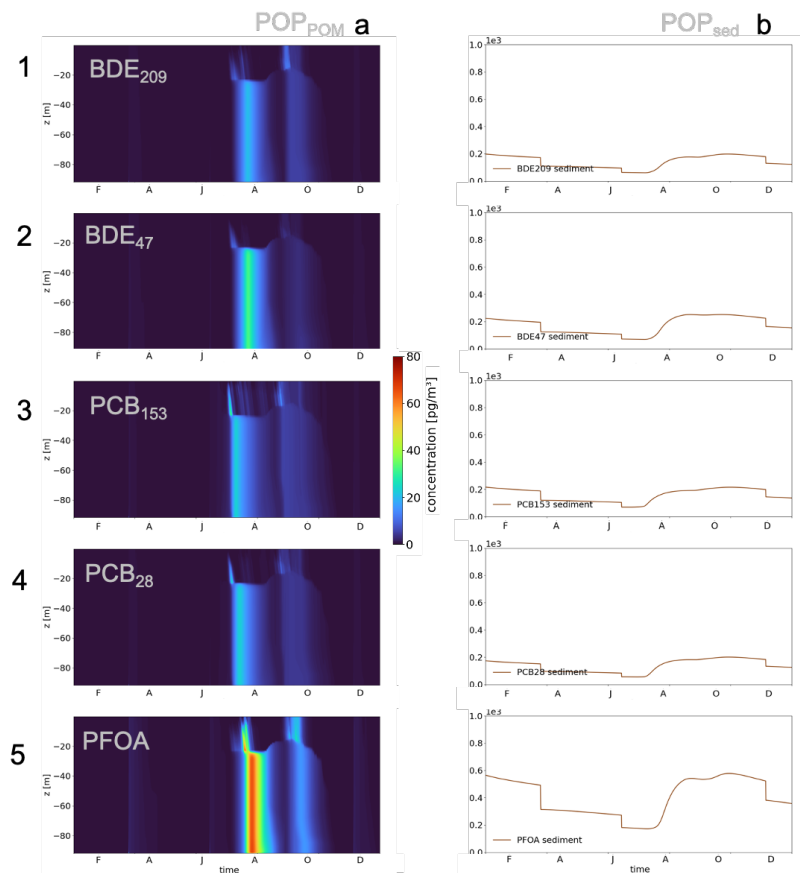


**Figure 21:** Results of simulation in the Bothnian Bay (year 2010): column **a** -  $POP_{POM}$  concentrations ( $pg\ m^{-3}$ ); **b** - sediment POP concentrations ( $pg\ m^{-2}$ ); row **1** - BDE<sub>209</sub>; row **2** - BDE<sub>47</sub>; row **3** - PCB<sub>153</sub>; row **4** - PCB<sub>28</sub>; row **5** - PFOA.

However, in this region, all five POPs are captured by detritus during the summer season

and can accumulate in the sediment (Figure 21, column b). The overall pattern and range of concentrations are constrained by bottom turbulence and the low influx of atmospheric pollutants, with the exception of PFOA, which exhibits a higher concentration range in the system.

In our model, we didn't incorporate the interactions of POPs with ice. However, it's conceivable that a portion of atmospheric POPs is sequestered in sea ice, potentially resulting in a more pronounced spring peak in POP concentrations upon ice melt.

#### 4.2.3 The North Sea — Tides Influenced Area with High Primary Production

##### 1. *Seasonally Stratified — Northern North Sea (NNS)*

The key process governing the differences between model runs with and without tides is the additional energy introduced by the tides which increases the turbulence and thus vertical mixing. Figure 22 depicts the seasonal turbulence and OM production patterns for the model run with and without tides.

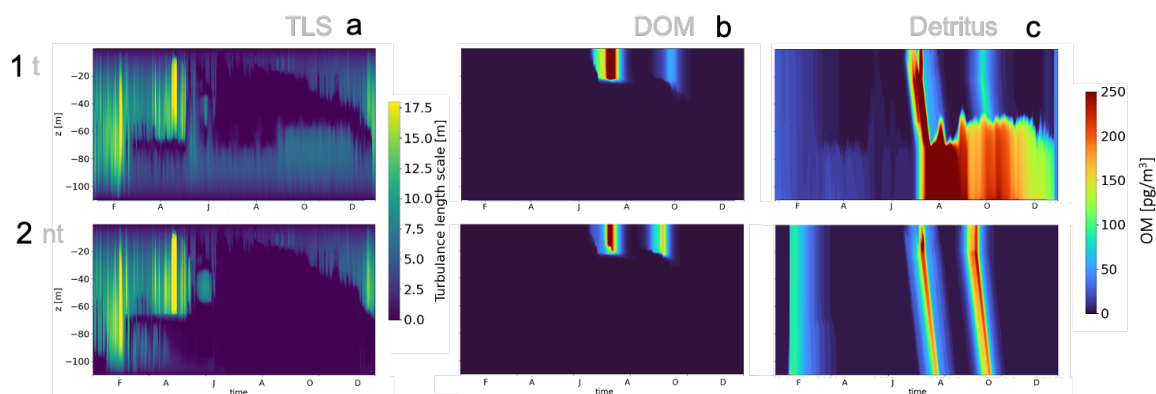


**Figure 22:** Conditions of the Northern North Sea (NNS) for 2 scenarios: column **a** - TLS (m); column **b** - DOM ( $\text{mgC m}^{-3}$ ); column **c** - POM ( $\text{mgC m}^{-3}$ ); row **1** - with tides (the water column stays stratified during summer season); row **2** - without tides.

The tides raise the depth and turbidity of the bottom mixed layer, leading to a breakdown of the stratification during winter (Figure 221a). This also increases sediment resuspension, introducing more particulate OM and nutrients into the water column (Figure 221c). In both model runs, the upper and bottom mixed layers are separated during summer.

POP cycling varies strongly between the two model runs. Common patterns are, like in the Baltic Sea, the scavenging of POP from the surface layer due to settling of POM. In the run without tides, all 5 POPs accumulate in the sediment and partially are resuspended during a short time of mixing in January (Figure 23, column c,d).

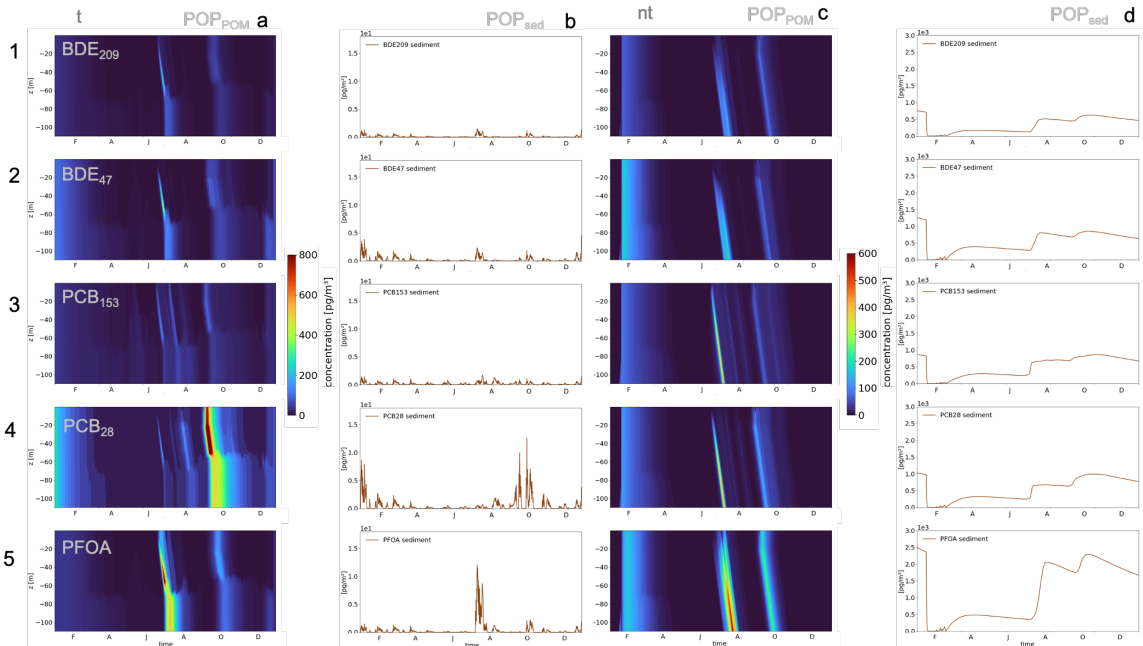


**Figure 23:** Results of simulations for all POPs related to POM in NNS: column **a** -  $POP_{POM}$  tide scenario ( $pg\ m^{-3}$ ); **b** - sediment concentration of POP tide scenario ( $pg\ m^{-2}$ ); **c** -  $POP_{POM}$  no-tide scenario ( $pg\ m^{-3}$ ); **d** - sediment concentration of POP no-tide scenario ( $pg\ m^{-2}$ ); row **1** - BDE<sub>209</sub>; row **2** - BDE<sub>47</sub>; row **3** - PCB<sub>153</sub>; row **4** - PCB<sub>28</sub>; row **5** - PFOA.

In scenarios involving tidal activity, the system possesses sufficient energy to resuspend POPs from the sediment, which then become mixed beneath the stratification layer (Figure 23, column a,b). Consequently, there is minimal or no net annual accumulation of POPs in sediments (Figure 23, column b), and concentrations of suspended  $POP_{POM}$  are generally elevated in the bottom layer (Figure 23, column a). This pattern is consistent across all POPs. However, for LSC PCB<sub>28</sub>, the concentration of the pollutant on detritus is notably high during the second bloom in July (Figure 23a4). This outcome is attributed to both the high atmospheric concentration of POP and the presence of DOM in the water column. With LSCs exhibiting a high affinity for DOM, this combination significantly boosts the influx of PCB<sub>28</sub> into the water column (Figure 24b3,c3). The abundant DOM effectively absorbs all incoming pollutants from the atmosphere, altering the partial pressure gradient. Consequently, this effect amplifies the atmospheric flux from air to water, resulting in exceedingly high concentrations of PCB<sub>28</sub> on DOM.

Over time, released from DOM, PCB<sub>28</sub> creates a notably concentrated area of freely dissolved pollutants near the surface, where detritus from the second bloom captures it and distributes it downward through the water column.

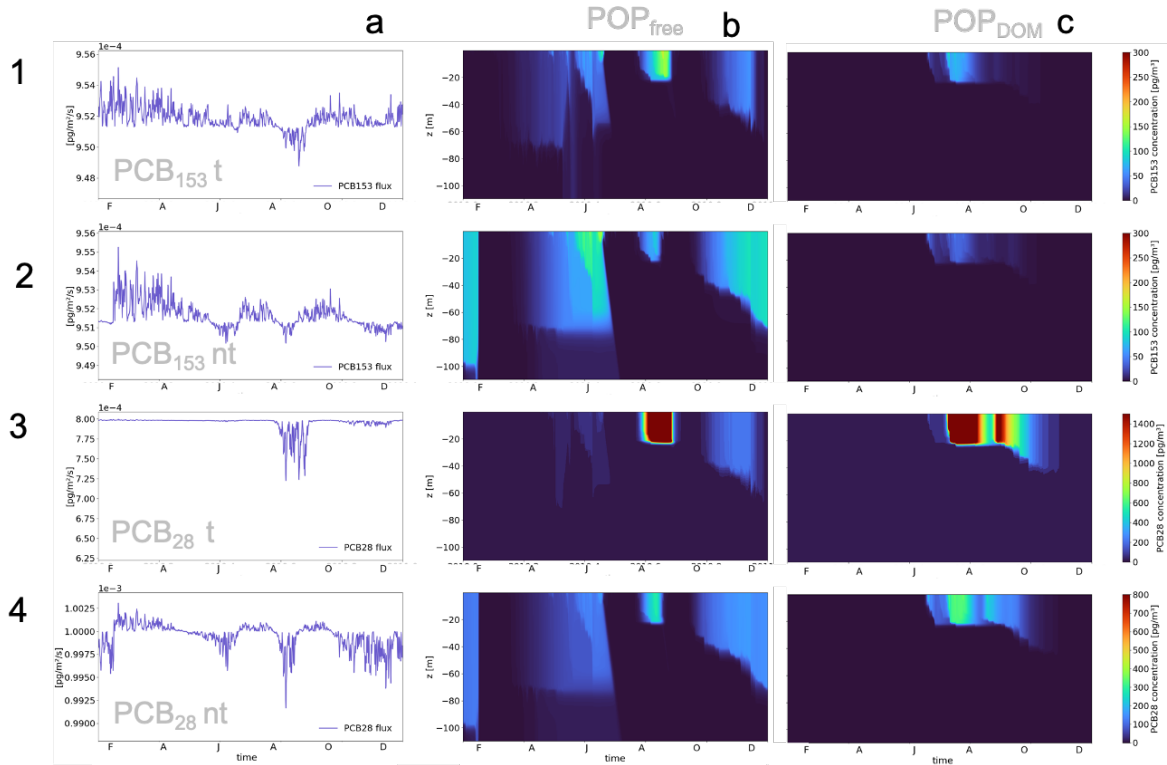


**Figure 24:** Results of PCB class simulations in NNS: column **a** - atmospheric flux of PCB ( $\text{pg m}^{-2} \text{s}^{-1}$ ); column **b** - freely dissolved PCB<sub>free</sub> ( $\text{pg m}^{-3}$ ); column **c** - PCB<sub>DOM</sub> ( $\text{pg m}^{-3}$ ); row **1** - results for PCB<sub>153</sub> with tides; row **2** - PCB<sub>153</sub> without tides; row **3** - PCB<sub>28</sub> with tides; row **4** - PCB<sub>28</sub> without tides.

Similar picture is observed in case of LSC BDE<sub>47</sub> (Figure 25b3,c3), however at lower extent. This can be explained by lower atmospheric concentrations of BDE<sub>47</sub> compared to PCB<sub>28</sub>, as well as the reduced mobility of the heavier BDE<sub>47</sub> over diffusive flux with the atmosphere.

For both BDEs and PCBs in both scenarios, the presence of detritus during winter increases scavenging, and dissolved POP<sub>free</sub> becomes, at times, completely depleted (Figure 25, column b; Figure 24, column b). With no-tide scenario, increased turbulence at the bottom of water column in January lead to resuspension of sediment POM, which removes residuals of dissolved POPs from the end of last year (Figure 25, column b; Figure 24, column b). All of those processes result increased POP flux from the atmosphere for BDEs and PCBs (Figure 25, column a; Figure 24, column a). The atmospheric POP is quickly absorbed to the abundant OM, which in turn increases the influx of atmospheric POP further.

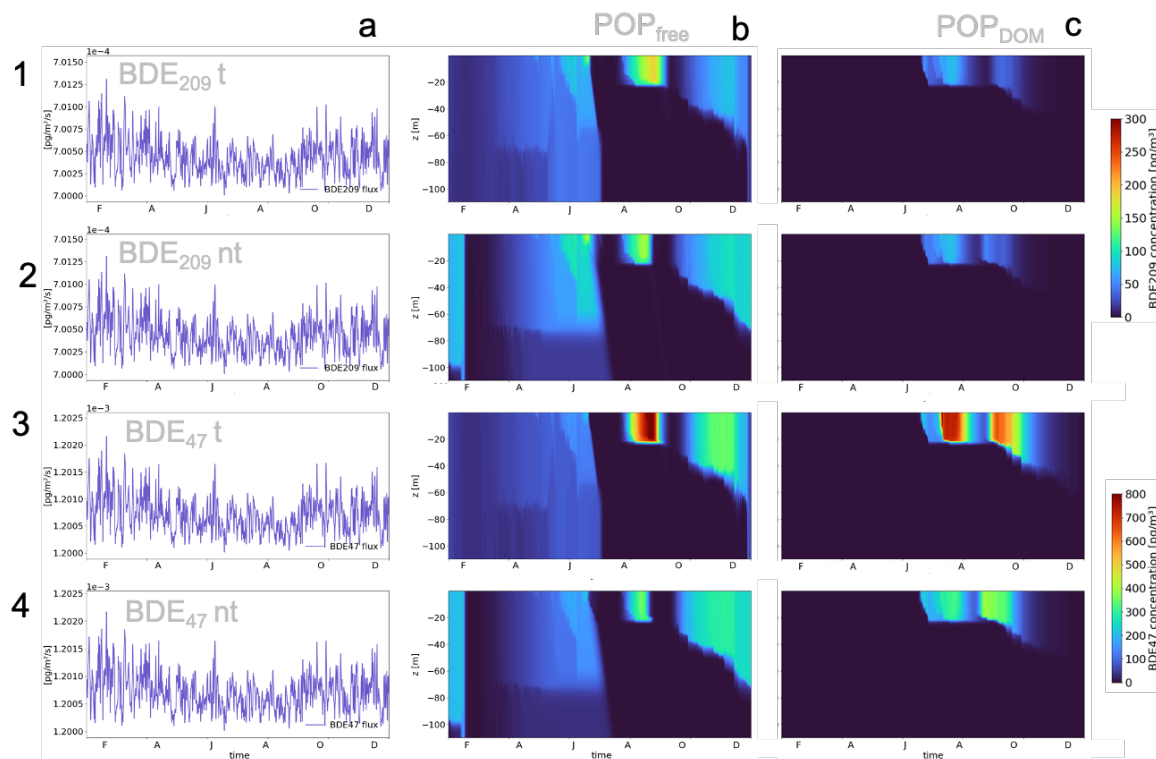


**Figure 25:** Results of BDE class simulations in NNS: column **a** - atmospheric flux of BDE ( $\text{pg m}^{-2} \text{s}^{-1}$ ); column **b** - freely dissolved BDE<sub>free</sub> ( $\text{pg m}^{-3}$ ); column **c** - BDE<sub>DOM</sub> ( $\text{pg m}^{-3}$ ); row **1** - results for BDE<sub>209</sub> with tides; row **2** - BDE<sub>209</sub> without tides; row **3** - BDE<sub>47</sub> with tides; row **4** - BDE<sub>47</sub> without tides.

In the absence of tides, winter wind-driven short-term resuspension events result in exceptionally high dissolved POP concentrations during spring, occurring before the phytoplankton bloom. Due to the lack of organic matter and well-mixed conditions, atmospheric POPs entering the water column contribute to the POP<sub>free</sub> fraction and distribute throughout the water column.

Although the pattern of pollutant adsorbed on POM is similar for PFOA, it exhibits its peak concentration with the first phytoplankton bloom in May (Figure 23a5). This phenomenon is attributed to the overall higher concentration of PFOA in the dissolved form during the winter, which subsequently adsorbs onto the first freshly produced detritus (Figure 26, column b). The higher dissolved concentration of PFOA is associated with its greater affinity for water compared to the other four POPs and its lower diffusive outflux back to the atmosphere, which occurs only via SSA.

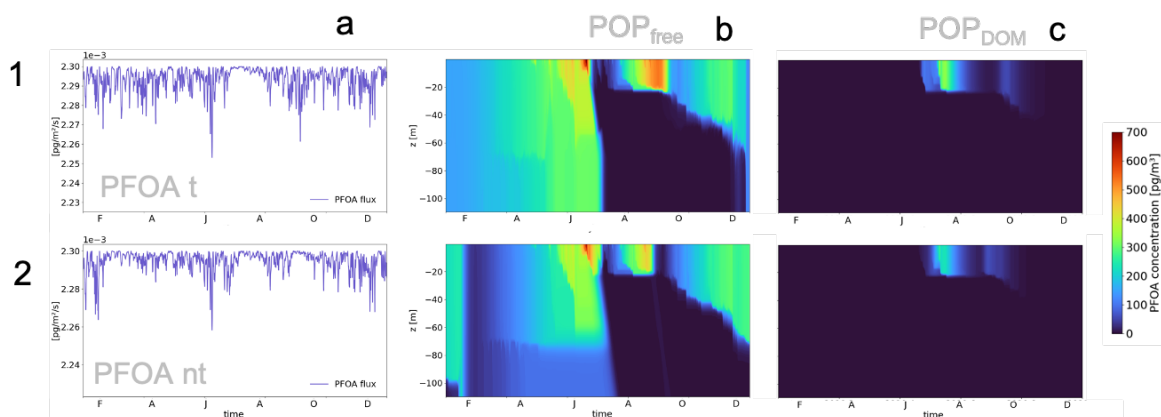


**Figure 26:** Results of PFOA class simulations in NNS: column **a** - atmospheric flux of PFOA ( $\text{pg m}^{-2} \text{s}^{-1}$ ); column **b** - freely dissolved PFOA<sub>free</sub> ( $\text{pg m}^{-3}$ ); column **c** - PFOA<sub>DOM</sub> ( $\text{pg m}^{-3}$ ); row **1** - results for PFOA with tides; row **2** - PFOA without tides.

The difference in POP concentrations between the two simulation scenarios is illustrated in Figure 27. In the tidal scenario, resuspension prevents pollutants from accumulating in sediment (refer to Figure 23). The surface mixed layer does not reach the bottom, resulting in a decrease in OM content before the spring bloom. Consequently, tidal activity reduces the concentration of freely dissolved POPs in the Northern North Sea in March and April. This effect is prominently observed for all PCBs and BDEs. However, BDEs, being heavier, are less prone to release from the water column via diffusive exchange. The increased resuspension in January in the no-tide scenario introduces additional OM into the water column, thereby removing freely dissolved BDEs. As a result, dissolved BDE concentrations decrease during the winter compared to the tidal scenario (refer to Figure 27,a1,b1). Similar trends are observed for PCB<sub>28</sub>, primarily due to its exceptionally high dissolved concentration (refer to Figure 27,b2). PCB<sub>153</sub>, characterized by lower concentrations and a high affinity to POM, exhibits an overall decrease in dissolved concentration in the tidal scenario (refer to Figure 27,b1). The higher content of dissolved PFOA in the water column does not have additional OM to partition with in the tidal scenario, allowing it to remain dissolved during the winter season, thus increasing PFOA<sub>free</sub> concentration (refer to Figure 27,c1). However, enhanced OM production significantly reduces PFOA in dissolved form, converting it into PFOA<sub>POM</sub>. Nevertheless, for all POPs, the increased content of DOM leads to a short but pronounced increase in POP<sub>free</sub> in July. Tidal activity does not affect the production of BDE-OH in this region.

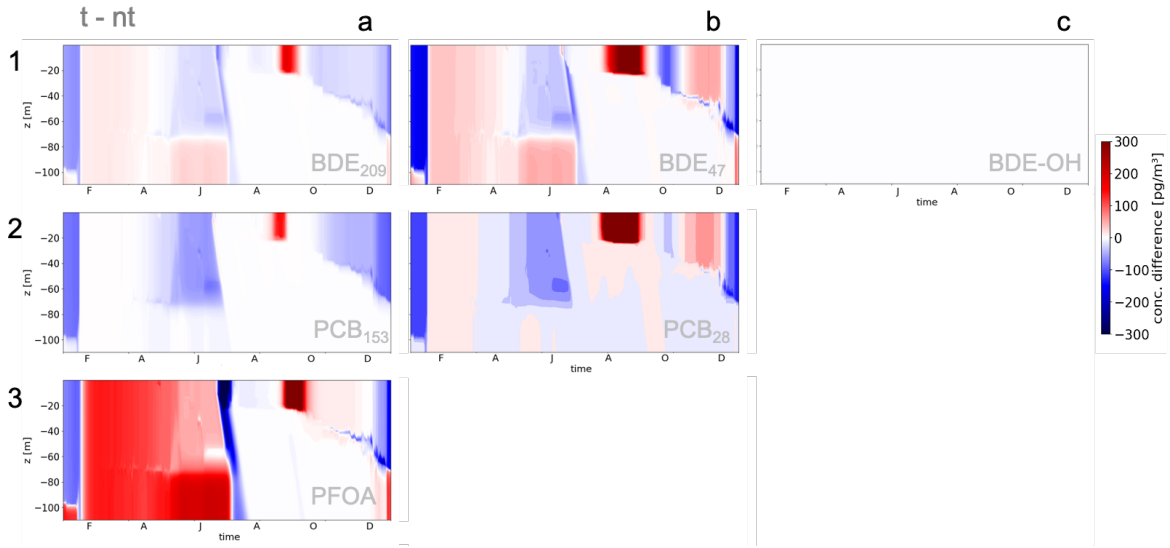


**Figure 27:** Differences in dissolved POP concentration ( $\mu\text{g m}^{-3}$ ) between tide–no-tide scenarios for NNS region: **1a** - BDE<sub>209</sub>; **1b** - BDE<sub>47</sub>; **1c** - BDE-OH; **2a** - PCB<sub>153</sub>; **2b** - PCB<sub>28</sub>; **3a** - PFOA.

## 2. Permanently Mixed — Southern North Sea (SNS)

In the Southern North Sea (SNS), the tidal amplitude range is higher than in the Northern North Sea, and the water column is shallower (41.5 m). Consequently, under these conditions, the bottom mixed layer even reaches the surface mixed layer during the summer months (refer to Figure 281a), resulting in the entire water column being mixed from surface to bottom. In contrast, without tides, the water column becomes stratified during summer (see Figure 282a).

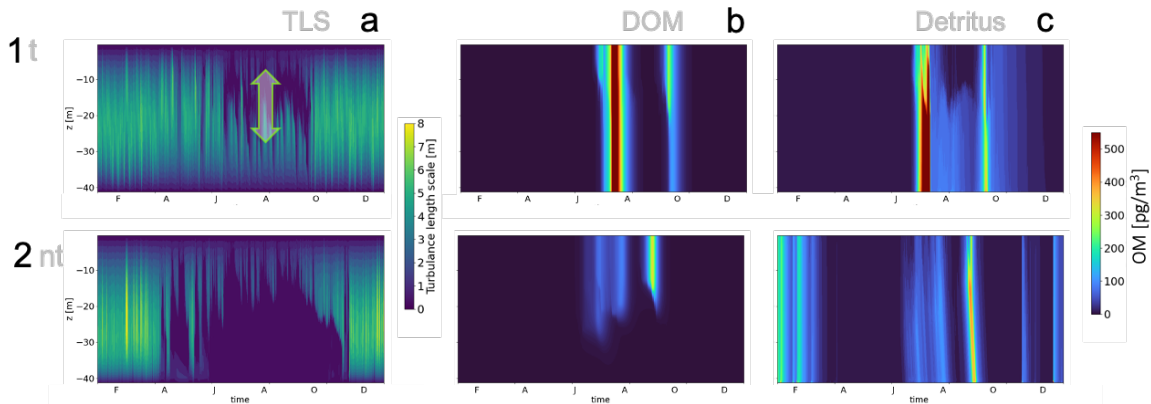


**Figure 28:** Conditions of the Northern North Sea (NNS) for 2 scenarios: column **a** - TLS (m); column **b** - DOM ( $\text{mgC m}^{-3}$ ); column **c** - POM ( $\text{mgC m}^{-3}$ ); row **1** - with tides (SML and BML (bottom mixed layer) meet during summer season — water column is permanently mixed); row **2** - without tides.

In the tidal scenario, nutrients resuspended from the sediment enhance biological produc-

tion at the subsurface layer, thereby increasing the content of organic matter (OM) in the water column. Additionally, OM from the sediment is mixed all the way to the surface (see Figure 28, columns b and c). Consequently, there is an abundance of OM throughout the year, leading to decreased concentrations of dissolved  $POP_{free}$  and increased atmospheric influx. Essentially, the tides alter the equilibrium between the atmosphere and ocean, resulting in higher POP concentrations in the water. Furthermore, due to the continuous mixing, tides prevent significant sedimentation (refer to Figure 29, column b).

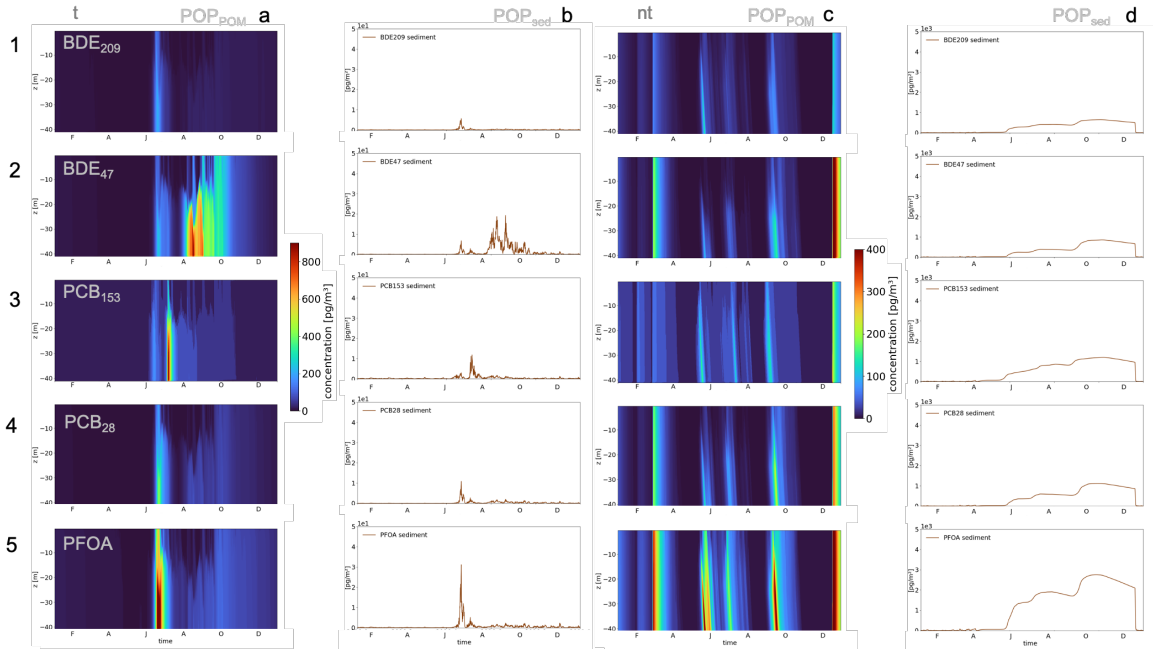


**Figure 29:** Results of simulations for all POPs related to POM in SNS: column **a** -  $POP_{POM}$  tide scenario ( $pg\ m^{-3}$ ); **b** - sediment concentration of POP tide scenario ( $pg\ m^{-2}$ ); **c** -  $POP_{POM}$  no-tide scenario ( $pg\ m^{-3}$ ); **d** - sediment concentration of POP no-tide scenario ( $pg\ m^{-2}$ ); row **1** - BDE<sub>209</sub>; row **2** - BDE<sub>47</sub>; row **3** - PCB<sub>153</sub>; row **4** - PCB<sub>28</sub>; row **5** - PFOA.

The first notable peak in  $POP_{POM}$  concentration in the tidal scenario occurs for all pollutants in April-May (refer to Figure 29, column a). The initial concentration is correlated with the dissolved concentration of the respective POP in the system over the winter period, with PFOA exhibiting the highest concentration (see Figure 29,5a). PCB<sub>153</sub>, possessing the highest affinity to POM, experiences a peak later in the late spring season (in May) (see Figure 29,3a), attributed to the increased atmospheric 'pump' coinciding with the removal of winter PCB<sub>153 $_{free}$</sub>  from the water column during the first phytoplankton bloom. With the augmented inflow of atmospheric PCB<sub>153</sub>, it directly accumulates due to the high content of freshly produced POM at the surface. Conversely, BDE<sub>47</sub> exhibits its highest concentrations on detritus during the summer months (refer to Figure 29,2a). This phenomenon is driven by the pollutant's high atmospheric concentration, its inability to undergo outflux from the water column back to the atmosphere, resulting in elevated concentrations of BDE<sub>47 $_{DOM}$</sub>  (see Figure 30,3c). With desorption and remineralization from

DOM, freshly released  $BDE_{47free}$  binds directly to resuspended POM in the system.

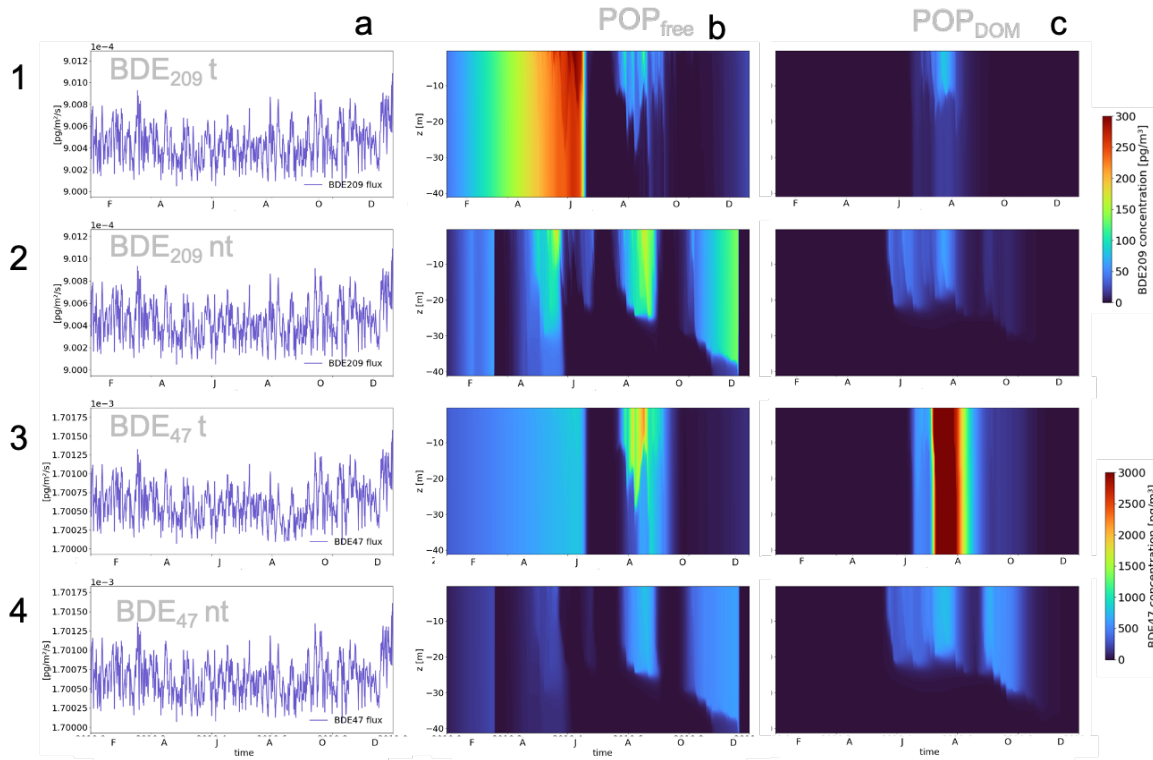


**Figure 30:** Results of BDE class simulations in SNS: column **a** - atmospheric flux of BDE ( $pg\ m^{-2}\ s^{-1}$ ); column **b** - freely dissolved  $BDE_{free}$  ( $pg\ m^{-3}$ ); column **c** -  $BDE_{DOM}$  ( $pg\ m^{-3}$ ); row **1** - results for  $BDE_{209}$  with tides; row **2** -  $BDE_{209}$  without tides; row **3** -  $BDE_{47}$  with tides; row **4** -  $BDE_{47}$  without tides.

In contrast, in the no-tide scenario, the initial peak of  $POP_{POM}$  is observed in January (refer to Figure 29, column c). This occurrence is triggered by intensified turbulence during a short period (see Figure 28,2a), leading to the release of additional POM into the water column, which absorbs dissolved pollutants. From April to August, in the stratified system, pollutants from the atmosphere bind with fresh detritus, transporting POPs to the sediments. Variations in concentrations are attributed to the specific properties of each POP and differences in atmospheric concentrations. During the summer season, all  $POP_{POM}$  accumulate in the sediment pool (refer to Figure 29, column d). In December, increased mixing releases all pollutants stored in the sediment, contributing to another peak of high  $POP_{POM}$  concentrations.

There is a distinct seasonality in  $POP_{free}$  concentrations, exhibiting a similar pattern in both scenarios for all POPs (refer to Figure 30, 31, 32, column b). When productivity halts in autumn and remaining OM remineralizes, absorbed pollutants in  $POP_{POM}$  are released back into the dissolved phase. Consequently,  $POP_{free}$  concentrations, nearly depleted by the end of summer, begin to accumulate again (refer to Figure 30, 31, 32, column b).

POP<sub>free</sub> peaks the following year when fresh OM is produced anew. This peak is more pronounced in the tidal scenario due to the higher content of POP<sub>POM</sub> and the smoother turbulent regime during winter, without pronounced high-intensity mixing events.

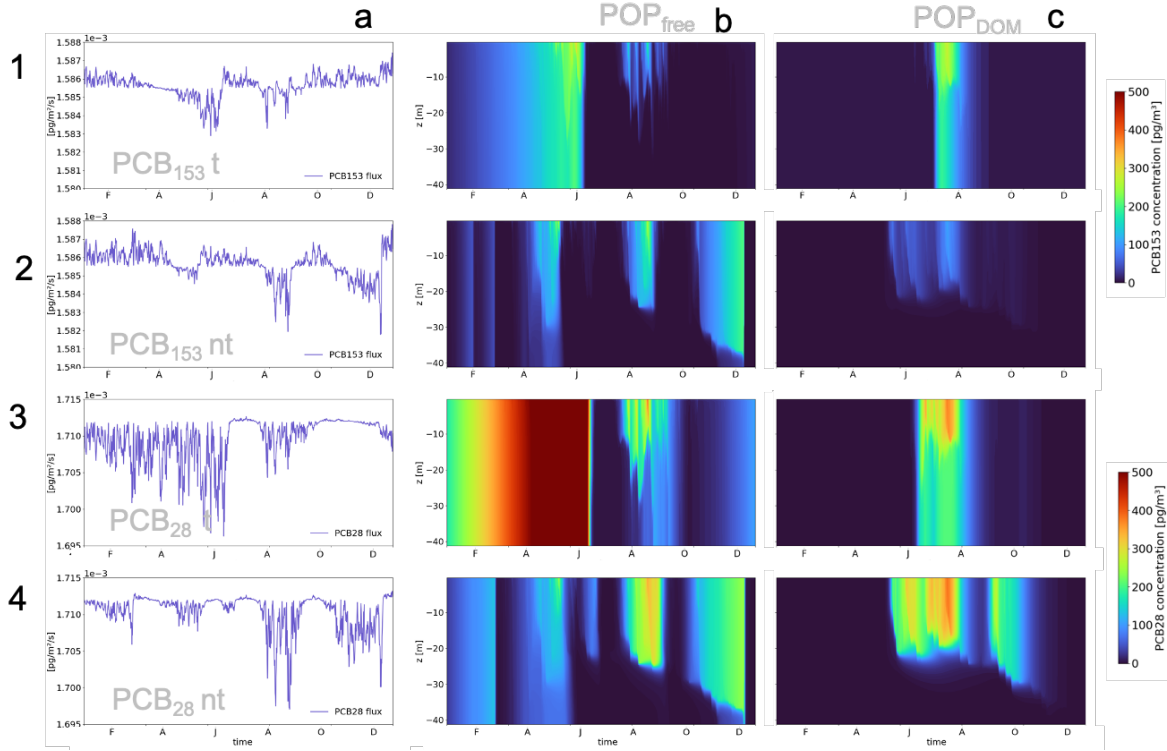


**Figure 31:** Results of PCB class simulations in SNS: column **a** - atmospheric flux of PCB ( $\text{pg m}^{-2} \text{ s}^{-1}$ ); column **b** - freely dissolved PCB<sub>free</sub> ( $\text{pg m}^{-3}$ ); column **c** - PCB<sub>DOM</sub> ( $\text{pg m}^{-3}$ ); row **1** - results for PCB<sub>153</sub> with tides; row **2** - PCB<sub>153</sub> without tides; row **3** - PCB<sub>28</sub> with tides; row **4** - PCB<sub>28</sub> without tides.

In regions characterized by high PFOA deposition rates and abundant DOM content, PFOA<sub>DOM</sub> is detected in substantial concentrations, exceeding  $2000 \text{ pg m}^{-3}$  in both scenarios (refer to Figure 32, column c). Towards the end of May through June, the SML undergoes a decline attributed to low wind speeds, resulting in the disruption between the SML and BML. With the elevated production of DOM, newly deposited PFOA predominantly binds directly to it. Furthermore, in the absence of resuspended POM, DOM becomes the primary organic matrix available for POP accumulation. However, this phenomenon is observed in both tidal and non-tidal scenarios across all POPs. The remarkably high concentrations of PFOA are primarily influenced by low wind speeds. Since PFOA is primarily influenced by SSA formation as the main pathway for outflux from water to atmosphere, under conditions of low wind speed and high deposition, PFOA accumulates in the water column at elevated concentrations.

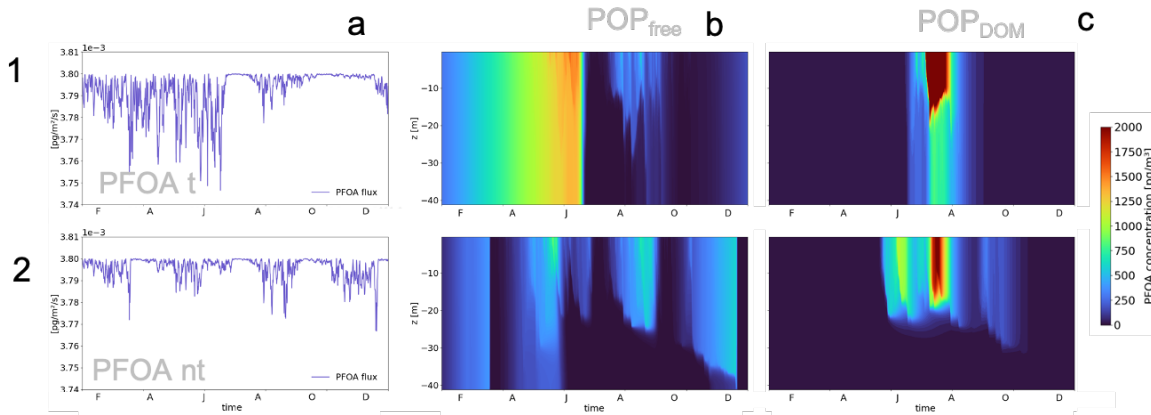


**Figure 32:** Results of PFOA class simulations in SNS: column **a** - atmospheric flux of PFOA ( $\text{pg m}^{-2} \text{s}^{-1}$ ); column **b** - freely dissolved PFOA<sub>free</sub> ( $\text{pg m}^{-3}$ ); column **c** - PFOA<sub>DOM</sub> ( $\text{pg m}^{-3}$ ); row **1** - results for PFOA with tides; row **2** - PFOA without tides.

To summarize, tidal activity enhances the overall load of POPs and particularly increases the concentration of bioavailable POP<sub>free</sub> by introducing additional organic matter through sediment resuspension. This organic matter, whether directly from sediments or indirectly through increased nutrient levels driving primary production, contributes to the retention of pollutants in the ocean. As POPs adsorbed onto organic matter gradually release into a dissolved form, POP<sub>free</sub> concentrations steadily rise over time. This phenomenon is noticeable across all pollutants, particularly during the winter season (see Figure 33).

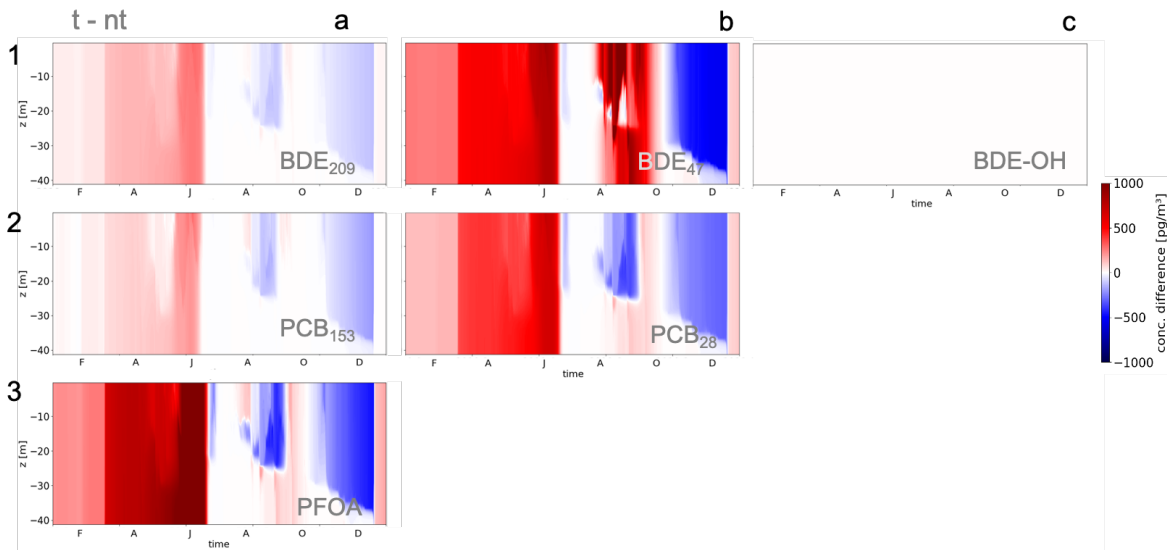


**Figure 33:** Differences in dissolved POP concentration ( $\text{pg m}^{-3}$ ) between tide–no-tide scenarios for SNS region: **1a** - BDE<sub>209</sub>; **1b** - BDE<sub>47</sub>; **1c** - BDE-OH; **2a** - PCB<sub>153</sub>; **2b** - PCB<sub>28</sub>; **3a** - PFOA.

In regions with increased biological production, a higher organic matter content accumulates POPs from their dissolved form, while elevated water column turbidity prevents

these pollutants from settling into the sediment. Both dissolved organic matter and detritus gradually release POPs back into the dissolved phase during remineralization. Consequently, in the SNS, the concentration of free POPs increases in the presence of tidal forces compared to scenarios without tides (Figure 33). During the initial phytoplankton bloom, dissolved POPs transition to the particulate organic matter matrix. The decline in POP concentrations observed in June and Autumn correlates with changes in OM distribution, as increased turbidity leads to the mixing of pollutants previously confined to the surface mixed layer (SML) throughout the water column in scenarios with tidal influence.

Notably, the concentration of BDE<sub>47</sub> experiences a significant increase in dissolved pollutants in June in tidal scenarios (Figure 33,1b). This phenomenon is driven by the high deposition of BDE<sub>47</sub>, its inability to return to the atmosphere, and its direct interaction with the abundant DOM. Consequently, dissolved concentrations rise in early June due to heightened atmospheric inflow, followed by further increases in late June to July via remineralization from DOM. Interestingly, the production of BDE-OH remains unaffected by tides in this region.

In the Southern North Sea, tidal activity leads to an increase in the concentration of dissolved forms of all five pollutants during the first four months of the year. Conversely, in the Northern North Sea, except for PFOA, most pollutants experience a decrease in April. By June, the scenario reverses: in the SNS, tides reduce the concentration of free POPs (with the exception of BDE<sub>47</sub>), while in the NNS, the opposite occurs. Overall, the variations in free POP concentrations are more pronounced in the SNS region, exceeding 1000 pg m<sup>-3</sup> compared to around 300 pg m<sup>-3</sup> in the NNS.

### 4.3 Changes in aquatic POPs distribution under the conditions of enhanced nitrate concentrations

The biological pump stands as a pivotal determinant in shaping the destiny of hydrophobic pollutants within marine ecosystems [Daewel et al., 2020]. This mechanism predominantly hinges on biological productivity, intricately intertwined with nutrient abundance in the environment. Elevated nutrient levels foster heightened concentrations of organic matter, thus catalyzing biological production. This study endeavors to explore the intricate interplay among nitrate (NO<sub>3</sub>) levels, biological productivity, and their consequential influence on the ultimate fate of POPs.

Over the course of the last three decades, there has been a noticeable decline of approximately 20% in the nitrogen load entering the Baltic Sea, stemming from both riverine influx and atmospheric deposition [Lønborg and Markager, 2021]. The actual nitrate (NO<sub>3</sub>) production varies across regions, contingent upon the prevailing biological processes orchestrating nutrient equilibrium. However, for the purposes of this investigation, which delves into the trajectory of POPs under varying biological scenarios, a uniform augmentation of 20% in NO<sub>3</sub> levels has been assumed across all simulated regions. Consequently, the system's response to extant POPs con-

centrations has been scrutinized, mirroring the broad trends of biological productivity prevalent during the 1990s.

#### **4.3.1 Gotland Basin - the stratified region of high nutrient content and UV irradiation**

Initially, nitrate ( $\text{NO}_3$ ) plays a pivotal role in regulating the production of organic matter in marine environment. The presence of hydrophobic organic pollutants is intricately linked to the quantity of OM within the system. Pollutants with a strong affinity to accumulate on particulate organic matter (detritus) are likely to exhibit higher concentrations in sediment. When the system undergoes heightened biological production due to elevated nitrate levels, it isolates more of these pollutants, effectively removing them from the water column through sedimentation. This process influences the atmospheric flux, resulting in an increased transfer of POPs from the atmosphere to the water column. This phenomenon is notably evident with higher substituted congeners such as BDE<sub>209</sub> and PCB<sub>153</sub>.

The hydrodynamic dynamics within the Gotland Basin establish conditions where dissolved organic matter and newly introduced dissolved POPs remain distinct from pollutants adhering to detritus. Despite the region boasting high biological productivity, the absence of resuspended detritus at the surface layer facilitates substantial UV irradiation. This phenomenon is attributed to enhanced light penetration facilitated by the basin's lower latitude relative to the Bothnian region.

In regions like the Gotland Basin, increased organic matter production due to high nitrate content results in a generally high flux of pollutants into the aquatic system. This leads to increased concentrations in the water column and especially in the sediment (Figure 34, columns b and d).

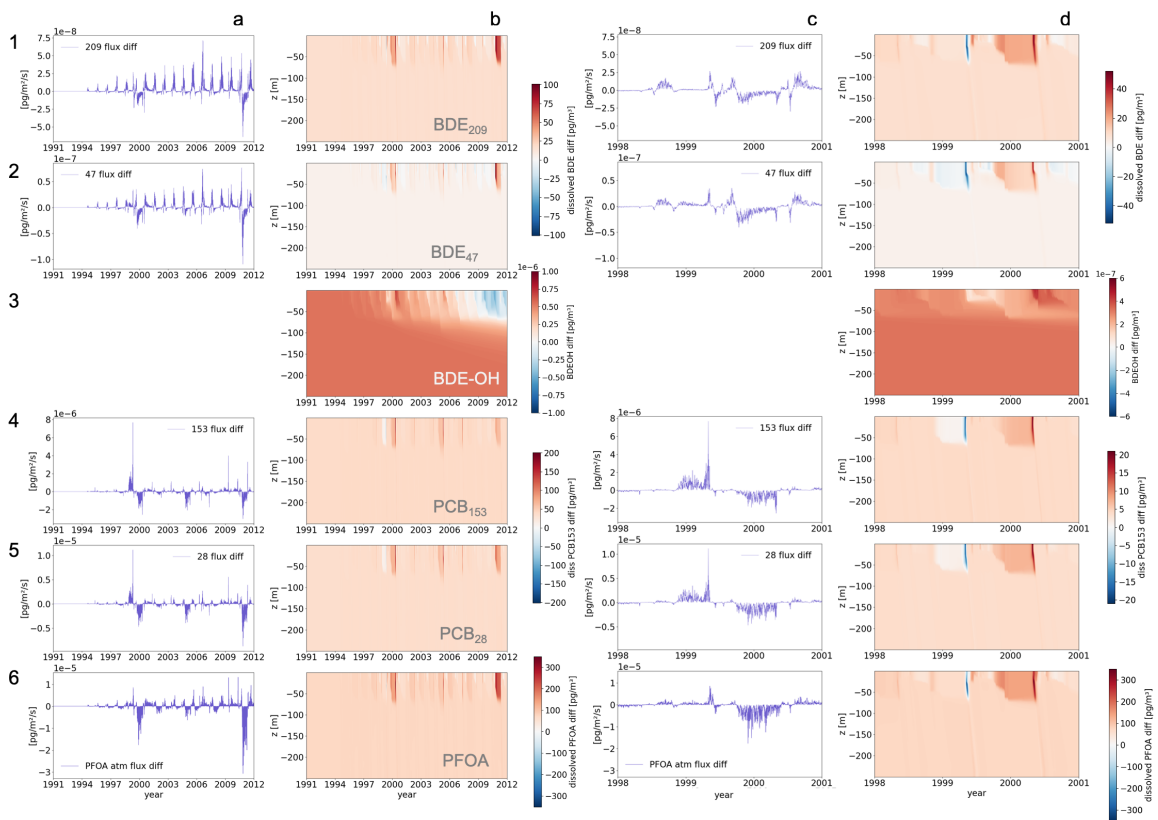


**Figure 34:** Differences in simulation between high-normal  $NO_3$  levels in Gotland Basin: column **a,c** - differences in atmospheric flux, simulations of 20 year and 3 year ( $pg\ m^{-2}\ s^{-1}$ ); column **b,d** - differences in dissolved concentrations of POP simulations of 20 year and 3 year ( $pg\ m^{-3}$ ); row **1** - BDE<sub>209</sub>; row **2** - BDE<sub>47</sub>; row **3** - BDE-OH; row **4** - PCB<sub>153</sub>; row **5** - PCB<sub>28</sub>; row **6** - PFOA.

The Gotland Basin is characterized by a deep water column and clear stratification, which diminishes the impact of POM on dissolved pollutants. When detritus is produced, it sinks, carrying all adsorbed POPs away from the surface layer. However, atmospheric input of POPs and biological production occur in the surface layer, leading to an overall increase in dissolved concentrations of all POPs (Figure 34, columns b and d).

In years with particularly high OM production (e.g., 1999, Figure 34, column d), detritus and DOM remove some dissolved POPs, resulting in decreased dissolved concentrations (Figure 35, column d). This effect is most pronounced for pollutants with the highest affinity for POM or DOM, such as PCBs and BDE<sub>47</sub> (Figure 34, d2, d4, d5). In years with lower bioproduction (e.g., 2000, Figure 34, column d), the opposite effect occurs, with increased dissolved concentrations of all five POPs.

In 1999, high  $NO_3$  levels contributed to an early phytoplankton bloom, increasing OM production early in the year (Figure 35, column d). This OM removed dissolved POPs mixed within the SML during winter. In contrast, in 2000, a late cyanobacteria bloom increased POM production, allowing pollutants to accumulate in the dissolved phase throughout the year, with

concentrations dropping in August (Figure 34, column d).

With increased concentrations of BDEs in the system, the production of BDE-OH also rises (Figure 34, 3b, 3d). Initially, the increased inflow of atmospheric pollutants serves as the limiting factor in the system. However, over time, the increased production of OM shifts the balance of factors influencing BDE-OH formation. Although high OM content enhances the diffusive flux from the atmosphere (Figure 34, 1a, 2a) and high  $NO_3$  levels boost OH radical production, it also reduces the amount of UV light in the surface water layer. Consequently, after 17 years (by 2008), UV irradiation becomes the limiting factor in BDE-OH formation (Figure 34, 3b). As a result, although BDE-OH concentrations increase in the water column, after 17 years of elevated  $NO_3$  concentrations, the BDE-OH concentration in the SML decreases, removing this dangerous pollutant from the zone of biological production.

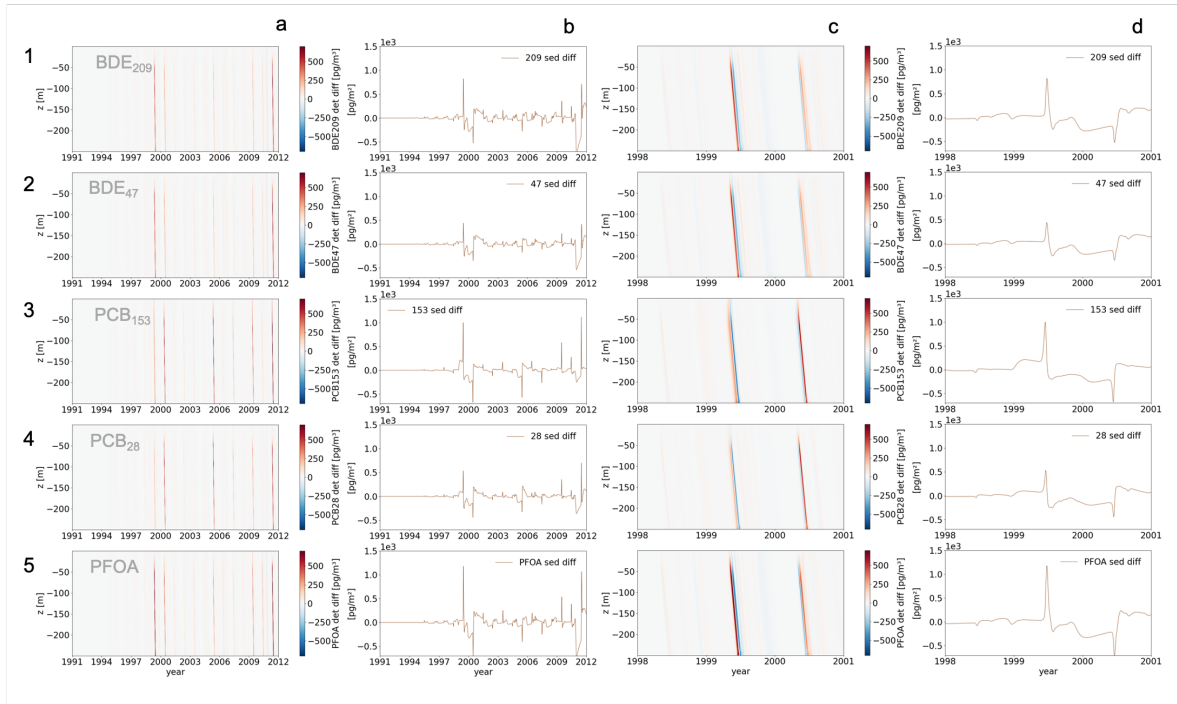


**Figure 35:** Differences in simulation between high-normal  $NO_3$  levels in Gotland Basin: column **a,c** - differences in concentrations of POP on POM ( $pg\ m^{-3}$ ); column **b,d** - differences in sediment concentrations of POP ( $pg\ m^{-2}$ ); row **1** - BDE<sub>209</sub>; row **2** - BDE<sub>47</sub>; row **3** - PCB<sub>153</sub>; row **4** - PCB<sub>28</sub>; row **5** - PFOA.

Changes in sediment concentrations are influenced by shifts in POM production within the system (Figure 35). In years when bioproduction is enhanced early in the year, the sediment concentration of POPs also increases early, with a ratio shift towards HSCs (Figure 35, 1d, 2d, 3d, 4d). Later in the year, the concentrations of all POPs in sediment decrease more gradually over a longer time frame (Figure 35, column d; year 1999). The total annual concentration of POPs in this region does not change significantly, but there is a noticeable shift in the distribution pattern.

In years with reversed OM production patterns, the decrease in sediment concentration early in the year shows a sharp pattern (e.g., May 2000), followed by a sharp increase in concentration. The pool of dissolved POPs increases during these years due to higher atmospheric input from the previous year and release from DOM via remineralization (Figure 34, columns c and d). The late bloom of cyanobacteria is less pronounced but extends over a longer period. This results in a less intense peak of OM production compared to the previous year, but it is sustained over a longer time frame. Consequently, pollutants on POM accumulate more slowly but over an extended period, leading to less intense but prolonged accumulation of all five POPs in sediment in 2000 (Figure 34, column d). As a result, the total concentration of all POPs in sediment increases compared to the previous year, with a dynamic rise in sediment pollutant content later in the year (Figure 34, column d; August-December 2000).

#### 4.3.2 Bothnian Bay - the region of low UV irradiation and winter sea ice coverage

The Bothnian Bay, located considerably farther north than the Gotland Basin, is characterized by distinct environmental factors. These include diminished UV irradiation owing to higher latitudes, lower atmospheric concentrations of persistent organic pollutants, the occurrence of sea ice formation, and heightened turbulence within the aquatic regime. Each of these system parameters exerts discernible effects on both biological productivity and the fate of POPs within the marine ecosystem. The interplay of factors such as elevated nitrate concentrations, prevailing mixing regimes, and the presence of sea ice governs the dynamics of organic matter production. Consequently, these factors collectively shape the distribution patterns of POPs throughout the marine environment.

The intense mixing regime in Bothnian Bay creates conditions where resuspended detritus from sediment interferes with areas of biological production, leading to increased sorption of pollutants on detritus throughout the year. Winter sea ice hampers the exchange of aquatic POPs with the atmosphere, resulting in reduced inflow and, consequently, a decrease in their overall total concentration (Figure 36, column b). This trend is particularly pronounced for the BDE and PCB classes. In the case of PFOA, sea ice restricts aerosol formation, thereby decreasing the outflow of dissolved PFOA back to the atmosphere. Consequently, the input of atmospheric pollutants to the water column increases, leading to a rise in dissolved PFOA concentration as well (Figure 36, a6, b6).

Although the total concentration of dissolved PFOA in the water column is slightly higher with a higher content of organic matter in the system, during the summer phytoplankton blooms, surface concentrations decrease for all POPs, including PFOA (Figure 36, column d). The most significant decreases in dissolved POP concentrations are observed for LSCs. With a mixture of higher content of both POM and DOM within the water column, more LSCs have the chance to sorb on detritus, leading to an increase in the concentration of these POPs in sediment over time (Figure 37, column b). Additionally, with low atmospheric concentrations and sea ice, the outflow of POPs from the water column decreases, especially for light, mobile PCB<sub>28</sub>, reducing its diffusive atmospheric flux (Figure 37, 4b; Figure 36, 5a).

The chosen persistent organic pollutants persistently accumulate on dissolved organic matter and/or particulate organic matter. The dissolved fraction of these pollutants is orders of magnitude lower compared to the Gotland Basin. An increase in nitrate leads to a higher rate of pollutant partitioning to organic matter, creating space for new atmospheric POPs to enter the water column. However, due to low atmospheric concentrations, the direction of the diffusive pump at the air-sea border does not change significantly. While this process is similar to that in the Gotland Basin, it is constrained by sea ice formation, which limits the exchange of aquatic POPs with the atmosphere.

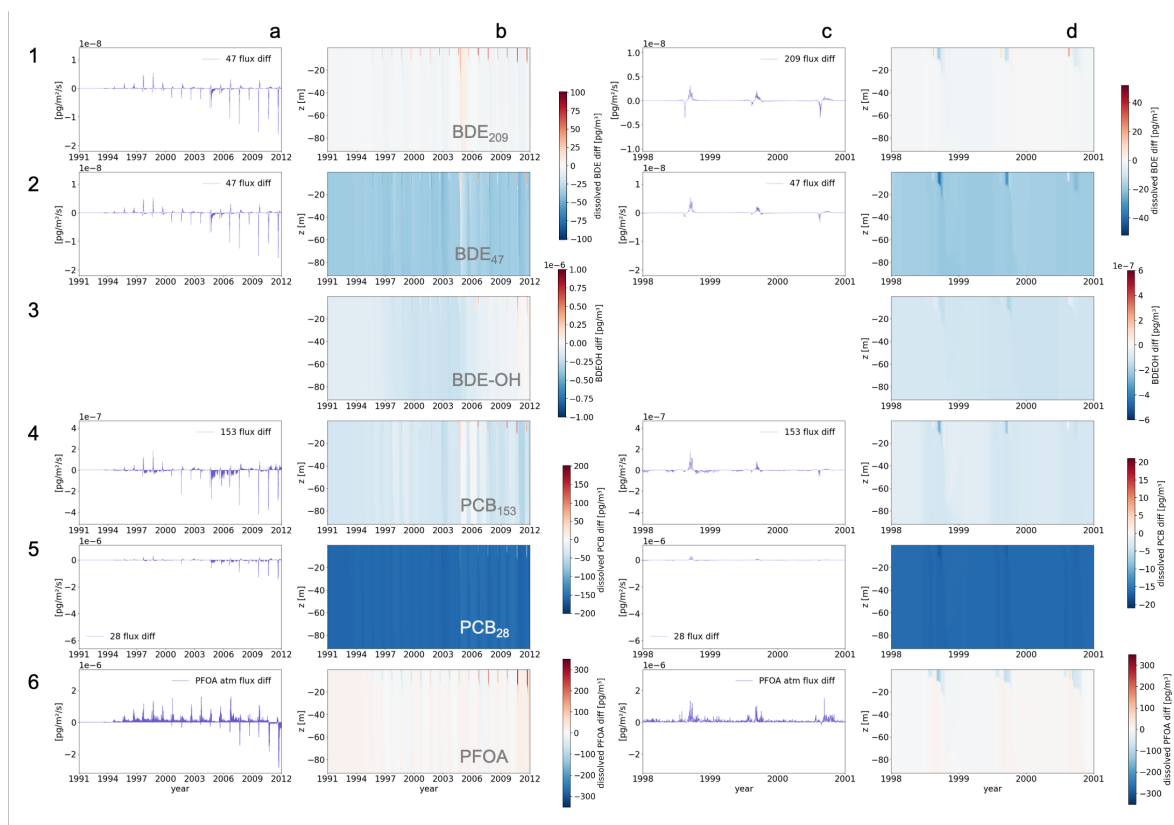


**Figure 36:** Differences in simulation between high-normal  $\text{NO}_3$  levels in Bothnian Bay: column **a,c** - differences in atmospheric flux ( $\text{pg m}^{-2} \text{s}^{-1}$ ); column **b,d** - differences in dissolved concentrations of POP ( $\text{pg m}^{-3}$ ); row **1** - BDE<sub>209</sub>; row **2** - BDE<sub>47</sub>; row **3** - BDE-OH; row **4** - PCB<sub>153</sub>; row **5** - PCB<sub>28</sub>; row **6** - PFOA.

Similar to the dynamics of POPs on detritus in the Gotland Basin region, here, a higher amount of POM early in the year increases the sorption of POPs earlier in the year and decreases later (Figure 37, column c). This effect is more pronounced for HSCs, which have a higher affinity for detritus. This results in a shift in the accumulation pattern in sediment, increasing the HSC content in early summer. Since BDEs have the lowest atmospheric concentrations in this region and cannot be released back into the atmosphere, the increased OM content in the system does not make a significant difference in their concentrations on POM and in sediment (Figure

37, 1c, 2c, 1d, 2d).

The dynamics in sediment distribution change for PCBs that are more oriented towards OM. However, due to the low POP concentrations in the system, these changes do not have a wide-ranging impact (Figure 37, 3c, 3c, 4d, 4d).

With increased dissolved concentrations of PFOA, the rates of sorption and desorption on detritus also rise. With the altered pattern of bioproduction and high dissolved PFOA content, concentrations of  $\text{PFOA}_{\text{POM}}$  increase early in May (refer to Figure 37,5c; May). Due to high bottom mixing in summer, the distribution pattern of  $\text{POP}_{\text{POM}}$  concentrations in the bottom mixed layer is less distinct than at the surface. Increased availability of nitrate leads to a generally sharper pattern in OM production, which, in turn, decreases  $\text{POP}_{\text{POM}}$  in June. With the bloom of cyanobacteria in August-September, more dissolved PFOA binds with detritus, leading to a second peak in  $\text{PFOA}_{\text{POM}}$  concentration (refer to Figure 37,5c; August-September). Over the years, this change in OM production pattern and high bottom resuspension not only alter the dynamics in sediment concentration of PFOA but also decrease it over time (Figure 37,5b). This is attributed to the higher affinity of PFOA to water and its higher concentration in the dissolved phase.

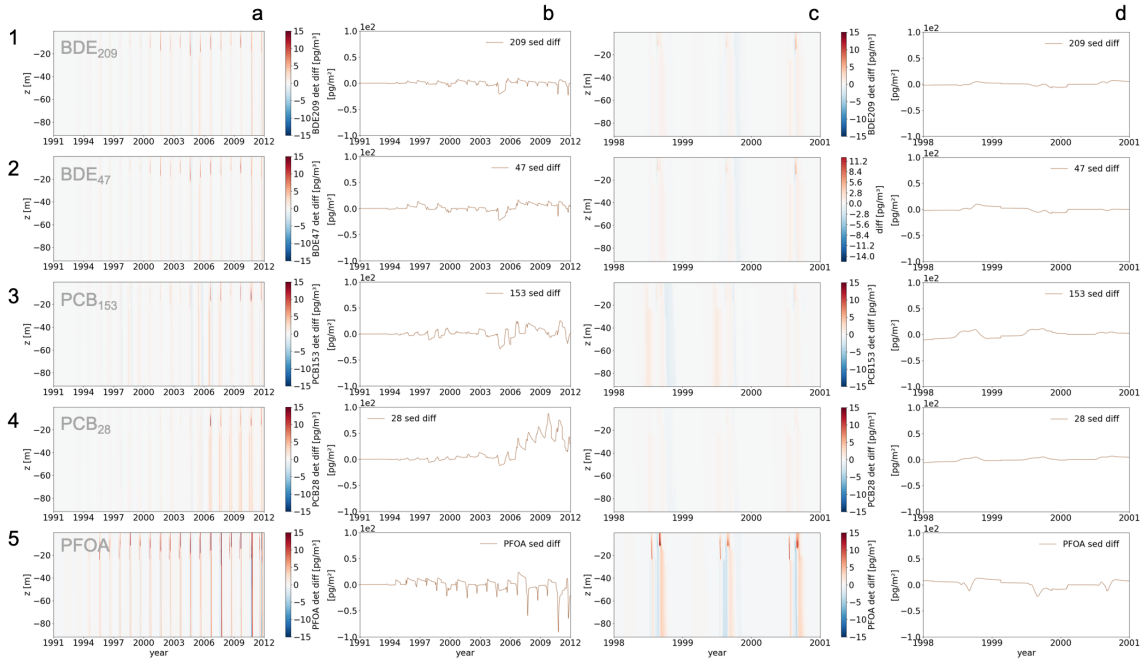


**Figure 37:** Differences in simulation between high-normal  $\text{NO}_3$  levels in Bothnian Bay: column **a,c** - differences in concentrations of POP on POM ( $\text{pg m}^{-3}$ ); column **b,d** - differences in sediment concentrations of POP ( $\text{pg m}^{-2}$ ); row **1** -  $\text{BDE}_{209}$ ; row **2** -  $\text{BDE}_{47}$ ; row **3** -  $\text{PCB}_{153}$ ; row **4** -  $\text{PCB}_{28}$ ; row **5** - PFOA.

In summary, the higher content of  $\text{NO}_3$  in the water column in Bothnian Bay leads to a decrease in the concentration of dissolved BDEs and PCBs due to a shift in distribution between

phases, with more hydrophobic POPs attaching to detritus. For LSC PCB<sub>28</sub>, this change in conditions results in a higher ability to bind with POM, leading to an increase in the sediment concentration of this congener. However, the dynamics of PFOA present the opposite picture. Due to its low affinity for diffusive flux and restricted outflux with sea salt aerosols in winter, PFOA accumulates in the water column over time. Higher dissolved concentration also leads to an increase in sorption on initially developed POM, with slight decreases occurring between phytoplankton blooms. Low wind speeds in the summer season result in higher deposition, and with remineralization from dissolved organic matter, PFOA concentrations on POM increase even further with cyanobacteria blooms later in the year.

For all POPs, an increase in NO<sub>3</sub> concentrations leads to shifts in the temporal distribution of pollutants in sediment.

Furthermore, due to the decrease in dissolved concentrations of BDEs and low UV irradiance levels in the water column, BDE-OH concentrations decrease compared to scenarios with normal nutrient content.

#### 4.3.3 Northern North Sea - seasonally stratified area of high nutrients content and UV irradiation

Despite the stratification characteristic of the North North Sea during the summer season, the region experiences bottom mixing, which prevents organic matter and pollutants from accumulating in the sediments throughout the year. The system's high nutrient content drives substantial biological production. However, the stratified water column in summer limits the ability of resuspended particulate organic matter to reach areas of active biological production. Under these conditions, elevated nitrate levels in the system further stimulate OM production. Additionally, the region is subject to high wind speeds, which influence the exchange of dissolved pollutants with the atmosphere. Furthermore, the North Sea is exposed to elevated atmospheric concentrations of POPs due to its proximity to industrial sources in surrounding countries.

Similar to the Bothnian Bay case, here increased content of OM shifts the ration between dissolved phase and sorbed on detritus. For NNS, not only detritus, but also DOM plays important role in pollutant distribution. Resuspended along with water column high content of POM insures the long storage of POPs on this matrix, however it is spread within water column. This can be observed in decreasing of POP<sub>free</sub> concentration for all five POPs (Figure 38, column b,d). In opposite to Bothnian Bay, here high wind speed and absance of sea ice provide substantial rate of SSA formation, insuring an outflux of PFOA from the system (Figure 38,6a). Atmospheric flux slightly increases over time of phytoplankton blooms. With time, when pollutants are released from DOM, it shortly increases dissolved concentration of PFOA, impacting removal of it with aerosol formation. Similar to the scenario in the Bothnian Bay, the increased content of organic matter in the North North Sea shifts the balance between pollutants in the dissolved phase and those sorbed onto detritus. In the NNS, both detritus and DOM play crucial roles in the distribution of pollutants. The resuspension of particulate organic matter throughout the water column ensures the prolonged storage of POPs within this matrix, although it becomes distributed throughout the water column. This distribution results in a decrease in the freely

dissolved concentrations of all five POPs (Figure 38, columns b and d).

In contrast to the Bothnian Bay, the NNS experiences high wind speeds and lacks sea ice, which facilitates a substantial rate of sea-spray aerosol formation. This dynamic ensures an effective outflux of PFOA from the system (Figure 38, 6a). The atmospheric flux of pollutants increases slightly during phytoplankton blooms. Over time, as pollutants are released from DOM, there is a brief increase in the dissolved concentration of PFOA, enhancing its removal via aerosol formation (Figure 38,6c,6d). For other POPs, remineralization from DOM leads to less pronounced negative variations compared to the normal nitrate content scenario.

Under conditions of decreased concentrations of dissolved BDEs, the concentration of BDE-OH also declines (Figure 38,3b,3d). The formation of BDE-OH is dependent on the production of OH radicals, UV irradiation, and the concentration of the parent POPs, restricting its formation to the surface mixed layer. However, due to the winter mixing regime, BDE-OH from the SML is dispersed throughout the entire water column. This results in the distribution of BDE-OH across the full depth of the water column, unlike the Gotland area where BDE-OH was confined to the surface. In the scenario with elevated nitrate levels, the concentration of BDE-OH decreases throughout the entire water column.

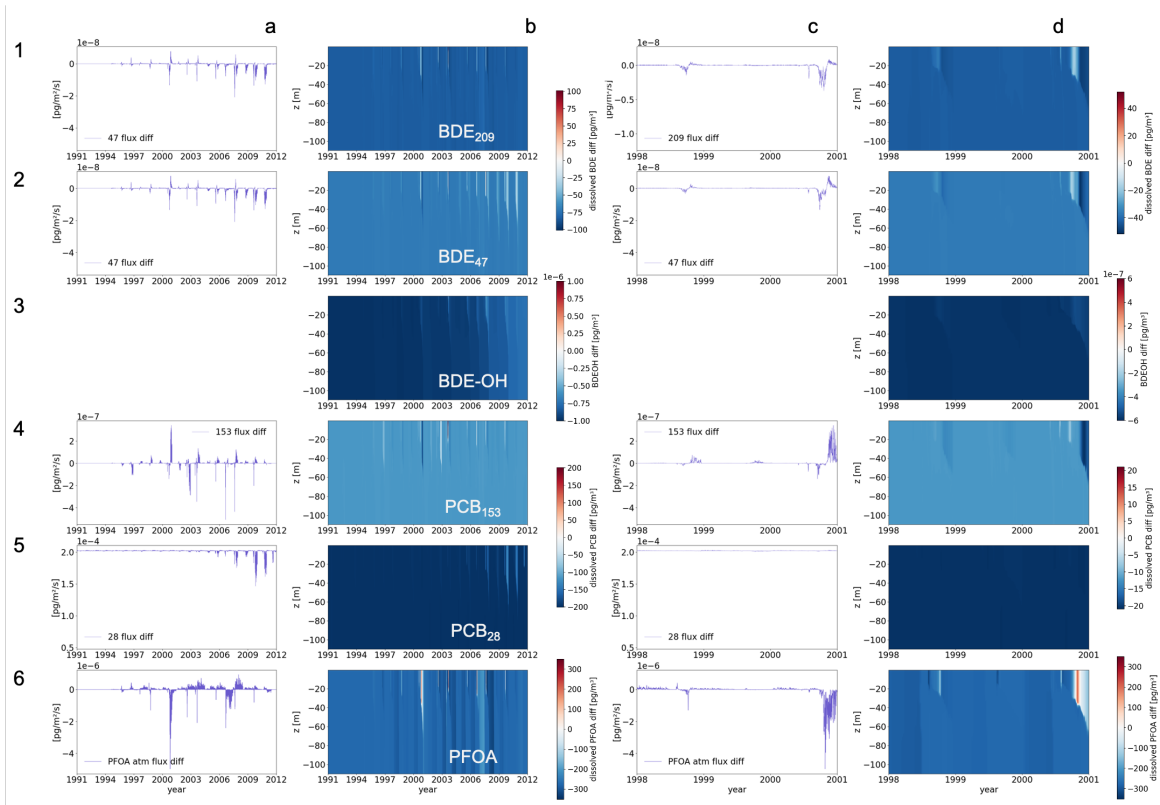


**Figure 38:** Differences in simulation between high-normal  $NO_3$  levels in Northern North Sea location: column **a,c** - differences in atmospheric flux ( $pg\ m^{-2}\ s^{-1}$ ); column **b,d** - differences in dissolved concentrations of POP ( $pg\ m^{-3}$ ); row **1** - BDE<sub>209</sub>; row **2** - BDE<sub>47</sub>; row **3** - BDE-OH; row **4** - PCB<sub>153</sub>; row **5** - PCB<sub>28</sub>; row **6** - PFOA.

Tidal activity in the NNS injects additional kinetic energy into the bottom mixed layer, preventing POPs from settling into sediment. The physical conditions in this region play a more significant role in determining the fate of OM and associated POPs than biological processes. Since POPs cannot be stored in sediment, the additional OM in the system, due to increased nitrate levels, does not alter the sedimentation pattern in the NNS (Figure 39, columns b and d). Instead, it influences the flux of  $POP_{POM}$  to and from the sediment, which is related to shifts in biological production. This, in turn, affects the temporal distribution of POP-POM in the water column.

In general, a higher content of detritus in the system alters the distribution of POPs between the dissolved and particulate phases in the water column. This trend is consistently observed across all simulated regions, including the NNS (Figure 39, column a). The presence of more detritus enhances the sorption of POPs onto particulate matter, thereby reducing their concentration in the dissolved phase.

Importantly, this dynamic fluctuates from year to year, altering the OM content in the system. In some years, increased nitrate levels have little impact on pollutant content on detritus (Figure 39, column c; year 1999). In other years, changes in biological dynamics lead to ef-

fects similar to those observed in previous regions, with high detritus content early in the year removing dissolved pollutants. This results in decreased concentrations of  $\text{POP}_{\text{POM}}$  with the subsequent phytoplankton bloom. However, later in the year, remineralized POPs from DOM become a source for a late  $\text{POP}_{\text{POM}}$  peak (Figure 39, column c; year 2000).

For  $\text{PCB}_{28}$ , which has elevated concentrations in this region (see section 4.2), the higher amount of detritus in the system helps to stabilize the system by decreasing dissolved  $\text{PCB}_{28}$  concentration and reducing its outflux back to the atmosphere. This stabilization is evidenced by the increased sorption of  $\text{PCB}_{28}$  onto particulate organic matter, leading to a permanent rise in  $\text{PCB}_{28\text{POM}}$  concentration, as shown in Figure 39, 4a and 4c. Over time, this increased concentration also enhances the exchange of  $\text{PCB}_{28\text{POM}}$  with sediments, elevating the flux between the water column and sediment (Figure 39,4b).

PFOA associated with POM exhibits higher fluctuations in this region due to the elevated organic matter content. Generally, PFOA deposition is high in the North Sea, leading to elevated dissolved concentrations. With an increased POM content in the system, more dissolved POPs rapidly accumulate on the condensed, high amount of detritus. This, in turn, reduces the availability of dissolved PFOA for accumulation during late OM blooms. Since PFOA is not significantly affected by diffusive atmospheric flux, the decrease in dissolved concentrations does not substantially increase the atmospheric influx of PFOA into the water column but rather decreases its removal via aerosol formation. The final peak in PFOA associated with POM in the year 2000 (Figure 39, 5c) is attributed to an increase in dissolved pollutants resulting from DOM remineralization.

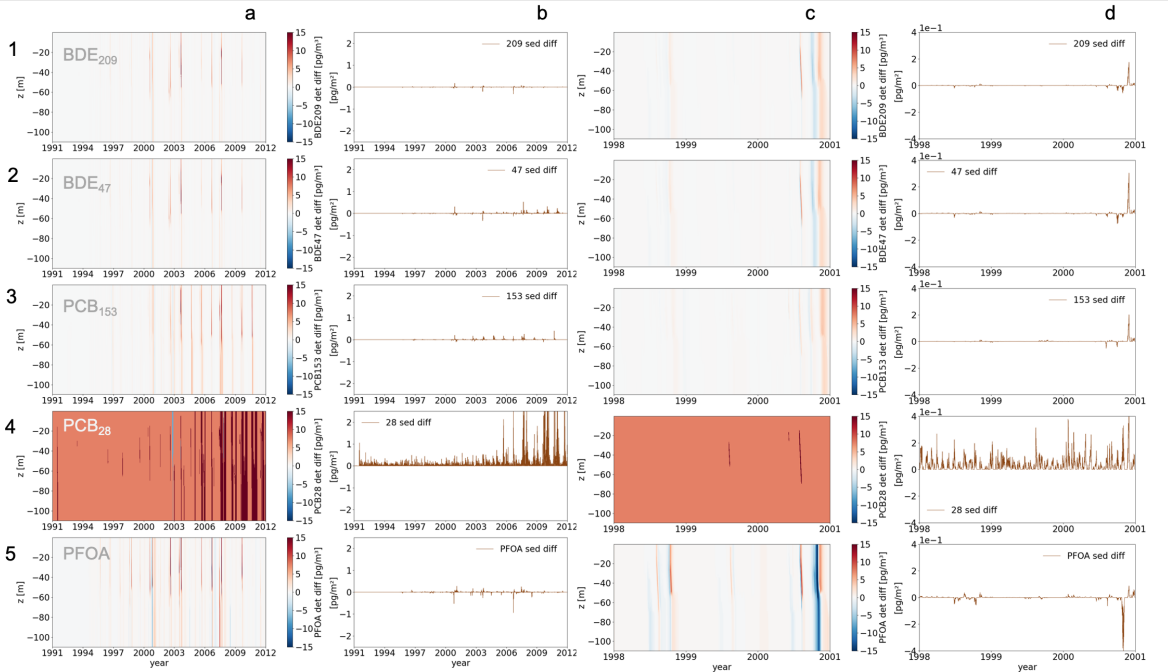


**Figure 39:** Differences in simulation between high-normal  $\text{NO}_3$  levels in Northern North Sea location: column **a,c** - differences in concentrations of POP on POM ( $\text{pg m}^{-3}$ ); column **b,d** - differences in sediment concentrations of POP ( $\text{pg m}^{-2}$ ); row **1** - BDE<sub>209</sub>; row **2** - BDE<sub>47</sub>; row **3** - PCB<sub>153</sub>; row **4** - PCB<sub>28</sub>; row **5** - PFOA.

In summary, elevated nitrate concentrations in the Northern North Sea lead to a decrease in the dissolved concentrations of all persistent organic pollutants, shifting the balance towards pollutants sorbed in detritus ( $\text{POP}_{\text{POM}}$ ). The continuous turbulence in the bottom mixed layer prevents the accumulation of pollutants in the sediment, and increased organic matter content only affects the fluxes between  $\text{POP}_{\text{POM}}$  and the sediment.

#### 4.3.4 Southern North Sea - shallow permanently mixed region with high UV irradiation and high biological production

The southern North Sea is characterized by its shallow water depth and abundant nutrient content, which fosters significant bioproduction. Tidal activity notably enhances bottom mixing in this region, and due to its limited depth, this phenomenon leads to interference between the Bottom Mixed Layer and Surface Mixed Layer. In an environment enriched with nitrate, this region experiences heightened bioproduction even in scenarios without elevated nitrate levels. Consequently, the distribution of pollutants between organic matter and the dissolved phase is established. Although increased nitrate levels augment the OM content in the system, they do not alter the temporal production dynamics.

Overall, the increased organic matter content in the system exhibits a similar effect on the fate of dissolved pollutants as observed in previous cases - concentrations tend to decrease (Fig-

ure 40, column b). Despite the high atmospheric concentrations of all POPs in the Southern North Sea, the additional OM in the water column does not significantly alter the diffusive pump mechanism (Figure 40, column a). However, a clear seasonality is evident in the case of heavy brominated flame retardants (BDEs) (Figure 40, 1c,2c). With a higher amount of OM present in the system, the overall decrease in atmospheric flux is less pronounced.

Although the overall dissolved concentrations of the five POPs decreased, there were specific years where all of them exhibited temporary increases. In 1999, the surface mixed layer experienced reduced turbulent kinetic energy due to slower wind speeds. This created conditions where the SML and BML briefly separated. The presence of a high amount of nutrients and increased light led to a surge in biological production, and consequently, an increase in organic matter content. Lower substituted congeners, which have a higher tendency to sorb onto DOM, accumulated on it. Over time, remineralization caused their release from DOM. All these pollutants remained dissolved in the surface layer, leading to increased concentrations of BDE<sub>47free</sub> and PCB<sub>28free</sub> (Figure 40, columns 2d and 5d). BDE<sub>47</sub>, having a lower atmospheric input compared to PCB<sub>28</sub>, was absorbed by DOM without significant changes in BDE<sub>47POM</sub> concentrations (Figure 41, column 2c). In contrast, PCB<sub>28</sub> is more mobile both within aquatic phases and at the air-water interface. This mobility means that differences in concentrations between air and water intensified the diffusive pump, leading to periods of elevated PCB<sub>28</sub> influx from the atmosphere when dissolved concentrations were particularly low (Figure 40, column 5c). Additionally, this process increased the concentration of PCB<sub>28</sub> on detritus (Figure 41, column 4c).

Highly substituted congeners HSCs and PFOA exhibit a stronger affinity for particulate organic matter. This characteristic significantly influences their accumulation on detritus and their dissolved concentrations in the subsequent year, 2000 (Figure 40, columns 1d, 4d, 6d; Figure 41, columns 1c, 3c, 5c). The year 2000 is patterned by increased wind speeds and elevated turbidity throughout the entire year. These conditions made POM more accessible to atmospheric pollutants and facilitated the accumulation of available dissolved POPs throughout the entire water column. Initially, this led to an increase in POP<sub>POM</sub> concentrations. However, through the process of remineralization, the dissolved concentrations of these pollutants also rose for a brief period (Figure 40, columns 1d, 4d, 6d; year 2000).

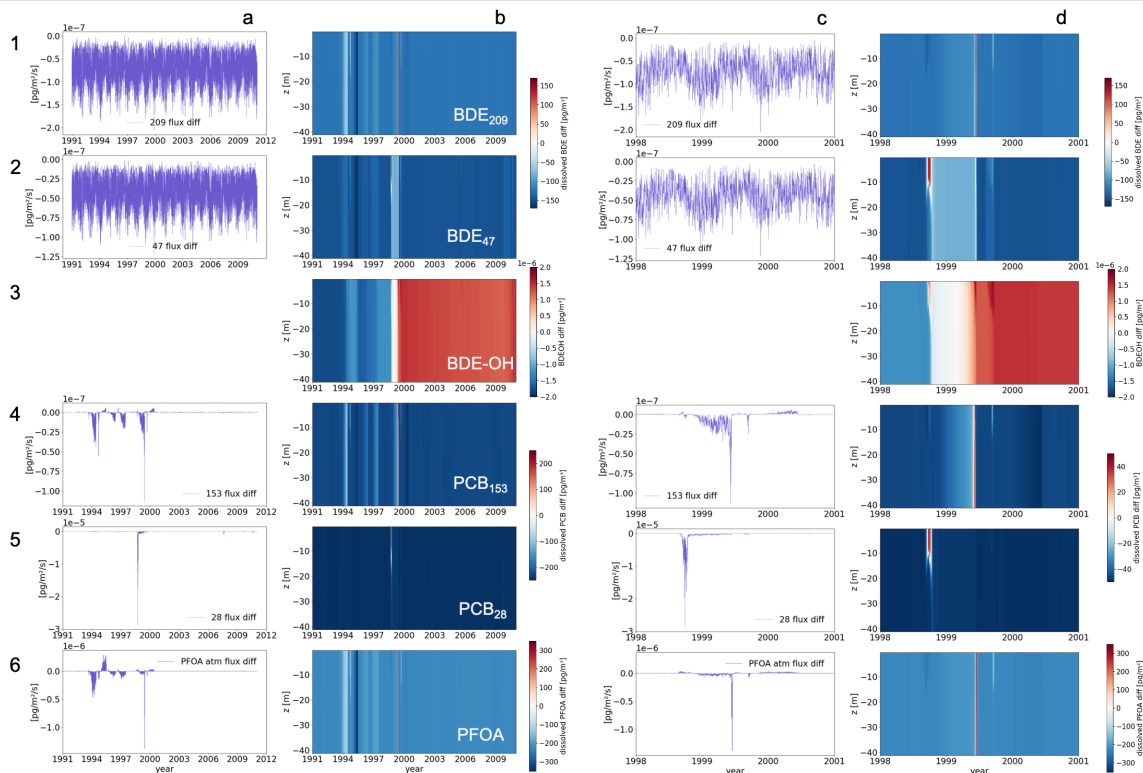


**Figure 40:** Differences in simulation between high-normal  $\text{NO}_3$  levels in Southern North Sea: column **a,c** - differences in atmospheric flux ( $\text{pg m}^{-2} \text{s}^{-1}$ ); column **b,d** - differences in dissolved concentrations of POP ( $\text{pg m}^{-3}$ ); row **1** - BDE<sub>209</sub>; row **2** - BDE<sub>47</sub>; row **3** - BDE-OH; row **4** - PCB<sub>153</sub>; row **5** - PCB<sub>28</sub>; row **6** - PFOA.

Following the examples of previous regions, the high bottom mixing in the southern North Sea prevents the accumulation of sediments. Consequently, all changes in POP concentrations in sediments primarily reflect variations in detritus concentration. The increased POM content associated with pollutants results in elevated fluxes to the sedimentation pool (Figure 41, columns b and d).

Although increased nitrate content in this region generally does not impact changes in  $\text{POP}_{\text{POM}}$  concentrations and decreases dissolved concentrations of the five POPs, it has an interesting effect on the production of BDE-OH.

Changes in  $\text{NO}_3$  content in aquatic systems have a profound impact on the fate of POPs beyond just the elevated content of organic matter matrices. An increase in nitrate concentration also affects photolytic processes. As the water column accumulates more organic matter particles, there is less light available for photolysis. Higher  $\text{NO}_3$  values lead to a decrease in direct UV irradiation, which affects all photon fluxes in the system, primarily impacting direct photolysis. Consequently, pollutant molecules receive less energy and fewer photons, resulting in a decreased rate of transformation.

However, the SNS is characterized by high turbidity and elevated biological production, which hinders light penetration. This means that even without extra nitrate, photon flux is low here, leading to a lower rate of photolytic processes.

From another perspective, high levels of DOM and nitrate  $\text{NO}_3$  can promote the generation of hydroxyl radicals  $\text{OH}\cdot$ . Although photon flux decreases, high concentrations of photoreactive species enhance the rate of indirect photolysis. Consequently, the formation of the previously mentioned BDE-OH also increases with high concentrations of extremely reactive  $\text{OH}$  radicals.

Following a period of intense mixing in 1999, the introduction of additional nitrate ceased to influence bioproduction or alter the concentration of  $\text{POP}_{\text{POM}}$ . However, within this scenario, the excess nitrate within the system affects the photolysis of BDE, shifting it from direct photolytical debromination towards indirect photolytical hydroxylation, thereby leading to the formation of BDE-OH. Since the nitrate remains unused for bioproduction, it persists within the system, thereby amplifying the production of  $\text{OH}$  radicals. This sequence of events results in an increase in toxic BDE-OH concentrations in southern North Sea region (Figure 40, 3b).

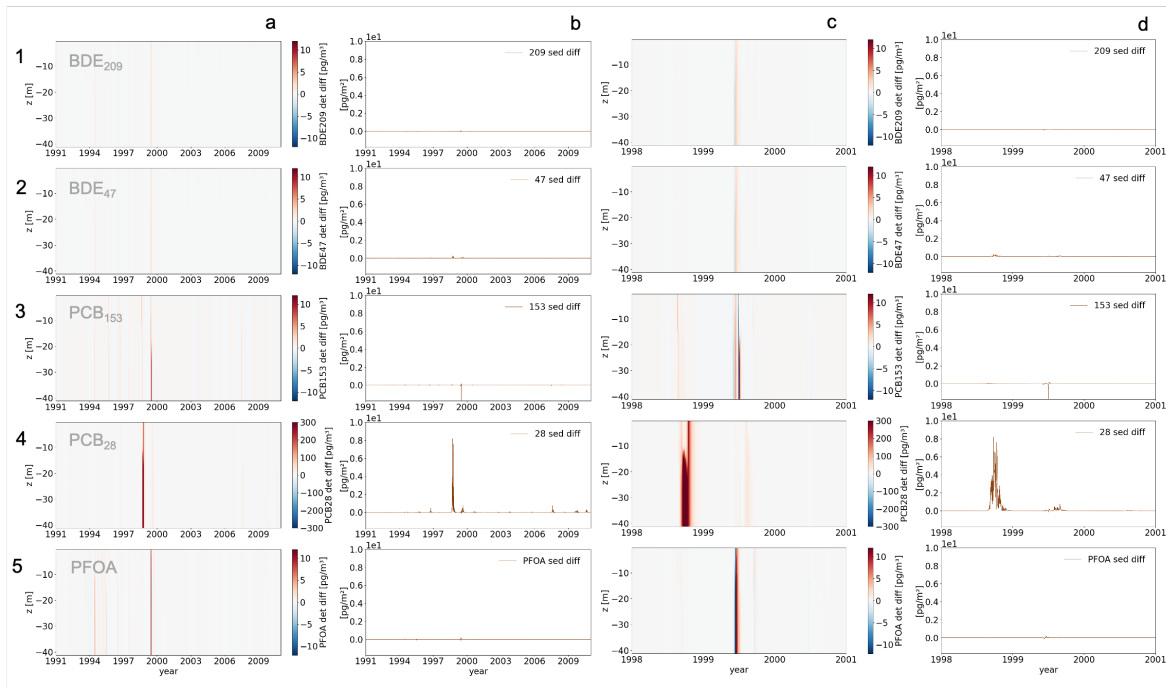


**Figure 41:** Differences in simulation between high-normal  $\text{NO}_3$  levels in Southern North Sea location: column **a,c** - differences in concentrations of POP on POM ( $\text{pg m}^{-3}$ ); column **b,d** - differences in sediment concentrations of POP ( $\text{pg m}^{-2}$ ); row **1** - BDE<sub>209</sub>; row **2** - BDE<sub>47</sub>; row **3** - PCB<sub>153</sub>; row **4** - PCB<sub>28</sub>; row **5** - PFOA.

In regions with high nutrient content, increased nitrate levels lead to a decrease in the dissolved concentration of POPs due to the higher availability of organic matter. However, the high turbidity in these regions evens out  $\text{POP}_{\text{POM}}$  concentrations throughout the year, resulting

in less pronounced pattern differences. During years of intense mixing, concentrations of higher substituted congeners BDE<sub>209</sub> and PCB<sub>153</sub>, and PFOA in both dissolved form and on detritus increase. Conversely, for lower substituted congeners BDE<sub>47</sub> and PCB<sub>28</sub>, dissolved concentrations rise due to their release from DOM during years characterized by less intense mixing and brief disruptions between the SML and BML.

Given the high turbidity of the water column and limited UV irradiation in both scenarios, additional organic matter does not significantly impact light penetration. Over time, the high nitrate content, not utilized by biota, increases the OH radical concentration in the system. This becomes a limiting factor for BDE-OH production. As a result, although BDE-OH concentrations were initially lower, they increase over time, making this region more hazardous for the bioaccumulation of toxic pollutants. Under an intense mixing regime, these toxic BDE-OH compounds remain dispersed throughout the water column year-round.

## 5 Summary and Conclusions

The behavior of persistent organic pollutants (POPs) in aquatic environments is influenced by the specific chemical properties of the individual pollutant, as well as the hydrodynamic and biogeochemical conditions of the region. In this study, I developed and employed a novel model to simulate the environmental fate of five different POPs from three distinct classes across five representative coastal regions, each with individual hydrodynamic and biogeochemical regimes. The primary objective of this research is to gain a comprehensive understanding of how chemical, physical, and biological factors impact the behavior of POPs, and to assess the system's response to changes in specific parameters.

A significant outcome of this thesis is the development of a novel model for simulating the behavior of various POPs in the marine environment. The model has been rigorously tested and was published in 2022 [Mikheeva et al., 2022]. For this study, the model was coupled to the hydrodynamic model GOTM (General Ocean Turbulence Model) and the biogeochemical NPZD (Nutrients, Phytoplankton, Zooplankton, Detritus) model ECOSMO. The GOTM model effectively represents the relevant hydrodynamic and thermodynamic processes associated with vertical turbulent mixing in a 1D framework, while ECOSMO captures the complex ecosystem dynamics and organic matter production in the water column. Additionally, the chemical module integrated into the model accounts for the detailed characteristics of each pollutant, including atmospheric and sedimentary diffusive exchange, as well as the parameters governing sorption, degradation, and transformation processes.

This study addresses three key research questions posed at the beginning of the thesis. To briefly recap, the research questions are:

1. How do the specific chemical properties of each pollutant influence their distribution throughout the water column?
2. To what extent do the hydrodynamic conditions of the selected region impact the fate of various classes of persistent organic pollutants?
3. How does a change in nitrate concentration influence the fate of POPs in the aquatic environment?

The following section provides a detailed summary of the overall findings and conclusions of each research question.

### 5.1 RQ1: The environmental fate of specific POP congeners

In addressing the first research question, we examined the differences in behavior among specific pollutants. Using identical conditions in the Gotland region and maintaining the same concentration levels, we analyzed the variations in pollutant accumulation and their distribution patterns. The Gotland Basin was selected for its unique environmental conditions. Those conditions include stratified waters, high biological productivity, and low turbulence, which together provide an ideal setting for analyzing pollutant behavior across different environmental compartments. The study explores how pollutants interact with particulate and dissolved

organic matter, how they accumulate in sediments, and how they are exchanged between the atmosphere and the water column.

In the aquatic environment, different POPs exhibit distinct distribution patterns based on their chemical properties. These variations are evident even at low concentration levels and among different congeners within the same class of pollutants. Such differences underscore the complexity of pollutant behavior in aquatic systems and highlight the importance of considering specific chemical properties when studying their distribution and impact.

Polychlorinated biphenyls (PCBs) and polybrominated diphenyl ethers (PBDEs) classes are both highly hydrophobic and share a wide range of properties, resulting in similar behavioral patterns. Lower substituted congeners (LSCs) tend to accumulate on particulate organic matter (POM) at a slower rate but continue to do so over an extended period of time. In contrast, higher substituted congeners (HSCs) rapidly bind to detritus. Differences in sorption/desorption processes dictate the final phase distribution of these POPs. HSCs prevail in the detritus-bound phase, while LSCs have higher concentrations associated with dissolved organic matter (DOM). Additionally, the intensity of diffusive atmospheric flux is linked to the mass of the POPs, leading to an increase in the outflux of POPs from the water column to the atmosphere in the order:  $BDE_{209} < BDE_{47} < PCB_{153} < PCB_{28}$ .

This variation in binding behavior leads to differences in sediment accumulation over time, thereby influencing the seasonal distribution patterns of these pollutants. HSCs dominate as the primary pollutants early in the year due to their fast binding affinity, leading to a higher initial concentration in sediments. However, as the year progresses, the steady accumulation of LSCs causes their levels in the sediment to gradually increase, eventually surpassing those of HSCs. This temporal shift highlights the dynamic nature of pollutant distribution and the varying impacts of LSCs and HSCs throughout the year.

Perfluorooctanoic acid (PFOA) exhibits a distinct behavior compared to other pollutants. PFOA exhibits a partitioning behavior similar to HSCs. However, it lacks diffusive atmospheric exchange but is released into the atmosphere through the formation of sea spray aerosols (SSA). Consequently, PFOA outflux from the system is predominantly influenced by wind speed, leading to enhanced PFOA concentrations in the water column compared to other POPs. While the release process depends on the concentration of PFOA, it is predominantly driven by wind speed. The formation of SSA significantly enhances the atmospheric deposition of PFOA, leading to elevated concentrations across various environmental matrices. Due to its tendency to dissociate in the water column, PFOA preferentially remains in the aquatic environment.

This study concludes that the distribution patterns of POPs in marine environments are intricately influenced by their specific chemical properties and the environmental conditions of the region. The unique physico-chemical characteristics of each pollutant play a crucial role in determining their distribution across different phases within the water column. By employing a kinetic partitioning approach, the study highlights the variations in pollutant accumulation behavior between dissolved and particulate organic matrices. This partitioning process not only affects the concentrations of pollutants within the aquatic environment but also influences their

temporal accumulation patterns in the sediment. Additionally, the study demonstrates that the specific properties of each POP govern their exchange with the atmosphere. Hydrophobic pollutants, which are accessible to diffusive exchange, exhibit a greater propensity for outflux back into the atmosphere. In contrast, the outflux of pollutants with surfactant properties is primarily regulated by wind speed at the water surface. Through the simulation of these processes, the research provides valuable insights into how different physico-chemical factors shape the fate of POPs in marine environments, emphasizing the importance of incorporating these variables in environmental modeling efforts.

## 5.2 RQ2: Hydrodynamic Impacts on the Fate of hydrophobic POPs in the Marine Environment

To address the second research question, the model was used to evaluate the fate of 5 different POPs under a variety of hydrophysical and biological conditions in different locations of the North and Baltic Seas.

In the northern part of the Baltic Sea, which is seasonally covered by sea ice, the atmospheric influx is blocked. Little primary production and turbulent mixing in winter season lead to dissolved POPs being evenly distributed in the beginning of the year with short window with no pollutants in dissolved form from the end of June to October. Elevated concentration in the surface layer during this period related to remineralisation from DOM. Elevated concentrations of PFOA can be explained by low outflux via SSA formation due to low wind and ice coverage.

In the deep Baltic basin, the water column is permanently stratified, with an oxic surface layer and an anoxic deep layer. With the onset of primary production in May, all five POPs become bound to particulate organic matter, which then settles with the organic particles. Beginning in August or September, the atmospheric influx of POPs gradually increases in concentration within the lighter surface layer. At the same time, the dissolved concentrations of pollutants rise due to the remineralization of DOM, a process particularly pronounced for LSCs like BDE<sub>47</sub> and PCB<sub>28</sub>. Additionally, the dissolved concentration of PFOA in the surface layer increases, primarily due to limited formation of SSA, a consequence of low salinity and restricted wind speed.

In the Northern North Sea, the water column is stratified during the summer and autumn and becomes mixed during the winter and spring. In summer, high biological production leads to dissolved pollutants binding to dissolved and particulate organic carbon, a process similar to that observed in the Gotland Deep. However, in winter, the deepening mixed layer dilutes POPs in the surface layer by spreading them over a larger volume. During this period, atmospheric POPs are introduced into the ocean. In spring, when the water column is fully mixed, pollutants that settled in the previous year are resuspended and evenly distributed throughout the water column until stratification and production cycles resume.

In the Southern North Sea, which remains well-mixed year-round, POPs are uniformly distributed throughout the water column. In summer, the surface layer is almost depleted of dis-

solved POPs, leading to a significant atmospheric influx and resuspension events, which can temporarily triple the total amount of POPs, particularly LSCs. The outflux of BDEs from the water column to the atmosphere is limited by their high molecular weight, causing them to accumulate in resuspended phases, both bound to organic matter and dissolved. PCBs exhibit a similar, though less pronounced, effect. The complete release of POPs from sediments back into the water column raises water concentrations and reduces the water column's capacity for diffusive gaseous uptake from the atmosphere. In this region, high wind speed, elevated water concentrations, and salinity (compared to the Baltic Sea) enhance the SSA outflux of PFOA. This pattern also applies to POPs entering the area from rivers.

This work established that the two primary driving processes of POPs fate in coastal water column are biological production and vertical mixing. Firstly, high biological production binds all simulated dissolved POPs to organic matter. This particulate organic matter then drives sedimentation, reducing the surface concentrations of POPs. The combination of reduced total POPs and a smaller fraction of total PCB in the dissolved phase alters the concentration gradient between the atmosphere and ocean, thereby increasing the atmospheric POP flux into the ocean. This process exhibits a similar nature for both PCB and BDE classes, which defines the general pattern of their distribution. However, differences in sorption/desorption processes dictate the final distribution of these POPs between different phases (dissolved, on DOM and on POM). HSCs prevail in the detritus-bound phase, while LSCs have higher concentrations associated with DOM.

Secondly, vertical mixing, which depends on tides, bathymetry, and wind regime, determined whether sedimentation is permanent, seasonal, or negligible. Regions of permanent sedimentation, such as the deep basins in the Baltic Sea, can be a major sink for POPs, and thus are an important factor when determining long-range transport from the coast to remote regions. In regions with seasonal sedimentation, we found that, typically, POPs are sedimented after the initial primary production peak and released in winter and spring. This leads to an enormous increase in bioavailable dissolved POP concentrations right at the onset of early primary production. Therefore, it has a major impact on the bioaccumulation of POPs. Here, we found that the underlying hydrodynamic characteristics strongly influence the fate and transport of POPs in the water column, the benthic–pelagic coupling and exchange as well as the uptake to or release from the atmosphere. In the coastal ocean, pronounced tides have a strong impact on vertical mixing and the stability of the summer stratified surface layer. Thus, implementing realistic tides and interactive benthic–pelagic coupling is vital to correctly reproduce vertical mixing and thus the fate of POP in shelf seas.

In addition, the impact of tides on POP concentrations exhibits seasonal variation in the Northern and Southern North Seas. In the Northern North Sea, tidal activity results in an increase in POP concentrations during early autumn, driven by enhanced DOM production. Conversely, a slight decrease is observed in late spring to early summer, likely due to the presence of resuspended detritus, which facilitates the removal of dissolved pollutants. In the Southern North Sea, POP concentrations generally rise in the first half of the year, followed by a decline from late autumn to early winter, influenced by the consistent availability of OM throughout the year. Across both regions, tides have a more significant effect on LSCs compared to HSCs,

with the impact being particularly pronounced for the more water-soluble PFOA.

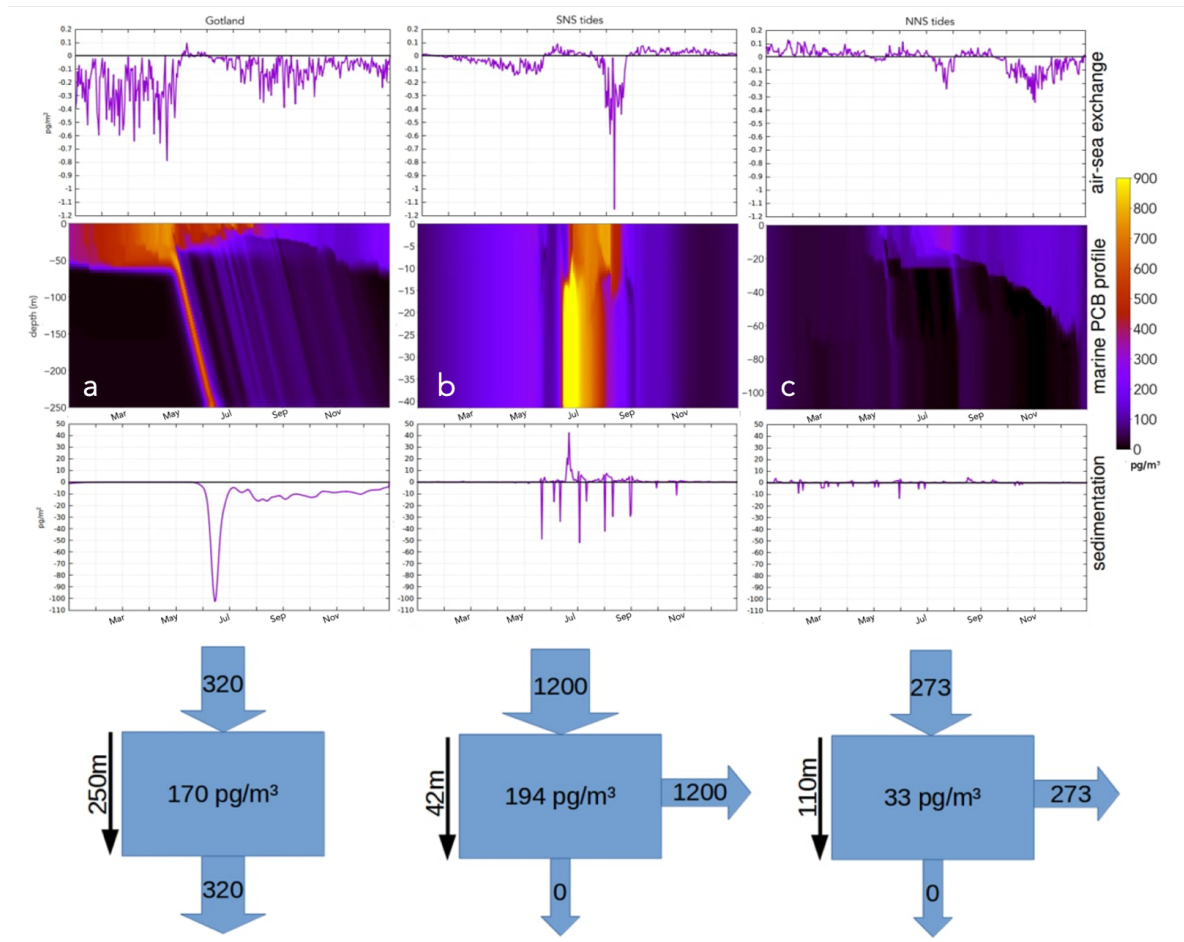


**Figure 42:** Summary picture of total PCB<sub>153</sub> concentrations and budgets for **a** – Gotland Basin, **b** – Southern North Sea (with tides) and **c** – Northern North Sea (with tides) locations.

The final summary of budgets is presented for PCB<sub>153</sub>, representing an average pollutant across all simulations. Although the values for other pollutants vary, the overall pattern remains consistent. In the Gotland Basin, the model predicts an annual atmospheric influx of 320  $\text{pg m}^{-3}$  of PCB, which is primarily transported to the sediment, with a significant initial deposition flux occurring in June (Figure 42a). In contrast, the Northern and Southern North Seas lack sediment deposition, preventing the storage of these pollutants in the sediments. On average, 273  $\text{pg m}^{-3}$  of PCB is transported from the atmosphere to the ocean in the Northern North Sea (Figure 42b), and 1200  $\text{pg m}^{-3}$  in the Southern North Sea (Figure 42c). These PCBs, along with any additional sources such as rivers, are subsequently advected toward the Atlantic Ocean.

### 5.3 RQ3: Changes in aquatic POPs distribution under the conditions of enhanced nitrate concentrations

In addressing the third research question, we investigated the differences between scenarios of enhanced nitrate levels, increased by 20%, versus normal concentrations. We ran the model for each scenario across four setups in the North and Baltic Seas to examine the effects of varying nitrate levels under different hydrodynamic and biogeochemical conditions.

As previously discussed, the biological pump plays a pivotal role in shaping the fate of POPs in the marine environment. The amount and type of organic matter present directly influence the distribution pathways of POPs, particularly those that are highly hydrophobic. This process is intrinsically linked to the nutrient levels within the system, as higher nutrient concentrations stimulate the production of organic matter, which in turn impacts POP partitioning.

Specifically, elevated nitrate ( $\text{NO}_3$ ) concentrations lead to increased production of organic matter, which binds to POPs and facilitates their removal from the dissolved phase. However, this also results in a greater proportion of POPs being associated with DOM, effectively maintaining their presence in the dissolved state. As the water becomes enriched with POPs, the atmospheric input of these pollutants diminishes, regardless of the concentrations in the atmosphere.

High levels of DOM and nitrate can promote the production of hydroxyl radicals ( $\text{OH}^\cdot$ ), which in turn enhances the rate of indirect photolysis. This process significantly influences the pathways of photolytic transformations of POPs. While the increased presence of hydroxyl radicals facilitates the formation of hydroxylated byproducts during photolysis, the extent of this transformation is still primarily governed by the initial concentrations of the parent POP compounds.

The behavior of POPs under elevated nitrate concentrations exhibits significant variability depending on the hydrophysical conditions of the region. This variability is observed across different types of stratification: permanently stratified regions, such as the Gotland Basin; seasonally stratified regions, including the Bothnian Bay and Northern North Sea locations; and permanently mixed regions, like the Southern North Sea. The strong influence of the region's physical characteristics on the biogeochemical processes within the water column underlies this variation, highlighting the interconnectedness of physical and biogeochemical dynamics in determining the fate of POPs under changing environmental conditions.

In regions with strong stratification, such as the Gotland Basin, the overall dissolved concentration of POPs tends to increase with rising nitrate levels. The elevated dissolved concentration accelerates partitioning processes, leading to an earlier accumulation of POPs on OM and a subsequent decrease later in the year. The significant depth of the Gotland Basin allows for a portion of POPs bound to detritus to be rapidly removed from the surface layer. Sedimentation processes in this region are particularly robust, resulting in substantial accumulation of POPs in the sediment layer and thus contributing to long-term storage. However, POPs bound to DOM remain within the surface mixed layer, and as DOM undergoes remineralization, the dissolved

POP concentration slowly increases over time.

The increase in dissolved POP concentrations also influences the production of hydroxylated byproducts such as BDE-OH. While a high DOM content contributes to the formation of hydroxyl radicals, beyond a certain threshold, DOM begins to have an opposing effect by reducing the amount of light available in surface waters, thereby limiting photolytic processes.

In regions where mixing regimes enable organic matter stored in sediments to reach the surface mixed layer, dissolved concentrations of all POPs tend to decrease with increasing nitrate levels. This decrease is attributed to the higher availability of organic matter for partitioning, which leads to an increase in pollutants bound to detritus. This effect is evident in both North Sea regions and in the Bothnian Bay of the Baltic Sea. However, in the Bothnian Bay, ice coverage restricts the exchange of POPs with the atmosphere, resulting in a less pronounced decrease compared to the North Sea regions. Additionally, for PFOA, low wind speeds and surface salinity inhibit its removal from the water via sea spray aerosols, leading to an increase in its dissolved concentration.

In the seasonally mixed area of Bothnian Bay, the rate of indirect photolysis does not increase dramatically due to low irradiation input, ice coverage, and shading of photon flux by permanently mixed POM. For Bothnian Bay and NNS, the reduced dissolved concentration remains a limiting factor, leading to a decrease in BDE-OH production.

In the permanently mixed Southern North Sea, enhanced nitrate concentrations generally result in a decrease in dissolved POP concentrations, with localized increases caused by the remineralization of organic matter. Specifically, DOM leads to higher concentrations of LSCs, while POM increases the concentrations of HSCs and PFOA. However, due to the presence of suspended organic matter throughout the year, even without enhanced nitrate levels, light penetration in this region is limited. This limitation shifts the factors influencing the process of indirect photolysis. Initially, lower dissolved concentrations are the primary factor in BDE-OH formation. However, over time, the increased rate of OH radical formation due to enhanced nitrate levels leads to a rise in the production of hydroxylated congeners.

## References

- [SC, 2019] (2019). Stockholm Convention on Persistent Organic Pollutants. <http://chm.pops.int/>. Last accessed May 2024.
- [NAO, 2024] (2024). NAOO Official Website. <https://maps.ngdc.noaa.gov/viewers/bathymetry/>. Last accessed May 2024.
- [Abbasi, 2015] Abbasi, G. (2015). *Story of Brominated Flame Retardants: Substance Flow Analysis of PBDEs from Use to Waste*. PhD thesis, University of Toronto, Toronto, Canada.
- [Agulló et al., 2019] Agulló, L., Pieper, D. H., and Seeger, M. (2019). Genetics and Biochemistry of Biphenyl and PCB Biodegradation. In *Aerobic Utilization of Hydrocarbons, Oils, and Lipids. Handbook of Hydrocarbon and Lipid Microbiology*, page 595–622. Springer.
- [Alava et al., 2018] Alava, J., Cisneros-Montemayor, A., Sumaila, U., and Cheung, W. (2018). Projected amplification of food web bioaccumulation of MeHg and PCBs under climate change in the Northeastern Pacific. *Scientific Reports*, 8(13460):196–211.
- [Aleksenko et al., 2018] Aleksenko, E., Thouvenin, B., Tronczyński, J., Carlotti, F., Garreau, P., Tixier, C., and Baklouti, M. (2018). Modeling of pcb trophic transfer in the gulf of lions; 3d coupled model application. *Marine Pollution Bulletin*, 128:140–155.
- [Alharbi et al., 2018] Alharbi, O. M., Basheer, A. A., Khattab, R. A., and Ali, I. (2018). Health and environmental effects of persistent organic pollutants. *Journal of Molecular Liquids*, 263:442–453.
- [Andrade et al., 2021] Andrade, H., Glüge, J., Herzke, D., Ashta, N. M., Nayagar, S. M., and Scheringer, M. (2021). Oceanic long-range transport of organic additives present in plastic products: an overview. *Environmental Sciences Europe*, 33(85).
- [Andvik et al., 2020] Andvik, C., Jourdain, E., Ruus, A., Lyche, J. L., Karoliussen, R., and Borgå, K. (2020). Preying on seals pushes killer whales from Norway above pollution effects thresholds. *Scientific Reports*, 10(1).
- [Bamford et al., 2000] Bamford, H., Poster, D., and Baker, J. (2000). Henry’s law constants of polychlorinated biphenyl congeners and their variation with temperature. *Journal of Chemical & Engineering Data*, 45:1069–1074.
- [Bao et al., 2011] Bao, L.-J., You, J., and Zeng, E. (2011). Sorption of PBDE in low-density polyethylene film: Implications for bioavailability of BDE-209. *Environmental toxicology and chemistry / SETAC*, 30:1731–8.
- [Berdowski et al., 1997] Berdowski, J., Baas, J., JP.J., B., Visschedijk, A., and Zandveld, P. (1997). *The European Emission Inventory of Heavy Metals and Persistent Organic Pollutants for 1990; Forschungsbericht 104 02 672/03; Umweltforschungsplan des Bundesministers für Umwelt, Naturschutz und Reaktorsicherheit*. TNO, Utrecht, The Netherlands.

- [Beyer and Biziuk, 2009] Beyer, A. and Biziuk, M. (2009). *Environmental Fate and Global Distribution of Polychlorinated Biphenyls*, pages 137–158. Springer US, Boston, MA.
- [Bodrato and Vione, 2013] Bodrato, M. and Vione, D. (2013). Apex (aqueous photochemistry of environmentally occurring xenobiotics): A free software tool to predict the kinetics of photochemical processes in surface waters. *Environmental science. Processes & impacts*, 16.
- [Borja et al., 2005] Borja, J., Taleon, D., Auresenia, J., and Gallardo, S. (2005). Polychlorinated biphenyls and their biodegradation. *Process Biochemistry*, 40:1999–2013.
- [Boyle et al., 1992] Boyle, A. W., Silvin, C. J., Hassett, J. P., Nakas, J. P., and Tanenbaum, S. W. (1992). Bacterial PCB biodegradation. *Biodegradation*, 3:285–298.
- [Breivik et al., 2002] Breivik, K., Sweetman, A., Pacyna, J., and Jones, K. (2002). Towards a global historical emission inventory for selected PCB congeners—A mass balance approach. 1. Global production and consumption. *Science of the Total Environment*, 290:181–198.
- [Breivik et al., 2007] Breivik, K., Sweetman, A., Pacyna, J. M., and Jones, K. C. (2007). Towards a global historical emission inventory for selected pcb congeners — a mass balance approach: 3. an update. *Science of The Total Environment*, 377(2):296–307.
- [Bruggeman and Bolding, 2014] Bruggeman, J. and Bolding, K. (2014). A general framework for aquatic biogeochemical models. *Environmental Modelling & Software*, 61:249–265.
- [Buck et al., 2011] Buck, R., Franklin, J., Berger, U., Conder, J., Cousins, I., Voogt, P., Jensen, A., Kannan, K., Mabury, S., and van Leeuwen, S. (2011). Perfluoroalkyl and polyfluoroalkyl substances in the environment: Terminology, classification, and origins. *Assessment and Management*, 7(4):513–541.
- [Burchard et al., 1999] Burchard, H., Bolding, K., and Ruiz-Villarreal, M. (1999). Gotm, a general ocean turbulence model. theory, implementation and test cases.
- [Calza and Vione, 2015] Calza, P. and Vione, D. (2015). *Surface Water Photochemistry*. The Royal Society of Chemistry.
- [ChemSpider, 2024] ChemSpider (2024). The free chemical database. <http://www.chemspider.com/>. Last accessed August 2024.
- [Cui et al., 2023] Cui, W., Hale, R. C., Huang, Y., Zhou, F., Wu, Y., Liang, X., Liu, Y., Tan, H., and Chen, D. (2023). Sorption of representative organic contaminants on microplastics: Effects of chemical physicochemical properties, particle size, and biofilm presence. *Ecotoxicology and Environmental Safety*, 251:114533.
- [Daewel and Schrum, 2013] Daewel, U. and Schrum, C. (2013). Simulating long-term dynamics of the coupled North Sea and Baltic Sea ecosystem with ECOSMO II: Model description and validation. *Journal of Marine Systems*, 119-120:30–49.
- [Daewel et al., 2020] Daewel, U., Yakushev, E., Schrum, C., Nizzetto, L., and Mikheeva, E. (2020). Understanding the role of organic matter cycling for the spatio-temporal structure of PCBs in the North Sea. *Water*, 12(3):817.

- [Davis, 2004] Davis, J. (2004). The long-term fate of polychlorinated biphenyls in San Francisco Bay (USA). *Environmental Toxicology & Chemistry*, 23:2396–2409.
- [de Wit et al., 2004] de Wit, C., Fisk, A., and Hobbs, K. (2004). Amap assessment 2002: Persistent organic pollutants in the arctic. *Arctic Monitoring and Assessment Programme*.
- [Degrendele et al., 2018] Degrendele, C., Wilson, J., Kukucka, P., Klanova, J., and Lammel, G. (2018). Are atmospheric pbde levels declining in central europe? examination of the seasonal and semi-long-term variations, gas–particle partitioning and implications for long-range atmospheric transport. *Atmospheric Chemistry and Physics*, 18:12877–12890.
- [Egbert and Erofeeva, 2002] Egbert, G. and Erofeeva, S. (2002). Efficient Inverse Modeling of Barotropic Ocean Tides. *Journal of Atmospheric and Oceanic Technology*, 19:183–204.
- [EMEP, 2024] EMEP (2024). European Monitoring and Evaluation Programme. <http://www.emep.int>. Last accessed August 2024.
- [Environment Agency, 2019] Environment Agency, U. (2019). Polybrominated diphenyl ethers (PBDEs): sources, pathways and environmental data. [https://consult.environment-agency.gov.uk/++preview++/environment-and-business/challenges-and-choices/user\\_uploads/polybrominated-diphenyl-ethers-pressure-rbmp-2021.pdf](https://consult.environment-agency.gov.uk/++preview++/environment-and-business/challenges-and-choices/user_uploads/polybrominated-diphenyl-ethers-pressure-rbmp-2021.pdf). Last accessed August 2024.
- [EPA, 2009] EPA (2009). Polybrominated diphenyl ethers (pbdes) action plan summary.
- [Eriksson et al., 2004] Eriksson, J., Green, N., Marsh, G., and Bergman, A. (2004). Photochemical decomposition of 15 polybrominated diphenyl ether congeners in methanol/water. *Environmental science & technology*, 38(11):3119–3125.
- [Fagbayigbo et al., 2021] Fagbayigbo, B., Opeolu, B., Fatoki, O., Olatunji, O., Akharam, M., and Human, I. (2021). Sorption and partitioning of perfluorooctanoic acid (pfoa) and perfluorooctane sulfonate (pfos) onto sediments of diep and plankenburg river systems western cape, south africa. *Environmental Technology & Innovation*, 25:102110.
- [Fernandes and Falandysz, 2020] Fernandes, A. and Falandysz, J. (2020). Polybrominated dibenzo-p-dioxins and furans (pbdd/fs): Contamination in food, humans and dietary exposure. *Science of The Total Environment*, 761:143191.
- [Friedman and Selin, 2016] Friedman, C. and Selin, N. (2016). PCBs in the Arctic atmosphere: Determining important driving forces using a global atmospheric transport model. *Atmospheric Chemistry & Physics*, 16:3433–3448.
- [Fulton and Matthews, 1936] Fulton, W. and Matthews, J. (1936). A Preliminary Report of the Dermatological and Systemic Effects of Exposure to Hexachloro-Naphthalene and Chloro-Diphenyl.

- [Garrido Reyes et al., 2021] Garrido Reyes, T. I., Mendoza Crisosto, J. E., Varela Echeverria, P. S., Mejías Barrios, E. G., and Álvarez Salgado, X. A. (2021). Interaction between polychlorinated biphenyls and dissolved organic matter of different molecular weights from natural and anthropic sources. *Journal of Environmental Management*, 299:113645.
- [Giri et al., 2011] Giri, R. R., Ozaki, H., Morigaki, T., Taniguchi, S., and Takanami, R. (2011). UV photolysis of perfluorooctanoic acid (PFOA) in dilute aqueous solution. *Water Science and Technology*, 63(2):276–282.
- [Gluege et al., 2020] Gluege, J., Scheringer, M., Cousins, I., Dewitt, J., Goldenman, G., Herzke, D., Lohmann, R., Ng, C., Trier, X., and Wang, Z. (2020). An overview of the uses of per- and polyfluoroalkyl substances (pfas). *Environmental Science: Processes and Impacts*, 22(12):2345–2373.
- [Gong, 2003] Gong, S. (2003). A parameterization of sea-salt aerosol source function for sub- and super-micron particles. *Global Biogeochemical Cycles - GLOBAL BIOGEOCHEM CYCLE*, 17.
- [Gouin et al., 2004] Gouin, T., Mackay, D., Jones, K., Harner, T., and Meijer, S. (2004). Evidence for the “grasshopper” effect and fractionation during long-range atmospheric transport of organic contaminants. *Environmental Pollution*, 128(1):139–148. Persistent Organic Pollutants.
- [Guo et al., 2019] Guo, W., Pan, B., Sakkiah, S., Yavas, G., Ge, W., Zou, W., Tong, W., and Hong, H. (2019). Persistent organic pollutants in food: Contamination sources, health effects and detection methods. *International Journal of Environmental Research and Public Health*, 16(22).
- [Hansen et al., 2004] Hansen, K. M., Christensen, J. H., Brandt, J., Frohn, L. M., and Geels, C. (2004). Modelling atmospheric transport of persistent organic pollutants in the Northern Hemisphere with a 3-D dynamical model: DEHM-POP. *Atmospheric Chemistry and Physics Discussions*, 4(2):1339–1370.
- [Hemond and Fechner, 2015] Hemond, H. and Fechner, E. (2015). *Chemical Fate and Transport in the Environment*. Elsevier, Amsterdam, The Netherlands, 3 edition.
- [Huang et al., 2007] Huang, P., Gong, S. L., Zhao, T. L., Neary, L., and Barrie, L. A. (2007). Gem/pops: a global 3-d dynamic model for semi-volatile persistent organic pollutants; part 2: Global transports and budgets of pcbs. *Atmospheric Chemistry and Physics*, 7(15):4015–4025.
- [IARC, 2016] IARC (2016). Monograph 107, monographs on the evaluation of carcinogenic risks to humans, Polychlorinated Biphenyls and Polybrominated Biphenyls. <https://monographs.iarc.who.int/wp-content/uploads/2018/08/mono107.pdf>. Last accessed May 2024.
- [Ilyina et al., 2006] Ilyina, T., Pohlmann, T., Lammel, G., and Sündermann, J. (2006). A fate and transport ocean model for persistent organic pollutants and its application to the North Sea. *Journal of Marine Systems*, 63:1–19.
- [ITRC, 2020] ITRC (2020). History and use of per- and polyfluoroalkyl substances (pfas) found in the environment.

- [ITRC, 2021] ITRC (2021). PFAS — Per- and Polyfluoroalkyl Substances. <https://pfas-1.itrcweb.org>. Last accessed August 2024.
- [Jamieson et al., 2017] Jamieson, A. J., Malkocs, T., Piertney, S. B., Fujii, T., and Zhang, Z. (2017). Bioaccumulation of persistent organic pollutants in the deepest ocean fauna. *Nature Ecology & Evolution*, 1(0051).
- [Johansson et al., 2019] Johansson, J. H., Salter, M. E., Acosta Navarro, J. C., Leck, C., Nilsson, E. D., and Cousins, I. T. (2019). Global transport of perfluoroalkyl acids via sea spray aerosol. *Environ. Sci.: Processes Impacts*, 21:635–649.
- [Jonker and Smedes, 2000] Jonker, M. and Smedes, F. (2000). Preferential Sorption of Planar Contaminants in Sediments from Lake Ketelmeer, The Netherlands. *Environmental Science & Technology*, 34:1620–1626.
- [Jurado et al., 2007] Jurado, E., Zaldívar, J.-M., Marinov, D., and Dachs, J. (2007). Fate of persistent organic pollutants in the water column: Does turbulent mixing matter? *Marine Pollution Bulletin*, 54(4):441–451.
- [Kallenborn et al., 2015] Kallenborn, R., Hung, H., and Brorström-Lundén, E. (2015). Chapter 13 - atmospheric long-range transport of persistent organic pollutants (pops) into polar regions. In Zeng, E. Y., editor, *Persistent Organic Pollutants (POPs): Analytical Techniques, Environmental Fate and Biological Effects*, volume 67 of *Comprehensive Analytical Chemistry*, pages 411–432. Elsevier.
- [Katsikantami et al., 2024] Katsikantami, I., Iatrou, E. I., Tzatzarakis, M. N., and Kalantzi, O.-I. (2024). Polychlorinated biphenyls (pcbs). In Wexler, P., editor, *Encyclopedia of Toxicology (Fourth Edition)*, pages 827–833. Academic Press, Oxford, fourth edition edition.
- [Khairy et al., 2021] Khairy, M., Brault, E., Dickhut, R., Harding, K. C., Harkonen, T., Karlsson, O., Lehnert, K., Teilmann, J., and Lohmann, R. (2021). Bioaccumulation of PCBs, OCPs and PBDEs in Marine Mammals From West Antarctica. *Frontiers in Marine Science*, 8.
- [Kohler et al., 2005] Kohler, M., Tremp, J., Zennegg, M., Seiler, C., Minder-Kohler, S., Beck, M., Lienemann, P., Wegmann, L., and Schmid, P. (2005). Joint sealants: An overlooked diffuse source of polychlorinated biphenyls in buildings. *Environmental Science & Technology*, 39(7):1967–1973.
- [Kong et al., 2014] Kong, D., MacLeod, M., and Cousins, I. (2014). Modelling the influence of climate change on the chemical concentrations in the Baltic Sea region with the POPCYCLING-Baltic model. *Chemosphere*, 110:31–40.
- [Kos Durjava et al., 2007] Kos Durjava, M., ter Laak, T., Hermens, J., and Struijs, J. (2007). Distribution of PAHs and PCBs to Dissolved Organic Matter: High Distribution Coefficients with Consequences for Environmental Fate Modeling. *Chemosphere*, 67:990–997.
- [Lamon et al., 2012] Lamon, L., MacLeod, M., Marcomini, A., and Hungerbühler, K. (2012). Modeling the influence of climate change on the mass balance of polychlorinated biphenyls in the Adriatic Sea. *Chemosphere*, 87:1045–1051.

- [Lechtenfeld, 2012] Lechtenfeld, O. (2012). *Biogeochemistry of Marine Dissolved Organic Matter: Molecular Composition, Reactivity and New Methods*. PhD thesis, Bremen University, Bremen, Germany.
- [Lehmann et al., 2022] Lehmann, A., Myrberg, K., Post, P., Chubarenko, I., Dailidienė, I., Hinrichsen, H.-H., Hüseyin, K., Liblik, T., Meier, H. E. M., Lips, U., and Bukanova, T. (2022). Salinity dynamics of the Baltic Sea. *Earth System Dynamics*, 13(1):373–392.
- [Lippold et al., 2019] Lippold, A., Bourgeon, S., Aars, J., Andersen, M., Polder, A., Lyche, J. L., Bytingsvik, J., Jenssen, B. M., Derocher, A. E., Welker, J. M., and Routti, H. (2019). Temporal trends of persistent organic pollutants in barents sea polar bears (*Ursus maritimus*) in relation to changes in feeding habits and body condition. *Environmental Science and Technology*, 53(2):984 – 995.
- [Lohmann et al., 2007] Lohmann, R., Breivik, K., Dachs, J., and Muir, D. (2007). Global fate of pops: Current and future research directions. *Environmental Pollution*, 150(1):150–165.
- [Lores et al., 2002] Lores, M., Llompart, M., González-García, R., González-Barreiro, C., and Cela, R. (2002). Photolysis of polychlorinated biphenyls by solid-phase microextraction: “on-fibre” versus aqueous photodegradation. *Journal of Chromatography A*, 963(1):37–47.
- [Luarte et al., 2023] Luarte, T., Gómez-Aburto, V. A., Poblete-Castro, I., Castro-Nallar, E., Huneeus, N., Molina-Montenegro, M., Egas, C., Azcune, G., Pérez-Parada, A., Lohmann, R., Bohlin-Nizzetto, P., Dachs, J., Bengtson-Nash, S., Chiang, G., Pozo, K., and Galbán-Malagón, C. J. (2023). Levels of persistent organic pollutants (pops) in the antarctic atmosphere over time (1980 to 2021) and estimation of their atmospheric half-lives. *Atmospheric Chemistry and Physics*, 23(14):8103–8118.
- [Lønborg and Markager, 2021] Lønborg, C. and Markager, S. (2021). Nitrogen in the baltic sea: Long-term trends, a budget and decadal time lags in responses to declining inputs. *Estuarine, Coastal and Shelf Science*, 261:107529.
- [Mackay et al., 2006] Mackay, D. and Shiu, W.-Y., Shiu, W.-Y., and Lee, S. (2006). *Handbook of Physical-Chemical Properties and Environmental Fate for Organic Chemicals*. CRC Press, Boca Raton, FL, USA, 2 edition.
- [MacLeod et al., 2001] MacLeod, M., Woodfine, D. G., Mackay, D., McKone, T., Bennett, D., and Maddalena, R. (2001). Betr north america: A regionally segmented multimedia contaminant fate model for north america. *Environmental Science and Pollution Research*, 8(3):156 – 163.
- [Markowitz, 2018] Markowitz, G. (2018). From industrial toxins to worldwide pollutants: A brief history of polychlorinated biphenyls. *Public Health Reports®*, 133(6):721–725.
- [McLachlan et al., 2018] McLachlan, M., Undeman, E., Zhao, F., and MacLeod, M. (2018). Predicting global scale exposure of humans to PCB 153 from historical emissions. *Environmental Science: Processes & Impacts*, 20:747–756.

- [McMurdo et al., 2008] McMurdo, C. J., Ellis, D. A., Webster, E., Butler, J., Christensen, R. D., and Reid, L. K. (2008). Aerosol Enrichment of the Surfactant PFO and Mediation of the WaterAir Transport of Gaseous PFOA. *Environmental Science & Technology*, 42(11):3969–3974.
- [Mikheeva et al., 2022] Mikheeva, E., Bieser, J., and Schrum, C. (2022). Hydrodynamic impacts on the fate of polychlorinated biphenyl 153 in the marine environment. *Water*, 14(23):39523.
- [Miniero et al., 2015] Miniero, R., Iamiceli, A., and De Felip, E. (2015). Persistent organic pollutants. In *Reference Module in Earth Systems and Environmental Sciences*. Elsevier.
- [Mishra et al., 2022] Mishra, A., Kumari, M., Swati, Kumar, R., Iqbal, K., and Thakur, I. S. (2022). Persistent organic pollutants in the environment: Risk assessment, hazards, and mitigation strategies. *Bioresource Technology Reports*, 19:101143.
- [Nadal et al., 2015] Nadal, M., Marquès, M., Mari, M., and Domingo, J. L. (2015). Climate change and environmental concentrations of pops: A review. *Environmental Research*, 143:177–185.
- [Neumann et al., 2016] Neumann, D., Matthias, V., J., B., Aulinger, A., and Quante, M. (2016). A comparison of sea salt emission parameterizations in northwestern Europe using a chemistry transport model setup. *Atmospheric Chemistry and Physics*, 16:9905–9933.
- [Ng and von Goetz, 2017] Ng, C. A. and von Goetz, N. (2017). The global food system as a transport pathway for hazardous chemicals: The missing link between emissions and exposure. *Environmental health perspectives*, 125(1):1–7.
- [Odabasi, 2008] Odabasi, M. (2008). Halogenated Volatile Organic Compounds from the Use of Chlorine-Bleach-Containing Household Products. *Environmental Science & Technology*, 42:1445–1451.
- [O’Driscoll et al., 2013] O’Driscoll, K., Mayer, B., Ilyina, T., and Pohlmann, T. (2013). Modelling the cycling of persistent organic pollutants (pops) in the north sea system: Fluxes, loading, seasonality, trends. *Journal of Marine Systems*, 111-112:69–82.
- [Olenycz et al., 2015] Olenycz, M., Sokołowski, A., Niewińska, A., Wołowicz, M., Namieśnik, J., Hummel, H., and Jansen, J. (2015). Comparison of PCBs and PAHs levels in European coastal waters using mussels from the *Mytilus edulis* complex as biomonitors. *Oceanologia*, 57:196–211.
- [Organisation for Economic Co-operation and Development (OECD), 2006] Organisation for Economic Co-operation and Development (OECD) (2006). Results of the 2006 Survey on Production and Use of PFOS, PFAS, PFOA, PFCA, Their Related Substances and Products / Mixtures Containing These Substances. *Env/Jm/Mono*, 36.
- [Pagni and Sigman, 1999] Pagni, R. and Sigman, M. (1999). *The Photochemistry of PAHs and PCBs in Water and on Solids*. Springer, Berlin/Heidelberg, Germany.
- [Pan et al., 2016] Pan, Y., Tsang, D., Wang, Y., Li, Y., and Yang, X. (2016). The Photodegradation of Polybrominated Diphenyl Ethers (PBDEs) in Various Environmental Matrices: Kinetics and Mechanisms. *Chemical Engineering Journal*, 297:74–96.

- [Paragot et al., 2020] Paragot, N., Bečanová, J., Karásková, P., Prokeš, R., Klánová, J., Lammel, G., and Degrendele, C. (2020). Multi-year atmospheric concentrations of per- and polyfluoroalkyl substances (pfass) at a background site in central europe. *Environmental pollution*, 265(Pt B):114851.
- [Placke et al., 2021] Placke, M., Meier, H., and Neumann, T. (2021). Sensitivity of the Baltic Sea Overturning Circulation to Long-Term Atmospheric and Hydrological Changes. *Journal of Geophysical Research: Oceans*, 126, e2020JC016079:4670–4686.
- [Qing Li et al., 2006] Qing Li, Q., Loganath, A., Seng Chong, Y., Tan, J., and Obbard, J. P. (2006). Persistent organic pollutants and adverse health effects in humans. *Journal of Toxicology and Environmental Health, Part A*, 69(21):1987–2005.
- [Rayne et al., 2006] Rayne, S., Wan, P., and Ikonou, M. (2006). Photochemistry of a major commercial polybrominated diphenyl ether flame retardant congener: 2,2,4,4,5,5-hexabromodiphenyl ether (bde153). *Environment International*, 32(5):575–585.
- [Ren et al., 2017] Ren, J., Wang, X., Wang, C., Gong, P., Wang, X., and Yao, T. (2017). Biomagnification of persistent organic pollutants along a high-altitude aquatic food chain in the tibetan plateau: Processes and mechanisms. *Environmental Pollution*, 220:636–643.
- [Ritter et al., 2011] Ritter, R., Scheringer, M., MacLeod, M., Moeckel, C., Jones, K. C., and Hungerbühler, K. (2011). Intrinsic human elimination half-lives of polychlorinated biphenyls derived from the temporal evolution of cross-sectional biomonitoring data from the United Kingdom. *Environmental health perspectives*, 119(2):225–231.
- [Rodhe et al., 2010] Rodhe, J., Tett, P., and Wulff, F. (2010). Chapter 26. THE BALTIC AND NORTH SEAS: A REGIONAL REVIEW OF SOME IMPORTANT PHYSICAL-CHEMICAL- BIOLOGICAL INTERACTION PROCESSES (20,S). In Allan R. Robinson, K. H. B., editor, *The Global Coastal Ocean*, volume 14. Harvard University Press, Cambridge, MA, USA.
- [Rodrigues et al., 2019] Rodrigues, J. P., Duarte, A. C., Santos-Echeandía, J., and Rocha-Santos, T. (2019). Significance of interactions between microplastics and pops in the marine environment: A critical overview. *TrAC Trends in Analytical Chemistry*, 111:252–260.
- [Rokni et al., 2023] Rokni, L., Rezaei, M., Rafieizonooz, M., Khankhajah, E., Mohammadi, A. A., and Rezaei, S. (2023). Effect of persistent organic pollutants on human health in south korea: A review of the reported diseases. *Sustainability*, 15(14).
- [Roszko et al., 2015] Roszko, M., Szymczyk, K., and Jędrzejczak, R. (2015). Photochemistry of tetra- through hexa-brominated dioxins/furans, hydroxylated and native BDEs in different media. *Environmental Science & Pollution Research*, 22:18381–18393.
- [Ruiz-Fernández et al., 2014] Ruiz-Fernández, A. C., Ontiveros-Cuadras, J. F., Sericano, J. L., Sanchez-Cabeza, J.-A., Liong Wee Kwong, L., Dunbar, R. B., Mucciarone, D. A., Pérez-Bernal, L. H., and Páez-Osuna, F. (2014). Long-range atmospheric transport of persistent organic pollutants to remote lacustrine environments. *Science of The Total Environment*, 493:505–520.

- [Sander, 2023] Sander, R. (2023). Compilation of Henry's law constants (version 5.0.0) for water as solvent. *Atmos. Chem. Phys.*, 23:10901–12440.
- [Savchuk and Wulff, 2009] Savchuk, O. and Wulff, F. (2009). Long-term modeling of large-scale nutrient cycles in the entire Baltic Sea. *Hydrobiologia*, 629:209–224.
- [Scheringer, 1996] Scheringer, M. (1996). Persistence and spatial range as endpoints of an exposure-based assessment of organic chemicals. *Environmental Science & Technology*, 30(5):1652–1659.
- [Scheringer et al., 2004] Scheringer, M., Salzman, M., Stroebe, M., Wegmann, F., Fenner, K., and Hungerbühler, K. (2004). Long-range transport and global fractionation of pops: insights from multimedia modeling studies. *Environmental Pollution*, 128(1):177–188. Persistent Organic Pollutants.
- [Scheringer et al., 2000] Scheringer, M., Wegmann, F., Fenner, K., and Hungerbühler, K. (2000). Investigation of the cold condensation of persistent organic pollutants with a global multimedia fate model. *Environmental Science & Technology*, 34(9):1842–1850.
- [Schlesinger et al., 2022] Schlesinger, D. R., McDermott, C., Le, N. Q., Ko, J. S., Johnson, J. K., Demirev, P. A., and Xia, Z. (2022). Destruction of per/poly-fluorinated alkyl substances by magnetite nanoparticle-catalyzed uv-fenton reaction. *Environ. Sci.: Water Res. Technol.*, 8:2732–2743.
- [Schmitt et al., 2021] Schmitt, L., Hinxlage, I., Cea, P. A., Gohlke, H., and Wesselborg, S. (2021). 40 years of research on polybrominated diphenyl ethers (pbdes)—a historical overview and newest data of a promising anticancer drug. *Molecules*, 26(4).
- [Schwarzenbach et al., 2016] Schwarzenbach, R. P., Gschwend, P. M., and Imboden, D. M. (2016). *Environmental Organic Chemistry*. Addison Wesley, Hoboken, NJ, USA, 3 edition.
- [Sha et al., 2022] Sha, B., Johansson, J. H., Tunved, P., Bohlin-Nizzetto, P., Cousins, I. T., and Salter, M. E. (2022). Sea spray aerosol (ssa) as a source of perfluoroalkyl acids (pfaas) to the atmosphere: Field evidence from long-term air monitoring. *Environmental Science & Technology*, 56(1):228–238.
- [Sişman et al., 2007] Sişman, T., Geyikoglu, F., and Atamanalp, M. (2007). Early life-stage toxicity in zebrafish (*Danio rerio*) following embryonal exposure to selected polychlorinated biphenyls. *Toxicology and industrial health*, 23:529–36.
- [Sobek et al., 2023] Sobek, A., Abel, S., Sanei, H., Bonaglia, S., Li, Z., Horlitz, G., Rudra, A., Oguri, K., and Glud, R. N. (2023). Organic matter degradation causes enrichment of organic pollutants in hadal sediments. *Nature Communications*, 14(2012).
- [Szymczycha et al., 2019] Szymczycha, B., Zaborska, A., Beldowski, J., Kuliński, K., Beszczyńska-Möller, A., Kędra, M., and Pempkowiak, J. (2019). *Chapter 4 — The Baltic Sea*, page 85–111. Academic Press, Cambridge, MA, USA, 2 edition.

- [Tehrani and Van Aken, 2014] Tehrani, R. and Van Aken, B. (2014). Hydroxylated polychlorinated biphenyls in the environment: sources, fate, and toxicities. *Environmental Science and Pollution Research*, 21:6334–6345.
- [Umlauf et al., 2024] Umlauf, L., Burchard, H., and Bolding, K. (2024). GOTM: Source Code and Test Case Documentation, Version 4.0. <https://gotm.net/manual/stable/pdf/letter.pdf>. Last accessed August 2024.
- [Usenko et al., 2012] Usenko, C., Hopkins, D., Trumble, S., and Bruce, E. (2012). Hydroxylated pbdes induce developmental arrest in zebrafish. *Toxicology and applied pharmacology*, 262:43–51.
- [Usenko et al., 2011] Usenko, C., Robinson, E., Usenko, S., Brooks, B., and Bruce, E. (2011). Pbde developmental effects on embryonic zebrafish. *Environmental toxicology and chemistry / SETAC*, 30:1865–72.
- [Van Jaarsveld et al., 1997] Van Jaarsveld, J., Van Pul, W., and De Leeuw, F. (1997). Modelling transport and deposition of persistent organic pollutants in the european region. *Atmospheric Environment*, 31(7):1011–1024.
- [Van Leeuwen et al., 2015] Van Leeuwen, S., Tett, P., Mills, D., and Van der Molen, J. (2015). Stratified and nonstratified areas in the North Sea: Long-term variability and biological and policy implications. *Journal of Geophysical Research: Oceans*, 120:4670–4686.
- [van Noort et al., 2003] van Noort, P., Cornelissen, G., Ten Hulscher, D., Vrind, B., Rigterink, H., and Belfroid, A. (2003). Slow and very slow desorption of organic compounds from sediment: Influence of sorbate planarity. *Water Research*, 37:2317–2322.
- [Vijgen et al., 2018] Vijgen, J., Weber, R., Lichtensteiger, W., and Schlumpf, M. (2018). The legacy of pesticides and pops stockpiles—a threat to health and the environment. *Environmental Science and Pollution Research*, 25:31793–31798.
- [Wang et al., 2020] Wang, J., Hoondert, R. P., Thunnissen, N. W., van de Meent, D., and Hendriks, A. J. (2020). Chemical fate of persistent organic pollutants in the arctic: Evaluation of simplebox. *Science of The Total Environment*, 720:137579.
- [Wang et al., 2018] Wang, R., Tang, T., Xie, J., Tao, X., Huang, K., Zou, M., Yin, H., Dang, Z., and Lu, G. (2018). Debromination of polybrominated diphenyl ethers (pbdes) and their conversion to polybrominated dibenzofurans (pbdfs) by uv light: Mechanisms and pathways. *Journal of Hazardous Materials*, 354:1–7.
- [Wania and Mackay, 1995] Wania, F. and Mackay, D. (1995). A global distribution model for persistent organic chemicals. *Science of The Total Environment*, 160-161:211–232. Ecological Effects of Arctic Airborne Contaminants.
- [Wasel et al., 2020] Wasel, O., Thompson, K., Gao, Y., Godfrey, A., Gao, J., Mahapatra, C., Lee, L., Sepulveda, M., and Freeman, J. (2020). Comparison of zebrafish in vitro and in vivo developmental toxicity assessments of perfluoroalkyl acids (pfaas). *Journal of toxicology and environmental health. Part A*, 84:1–12.

- [Webster et al., 2004] Webster, E., Mackay, D., Di Guardo, A., and Kane, D. (2004). Regional differences in chemical fate model outcome. *Chemosphere*, 55:1361–1376.
- [Wolska et al., 2012] Wolska, L., Mechlińska, A., Rogowska, J., and Namieśnik, J. (2012). Sources and Fate of PAHs and PCBs in the Marine Environment. *Critical Reviews in Environmental Science and Technology*, 42(11):1172–1189.
- [Wong and Wong, 2006] Wong, K. and Wong, P. (2006). Degradation of Polychlorinated Biphenyls by UV-Catalyzed PhotoFysis. *Human and Ecological Risk Assessment*, 12:259–269.
- [Wong et al., 2005] Wong, M., Leung, A., Chan, J., and Choi, M. (2005). A review on the usage of pop pesticides in china, with emphasis on ddt loadings in human milk. *Chemosphere*, 60(6):740–752. Science-Based Decision Making to Reduce Risks from persistent Organic Pollutants (POPS).
- [Wu et al., 2022] Wu, X., Zheng, X., Yu, L., Lu, R., Zhang, Q., Luo, X.-J., and Mai, B.-X. (2022). Biomagnification of persistent organic pollutants from terrestrial and aquatic invertebrates to songbirds: Associations with physiochemical and ecological indicators. *Environmental Science & Technology*, 56(17):12200–12209.
- [Xin et al., 2023] Xin, X., Kim, J., Ashley, D. C., and Huang, C.-H. (2023). Degradation and defluorination of per- and polyfluoroalkyl substances by direct photolysis at 222 nm. *ACS ES&T Water*, 3(8):2776–2785.
- [Yan et al., 2016] Yan, Y., Ma, W., Zhang, Y., Nie, C., Guo, H., and Lun, X. (2016). Competitive sorption and desorption between BDE-47 and BDE-99 by different river- and farmland-based aquifer media. Desalination and Water Treatment. *Desalination and Water Treatment*, 57(60):29328–29339.
- [Yang and Chan, 2014] Yang, J. and Chan, K. M. (2014). Evaluation of the toxic effects of brominated compounds (bde-47, 99, 209, tbbpa) and bisphenol a (bpa) using a zebrafish liver cell line, zfl. *Aquatic Toxicology*, 159.
- [Zhang et al., 2015] Zhang, H., Jiang, X., Lu, L., and Xiao, W. (2015). Biodegradation of polychlorinated biphenyls (PCBs) by the novel identified cyanobacterium Anabaena PD-1. *PLoS One*, 10(7):e0131450.
- [Zhang et al., 2013] Zhang, S., Xia, X., Xia, N., Wu, S., Gao, F., and Zhou, W. (2013). Identification and biodegradation efficiency of a newly isolated 2,2,4,4-tetrabromodiphenyl ether (bde-47) aerobic degrading bacterial strain. *International Biodeterioration Biodegradation*, 76:24–31. Geomicrobial Ecotoxicology.
- [Zhao et al., 2019] Zhao, C., Daewel, U., and Schrum, C. (2019). Tidal impacts to primary production in the North Sea. *Earth System Dynamics*, 10(1):287–317.
- [Zhao et al., 2015] Zhao, Q., Zhao, H., Quan, X., He, X., and Chen, S. (2015). Photochemical Formation of Hydroxylated Polybrominated Diphenyl Ethers (OH-PBDEs) from Polybrominated Diphenyl Ethers (PBDEs) in Aqueous Solution under Simulated Solar Light Irradiation. *Environmental Science & Technology*, 49:9092–9099.

[Zhou et al., 2005] Zhou, W., Zhai, Z., Wang, Z., and Wang, L. (2005). Estimation of n-octanol/water partition coefficients (KOW) of all PCB congeners by density functional theory. *Journal of Molecular Structure: THEOCHEM*, 755(1):137–145.